

FINITE ELEMENT MODEL UPDATING OF AEROSPACE STRUCTURES

A THESIS SUBMITTED TO THE GRADUATE SCHOOL
OF NATURAL AND APPLIED SCIENCES
OF
MIDDLE EAST TECHNICAL UNIVERSITY

DOĞUŞ ÜNLÜ

IN PARTIAL FULFILLMENT OF THE REQUIREMENTS
FOR
THE DEGREE OF MASTER IN SCIENCE
IN
MECHANICAL ENGINEERING

DECEMBER 2017

Approval of the thesis:

FINITE ELEMENT MODEL UPDATING OF AEROSPACE STRUCTURES

submitted by **DOĞUŞ ÜNLÜ** in partial fulfillment of the requirements for the degree of **Master in Science in Mechanical Engineering Department, Middle East Technical University** by,

Prof. Dr. Gülbin Dural Ünver

Dean, Graduate School of **Natural and Applied Sciences**

Prof. Dr. Sahir Arıkan

Head of Department, **Mechanical Engineering**

Assoc. Prof. Dr. Ender Ciğeroğlu

Supervisor, **Mechanical Engineering Department, METU**

Assist. Prof. Dr. Gökhan O. Özgen

Co-Supervisor, **Mechanical Engineering Department, METU**

Examining Committee Members:

Assist. Prof. Dr. Ulaş Yaman

Mechanical Engineering Department, METU

Assoc. Prof. Dr. Ender Ciğeroğlu

Mechanical Engineering Department, METU

Assist. Prof. Dr. Gökhan O. Özgen

Mechanical Engineering Department, METU

Assist. Prof. Dr. Kerem Bayar

Mechanical Engineering Department, METU

Assist. Prof. Dr. Can Ulaş Doğruer

Mechanical Engineering Department, Hacettepe University

Date:

I hereby declare that all information in this document has been obtained and presented in accordance with academic rules and ethical conduct. I also declare that, as required by these rules and conduct, I have fully cited and referenced all material and results that are not original to this work.

Name, Last Name : DOĐUŐ ÜNLÜ

Signature :

ABSTRACT

FINITE ELEMENT MODEL UPDATING OF AEROSPACE STRUCTURES

Ünlü, Dođuş

M.Sc., Department of Mechanical Engineering

Supervisor: Assoc. Prof. Dr. Ender Ciđerođlu

Co-Supervisor: Assist. Prof. Dr. Gökhan O. Özgen

December 2017, 119 pages

Model updating methods can be used to obtain more accurate mathematical models. Results of linear finite element models which can be assumed as mathematical models for structural dynamics studies almost never match with the real test results. Accurate mathematical models are used to extract more precise results from structural analyses. The model update theory is classified with respect to the solution method as direct and iterative methods. As a summary, direct methods use structural matrices while iterative methods use the modal or response function results in an iterative manner. Selection of the model updating method is initiated with the application of the methods to simple spring-mass system. The advantages and disadvantages of the methods are clarified by extracting the results for direct and iterative methods. Modal based iterative methods are selected to be applied effectively to large order finite element models. Algorithm

is developed by using Inverse Eigensensitivity method with the enhancement which reduces the total time of the updating procedure. Improved method is applied to case studies to see the effect of enhancement and it is concluded that it can reduce the elapsed time great amount. Additionally, Femtools commercial software is used to analyze a test fixture and to update the finite element model to build insight and know-how about the commercial finite element updating software.

Keywords: Finite Element Model Updating, Large Order Finite Element Models, Sensitivity Based Model Updating, Computational Model Updating, Inverse Eigensensitivity Method

ÖZ

HAVACILIK YAPILARINA AİT SONLU ELEMAN MODELLERİNİN GÜNCELLEŞTİRİLMESİ

Ünlü, Dođuş

Master, Makina Mühendisliđi Bölümü

Tez Yöneticisi: Doç. Dr. Ender Ciđerođlu

Ortak Tez Yöneticisi: Yrd. Doç. Dr. Gökhan O. Özgen

Aralık 2017, 119 sayfa

Model güncelleştirme yöntemleri daha dođru ve hassas matematiksel modellerin elde edilmesi için kullanılabilir. Dinamik analizler için matematiksel modeller olarak kabul edilebilen lineer sonlu eleman modellerine ait sonuçlar ile gerçek test sonuçları neredeyse hiçbir zaman eşleşmez. Hassas matematiksel modeller yapısal analizlerden daha dođru sonuçlar elde etmek için kullanılmaktadır. Model güncelleme teorisi çözüm yöntemine göre, direkt ve iteratif olarak ayrılır. Özetle, direkt yöntemler yapısal sistem matrislerini kullanırken; iteratif yöntemler ise modal ve frekans cevap sonuçlarını döngü içerisinde olacak şekilde kullanır. Model güncelleştirme yöntem seçimi basit kütle-yay sistemi uygulamasıyla başlatılmıştır. Yöntemlerin birbirine göre olan avantaj ve dezavantajları, direkt ve iteratif yöntemlerin uygulanmasıyla açığa çıkarılmıştır. Elde edilen sonuçlara göre, modal sonuç tabanlı iteratif yöntemlerin yüksek sayıda serbestlik derecesine sahip sonlu eleman modellerine verimli şekilde uygulanabileceđi sonucuna ulaşılmıştır. Güncelleme işlem süresini kısaltacak bir geliştirme ile birlikte modal

sonuç tabanlı bir algoritma oluşturulmuştur. Oluşturulan algoritmanın zaman açısından sağladığı iyileştirmenin görülmesi için farklı uygulama örnekleri ile denenmiş ve toplam güncellenme zamanını büyük oranda azaltabildiği sonucuna ulaşılmıştır. Ek olarak, ticari bir yazılım olan Femtools hakkında bilgi kaynağı oluşturmak için bir test fikstürüne ait bir sonlu eleman modeli ilgili yazılım vasıtasıyla güncelleştirilmiştir.

Anahtar Kelimeler: Sonlu Eleman Model Güncelleştirme, Yüksek Sayıda Serbestlik Derecesine Sahip Sonlu Eleman Modelleri, Hassasiyet Tabanlı Model Güncelleştirme, Hesaplamalı Model Güncelleştirme, Modal Sonuç Tabanlı Model Güncelleştirme

ACKNOWLEDGMENTS

The author would like to thank to his supervisor Assoc. Prof. Dr. Ender Ciğerođlu and cosupervisor Assist. Prof. Dr. Gökhan O. Özgen for their advice, assistance, feedback and insight throughout the research.

The author would also like to thank Bülent Acar, Tarık Olđar for his suggestions and comments.

The technical and physical assistance of Mr. Kenan Gürses about modal tests of structures used as case studies is acknowledged.

Author would like to gratefully acknowledge the support provided by Undersecretariat for Defence Industries and Roketsan Missile Ind., Grant No: BLS.MH.1000-14/094-4948, SAYP.

TABLE OF CONTENTS

ABSTRACT	v
ÖZ	vii
ACKNOWLEDGMENTS	ix
TABLE OF CONTENTS	x
LIST OF TABLES	xiii
LIST OF FIGURES.....	xv
CHAPTER 1.....	1
INTRODUCTION	1
CHAPTER 2.....	3
THE LITERATURE REVIEW AND MODEL UPDATE THEORY.....	3
2.1 LITERATURE REVIEW.....	3
2.2 MODEL UPDATE THEORY.....	9
2.2.1. Direct Matrix Methods.....	12
2.2.2. Iterative (Indirect) Methods	15
CHAPTER 3.....	19
SELECTION OF THE APPROPRIATE METHOD FOR LARGE ORDER FINITE ELEMENT MODELS WITH CASE STUDIES	19
3.1 CASE STUDIES ON SIX DOF SPRING MASS SYSTEM	19
3.1.1. Results for Update by Direct Matrix Method.....	21
3.1.2. Results for Update by Error Matrix Method	35
3.1.3. Results for Update by Inverse Eigensensitivity Method (IEM).....	41
CHAPTER 4.....	53
DEVELOPED ALGORITHM AND FLOWCHART	53
CHAPTER 5.....	57

APPLICATION OF THE DEVELOPED ALGORITHM TO GARTEUR MODEL AND MISSILE LAUNCHER.....	57
5.1 CASE STUDY ON A SCALED AIRCRAFT MODEL USING THE DEVELOPED ALGORITHM WITH INVERSE EIGENSENSITIVITY METHOD.....	57
5.2 CASE STUDY ON A LAUNCHER OF A GUIDED MISSILE USING THE DEVELOPED ALGORITHM WITH INVERSE EIGENSENSITIVITY METHOD.....	73
CHAPTER 6.....	81
CASE STUDY ON VIBRATION TEST FIXTURE USING FEMTOOLS SOFTWARE.....	81
CHAPTER 7.....	95
RESULTS AND DISCUSSION.....	95
REFERENCES	98
APPENDIX	101
Finite Element Model Reduction and Expansion Techniques	101
I. Guyan or Static Reduction.....	101
II. Dynamic Reduction	103
III. Improved Reduced System.....	103
IV. SEREP(System Equivalent Reduction Expansion Process)	105
I. Expansion using Theoretical Spatial Model – Kidder’s Method.....	107
II. SEREP Expansion Technique	108
Measurement Coordinate Numbers in IEM	109
I. More Measurement Coordinates than the Number of Design Parameters	109
II. Less Measurement Coordinates than the Number of Design Parameters.....	111

Finite Element Method and Model Testing 113

LIST OF TABLES

Table 1. Parameter Values for Experimental Model and Mathematical Model....	21
Table 2. The Case Definitions for Direct Matrix Updating Method	23
Table 3. The MAC Numbers before Updating for Case-1 that Belong to Figure 2	24
Table 4. The MAC Numbers before Updating for Case-1 that Belong to Figure 3	25
Table 5. The MAC Numbers before Updating for Case-2 that Belong to Figure 6... ..	27
Table 6. The MAC Numbers after Updating for Case-2 that Belong to Figure 7	28
Table 7. The MAC Numbers before Updating for Case-3 that Belong to Figure 11	31
Table 8. The MAC Numbers after Updating for Case-3 that Belong to Figure 12	32
Table 9. The MAC Numbers before Updating that Belong to Figure 17	38
Table 10. The MAC Numbers before Updating that Belong to Figure 18	39
Table 11. The Erroneous Values of the Parameters	44
Table 12. The MAC Numbers before Updating that Belong to Figure 23	46
Table 13. The MAC Numbers after Updating that Belong to Figure 24	47
Table 14. The Natural Frequency and Damping Ratios for the Calculated Modes in the Selected Frequency Range.....	60
Table 15. The Material Properties of Al 7071-T6.....	63
Table 16. The MAC Matrix for the Aircraft Model before Updating	64
Table 17. The Natural Frequencies for Experimental and Mathematical Models Before Updating	65
Table 18. The Change of Design Variables with respect to the Iteration Number	67
Table 19. The Natural Frequencies for Experimental and Mathematical Models after Updating.....	71
Table 20. The MAC Matrix for the Aircraft Model after Updating	72

Table 21. The Comparison of the Natural Frequencies of Mathematical and Experimental Models	73
Table 22. MAC Matrix for the Missile Launcher Model before Updating.....	78
Table 23. Comparison of the Natural Frequencies and MAC Values	80
Table 24. Modal Frequency Values Extracted from Modal Test	88
Table 25: Initial Design Paramater Value	91
Table 26: Modal Results before Updating	92
Table 27: Modal Results after Updating	92

LIST OF FIGURES

Figure 1. Reference Spring Mass System	20
Figure 2. MAC Plot before Updating for Case 1	24
Figure 3. MAC Plot after Updating for Case 1	25
Figure 4. The Semi Log Point FRF Plot of the 6 th DOF for Experimental and Mathematical Model for Case 1	26
Figure 5. The Semi Log Point FRF Plot of the 6 th DOF for Experimental, Mathematical and Updated Model for Case 1	26
Figure 6. MAC Plot before Updating for Case 2	27
Figure 7. MAC Plot after Updating for Case 2	28
Figure 8. The Semi Log Point FRF Plot of the 5 th DOF for Experimental and Mathematical Model for Case 2	29
Figure 9. The Semi Log Point FRF Plot of the 5 th DOF for Experimental, Mathematical and Updated Model for Case 2	29
Figure 10. The Semi Log Point FRF Plot of the 6 th DOF for Experimental, Mathematical and Updated Model for Case 2	30
Figure 11. MAC Plot before Updating for Case 3	31
Figure 12. MAC Plot after Updating for Case 3	32
Figure 13. The Semi Log Point FRF Plot of the 4 th DOF for Experimental and Mathematical Model for Case 3	33
Figure 14. The Semi Log Point FRF Plot of the 4 th DOF for Experimental, Mathematical and Updated Model for Case 3	33
Figure 15. The Semi Log Point FRF Plot of the 5 th DOF for Experimental, Mathematical and Updated Model for Case 3	34
Figure 16. The Semi Log Point FRF Plot of the 6 th DOF for Experimental, Mathematical and Updated Model for Case 3	34
Figure 17. MAC Plot before Updating	38
Figure 18. MAC Plot after Updating	39
Figure 19. The Semi Log Point FRF Plot of the 6 th DOF for Experimental and Mathematical Model	40

Figure 20. The Semi Log Point FRF Plot of the 6 th DOF for Experimental, Mathematical and Updated Model.....	40
Figure 21. The Natural Frequencies of the Experimental and Mathematical Models before Updating.....	45
Figure 22. The Natural Frequencies of the Experimental and Mathematical Models after Updating	45
Figure 23. MAC Plot of the Experimental and Mathematical Models before Updating.....	46
Figure 24. MAC Plot of the Experimental and Mathematical Models after Updating.....	47
Figure 25. The Convergence of Erroneous Parameter k_1	48
Figure 26. The Convergence of Erroneous Parameter k_2	48
Figure 27. The Convergence of Erroneous Parameter k_3	49
Figure 28. The Convergence of Erroneous Parameter k_4	49
Figure 29. The Convergence of Parameters With Respect to Number of Iterations	50
Figure 30. The Semi Log Point FRF Plot of the 6 th DOF for Experimental and Mathematical Model.....	51
Figure 31. The Semi Log Point FRF Plot of the 6 th DOF for Experimental, Mathematical and Updated Model.....	51
Figure 32. The Model Updating Methods.....	54
Figure 33. Flowchart of the developed algorithm	56
Figure 34. Geometry of the aircraft model.....	57
Figure 35. The Test Configuration for the GARTEUR Aircraft Model	58
Figure 36. The Properties Identity Numbers of Aircraft Model.....	61
Figure 37. The Finite Element Model of the Aircraft Model.....	62
Figure 38. The Coordinates and Grid Numbers of Nodes that the Eigenvectors Are Extracted From	63
Figure 39. The MAC Plot for the Aircraft Model before Updating	64
Figure 40. The Comparison of the Natural Frequencies before Updating	65
Figure 41. Visual representation of the mode shapes extracted from Nastran.....	66

Figure 42. Change of 1 st Design Parameter with the iterations	68
Figure 43. Change of 2 nd Design Parameter with the iterations	68
Figure 44. Change of 3 rd Design Parameter with the iterations	69
Figure 45. Change of 4 th Design Parameter with the iterations.....	69
Figure 46. Change of 5 th Design Parameter with the iterations.....	70
Figure 47. The MAC Plot for the first 6 Mode Shapes After Updating Procedure	71
Figure 48. The Comparison of the Experimental and Mathematical Natural Frequency Values After Updating Procedure	72
Figure 49. Normalized Sensitivity Values for 1 st Natural Frequency.....	75
Figure 50. Normalized Sensitivity Values for 2 nd Natural Frequency	75
Figure 51. Normalized Sensitivity Values for 3 rd Natural Frequency	76
Figure 52. Missile Launcher.....	76
Figure 53. Parameter Sets Defined In Updating Algorithm.....	77
Figure 54. MAC Plot before Updating.....	79
Figure 55. Change of Design Variable for Case I	79
Figure 56. Change of Design Variable for Case II	80
Figure 57. Finite Element Model of Fixture	82
Figure 58. Results of modal analysis of fixture.....	84
Figure 59. Measurement locations of test fixture	85
Figure 60. Excitation locations and directions of test fixture.....	85
Figure 61. Impact hammer with plastic tip	86
Figure 62. Modal test configuration of test fixture.....	86
Figure 63. Measurement directions of test fixture.....	87
Figure 64. Driving-point FRF functions	87
Figure 65. CAD Model of Fixture	88
Figure 66. Design Parameters.....	90
Figure 67. Design Sensitivity Graph.....	90
Figure 68. Change of design parameters 1, 2 and 3.....	91
Figure 69. Change of design parameters 4, 5	92
Figure 70. Femtools interface-1.....	93

Figure 71. Femtools interface-2..... 93

CHAPTER 1

INTRODUCTION

This work covers the details of application of model updating methods to large order finite element models to obtain more accurate mathematical models. Large order finite element models are extensively for aerospace structure analyses. There are plenty of model updating methods that can be applied to aerospace structures. The choice of a specific method among various existing updating methods considering their advantages and disadvantages in regards to practicality and model correlation performance is one of main tasks accomplished in this thesis work.

The motivation of the work can be summarized to develop and build practical experience on obtaining experimentally verified mathematical structural dynamics models of aerospace structures. For aerospace structures, usually large mechanical structures, design requirements must be satisfied according to operational loading conditions which are based on the dynamic characteristics of the structures. Operational loading conditions are simulated with dynamic analyses such as random vibration, identification of aeroelastic behavior of aerospace structures. Accuracy of the dynamic analyses depends on the structural matrices which must be well representing the real structural dynamics behavior of the actual physical systems. Results such as the eigenvalues obtained by using the mathematically derived structural matrices are major design parameters to be checked in regards to design requirements of structures. Additionally, carrying out a test is not a simple and fast procedure. Small modification with the structure can change the dynamic behavior substantially. Using structural dynamics models correlated with experiments through the use of model updating procedure for doing design

iterations can prevent the repetition prototype fabrication for revised designs and testing of these prototypes, which saves time and decrease design expenses.

The objective of the thesis work is to search, find model updating techniques that can be practically applied for the aerospace structures and to build background information for model updating theory. Additionally, commercial software Femtools is used to update the finite element model of test fixture to gain insight, know how about the application of the model update procedure on a complicated large mechanical structure.

The overview of the thesis is given to summarize the flowchart of the topics that was covered. Chapter 2 covers the literature review about model update and the theory of the techniques used in model updating. Case studies that used to identify the advantages of techniques are given in Chapter 3. Additionally, the selection of proper method applicable to larger order finite element models is made with the application of the Matlab based code to 6 DOF mass spring system to verify the advantages and disadvantages of the model update techniques. Chapter 4 covers the details flowchart of the code generated to be applied to the large order finite elements and modification added to method that decreases the time elapsed for whole model updating procedure. Chapter 5 covers the application of the Matlab based code to GARTEUR structure and launcher of a guided missile. Additionally, Femtools software is used to analyze the test fixture and to update the finite element model in Chapter 6. As a final section, Chapter 7 includes the discussions and results obtained in Chapter 5 and 6.

CHAPTER 2

THE LITERATURE REVIEW AND MODEL UPDATE THEORY

In this section, literature review and model update theory are explained in detail. Literature review includes the old and recent works about model updating to gain insight about the topic; whereas model update theory covers the theoretical details of the method.

2.1 LITERATURE REVIEW

The literature about the techniques used with model updating and model updating theory is investigated to have information about the development of the methods and to understand the applicability of the methods to the real case structures. This section includes the old model updating methods and recent techniques about model updating.

In model updating theory, the first developments was made through modification of the mass and stiffness matrices of the finite element models to make the results be closer to test results. These techniques are collected in the group called direct model updating techniques.

Fox and Kapoor [1] used eigenvector equation to calculate the derivative of an eigenvalue with respect to a design parameter. After that formulation, by using the mass orthogonality and eigensystem equation the eigenvector sensitivity equation is derived.

Link and Santiago [2] involved an updating method that also covers to detect localized erroneous regions. Proposed method works with measured DOF from modal test of structures and creates error indicator functions. Mass and stiffness matrices are updated by using correction factors and localized erroneous region

properties. Method is applied to satellite structures and mathematical model of the structures are updated with the identification of the erroneous regions.

Lin and Zhu [3] worked on the based excitation on the structures to update the mathematical models. They aimed at getting the accurate dynamic model of the structure by finite element methods and updating. They tried to minimize the objective function by using FRF data of the real structure. Mass and stiffness matrices of the mathematical model assumed to have errors. Since the base displacement and the node fixed to base displacement was known, the mathematical errors was identified by modifying the structural eigensystem equations.

Kwon and Lin [4] introduced a new method to select frequency point for updating procedure. The measured FRF values were assumed to be reference basis for updating. The sensitivity matrix was used in the analysis. Frequency response matrix sensitivity was calculated with respect to the related parameter. The frequency points were compared according to their sensitivity values. The frequency points with high sensitivity values were selected for the updating procedure. To compare the eigenvectors, MAC (Modal Assurance Criterion) was used.

Schwarz, Richardson and Formenti [5] worked about a method that includes the structural modification and the parameter selection for the updating algorithm. In that method, the use of orthogonality was proposed by eliminating the updating of damping terms. Another aspect of the work was to use the modal domain transformation which means the number of DOFs is decreased. The mass and stiffness matrices were modified by changing the selected parameters like point translational masses, beam cross sectional areas, etc. After formulation of the cost function that includes the difference between the eigenvectors and eigenvalues of the experimental and mathematical models, the upper and lower limits of the

parameters were chosen. At last stage, the most physically reliable parameter set was chosen to reflect the experimental results.

Wu and Simin [6] proposed an updating method that used the substructures and subsets. The method was developed to identify the erroneous regions and to select the parameter subsets. Subset selection method was demonstrated to find the design parameters which have dominant influence on the real dynamic characteristics of the structure. SEREP (System Equivalent Reduction Process) method was used to expand the experimental mode shapes and the sensitivity values of the eigenvalues, eigenvectors were calculated from the theory given by Fox and Kapoor [1].

Carvalho, Datta, Gupta and Lagadapati [7] proposed a direct method for updating. Incomplete data from the modal test was the main reference data for the method. In the method, only the stiffness matrix was updated to decrease the difference between the experimental and mathematical values. The mathematical eigenvalue and eigenvector was partitioned into 2 parts according to the updating requirement. QR decomposition and SVD (Singular Value Decomposition) was used to solve the numerical problems.

Ren and Chen [8] proposed response surface method for updating procedure. The method consisted of 3 steps:

- Formulation of the objective function
- Selection of the design parameters
- Application of the developed algorithm

The comparison of the sensitivity based method and response surface method was done. The ability to construct the surrogate model of the mathematical model with RSM (Response Surface Method) was pointed out as the most important advantage over sensitivity based methods. Root Mean Square Error (RMSE) term was used to quantify the error between the mathematical and experimental

eigenvalues. Comparison of the number of the iterations up to convergence criteria was made between RSM and sensitivity based method.

Göge [9] proposed a method by using inverse eigensensitivity technique to modify the mathematical parameters. The method included the least square optimization and 1st order linearization. In the each iteration, sensitivity matrix and mathematical system matrices were needed to be updated. Half aero plane model was selected for the updating algorithm. In the 1st stage, the initial correlation was made through sensitivity analysis. The most effective parameter sets on the dynamic properties of the structures were selected and the use of separate values for the weightings was pointed out. As a consequence, it was pointed out that the method has been used effectively with large FE models by substructuring the whole mathematical model. The inverse eigensensitivity method was iteratively worked with the aero plane model to modify the selected design parameter sets.

Göge and Link [10] worked on a comparative study each includes the sensitivity approach. The 1st method was based on the eigenvalue and eigenvector difference values. 2nd method was based on the eigenvalue and frequency response function difference. The advantages and disadvantages of the methods were compared according to different aspects. It was pointed out that validated mathematical model, some requirements needed to be satisfied:

- Representation the test data in frequency range of interest
- Estimation of the frequency response function and eigendata apart from the frequency range of interest
- Estimation of the test data of adjusted structure

The methods were applied to GARTEUR SM-AG19 test bed aircraft design and the solutions were compared. The ability to update the viscous damping data was stated for the 2nd method which includes the FRF (Frequency Response Function)

residuals. For the data range that was measured from test data, the both models were able to represent the test data with high accuracy. But if the aim was to estimate the test data outside the frequency range of interest, the method, in which eigenvalue and eigenvector residues were used, could represent more physically the test data.

Schedlinski [11] worked on the method that includes the eigenvalue and eigenvector residues in the updating algorithm. It was pointed out that the test planning has a crucial role in estimating the dynamic properties of the structure and updating. The important key points of the test must consist of:

- The identification of the modes that can be extracted from the modal test. Rotational degrees of freedom cannot be measured by modal test.
- The choice of the accelerometer locations must be made by great care. Because the location must not be nodal point and have the property to reflect the target mode shape.
- The position of the exciter must be chosen to distribute the energy to whole structure and to effectively excite the modes in interest.
- The resolution must be chosen to clarify the FRF of the selected frequency range.

After the modification of the design parameters, the damping ratios were changed to decrease the difference in the resonance and anti-resonance regions. Automobile body finite element was updated by checking the linearity of the structure up to 100 Hz. It was also emphasized that the roving hammer method with stable accelerometer location was used to overcome the mass effect.

Writing the literature reviews about model updating, the selection of which model updating technique is applicable to the large order finite element models turns out to be indirect methods. Because, recent mathematical models can have so many degrees of freedom and it is hard to cope with procedure of inverting the mass and

stiffness matrices of the whole system which takes so much time and brings error to the procedure. Sipple and Sanayei [13] introduced a finite element model updating method which using frequency response function to perform parameter estimation and damage detection of benchmark model. Updating procedure is used to detect the magnitude and location of damage in the structure. UCF grid structure is treated as an application model. Sensitivity and grouping studies are carried out to increase the effectiveness of updating time. Firstly, initial finite element model is updated by the help of FRF based method. Extracting new set of measured FRFs to represent the damaged structure, damage locations, magnitude combinations are obtained for the structure. It is concluded that newly proposed method can able to predict the location, magnitude of the damage in the structure by using updating method based on frequency response functions and it is also applicable to actual structures as bridges.

Gou, Zhang, Lu, Wang [14] proposed a modified response surface method to update the finite element models. Procedure is applied to simple beam and brake disc model as real life application. Improving the response surface method by implementation of successive selection method (SSM), it is concluded that modified method faster and more effective than traditional response surface method. As another conclusion, it is pointed out that the response surface can be constructed more accurately with the method.

2.2 MODEL UPDATE THEORY

The theory behind model update and the techniques used with model update are given in this section. The model update theory is classified with respect to the solution method as direct and iterative methods. As a brief summary, direct methods use structural matrices however iterative methods use the modal or response function results in an iterative manner [16].

The initial mathematical matrices must be obtained before the updating algorithm is applied. The mathematical structural matrices $[M_A]_{NxN}$ and $[K_A]_{NxN}$, the modal matrices of the mathematical model $[w_A]_{NxN}$ and $[\varphi_A]_{NxN}$, the response matrix as frequency response function(FRF) $[H_A(w)]_{NxN}$ are the source matrices for the updating algorithm [16].

The size of the experimental results such as FRF and modal matrices are smaller than the mathematical model. To increase the correlation and effectiveness of the model updating algorithm, the maximum number of degrees of freedom must be measured in modal test. Because the reference data is assumed as the modal test result [15].

The general problem with real case situations is to have much more degrees of freedom in mathematical model than experimental results. That causes to the under determined problem which means there are more unknowns than number of equations. To solve that problem, there are some mathematical techniques such as Singular Value Decomposition (SVD) [16].

There is an option to find the regions which are sources for the high discrepancy between the results and it is possible to decrease the amount of the parameters to be updated. In that situation, the mathematical model will be over determined which can be solved more easily [16]. The initial effort must be accomplished on the mathematical model before the model updating. The modes that are in concern

must be correlated and the eigenvalues must be close enough to be updated [16]. If there is a substantial difference between mathematical and experimental results, the algorithm will have a divergent behavior [16].

There are several methods to obtain the quantification of the correlation between the mathematical and experimental model.

Comparison techniques cover the quantification of the difference between the results of models. Results can include modal or frequency based values such as natural frequency, mode shapes, FRF. Modal results can be compared individually and the frequency range can be selected. These advantages make modal property comparison much useful and applicable with respect to the frequency based results like frequency response functions. Extraction of modal characteristics needs some steps to be covered. Modal synthesis that includes the curve fitting procedure is needed to extract the modal properties from the experimental model [15].

The natural frequencies of the selected modes are compared between the mathematical and experimental models. It is more convenient to plot a 2D graph with a reference line with 45° from the x axis [15]. Then the mathematical and experimental eigenfrequencies are plotted respectively on the x and y axis. The frequencies that are needed to be compared must be selected after mode shape correlation [15]. Because, there is a possibility to take into account an irrelevant mode which can be a mathematical mode. Mathematical mode is defined as the mode that can be found from mathematical formulation but there is no possibility to have a mode shape in reality [15]. That case is often experienced in finite element model solutions [15].

After applying the correlation for the mode pairs, both eigenfrequencies must lie close to a straight line which has a slope value of 1 [15].

Due to the visual difficulties to differentiate the mode shapes between mathematical and experimental model, the numerical technique was developed to overcome this issue. Model Assurance Criterion (MAC) quantifies the comparison between two mode shapes [15]. By assuming the mathematical mode shape vector is $\{\varphi_A\}$ and the experimental mode shape vector is $\{\varphi_X\}$, then the following formula is derived [15],

$$MAC(A, X) = \frac{|\{\varphi_X\}^T \{\varphi_A\}|^2}{(\{\varphi_X\}^T \{\varphi_X\})(\{\varphi_A\}^T \{\varphi_A\})} \quad (2.1)$$

No matter how much the mode shape data is complex, MAC number will be a scalar quantity [15]. If two modes are correlated perfectly, the MAC number will be 1. The deviation from that value means that the mode correlation deteriorates [15].

In real case problems, the MAC number close to 1 means the modes are correlated well between mathematical and experimental model. Whereas the MAC number close 0 means that the mode shapes belong to different modes. In general, the MAC number value of 0.9 and more defines the well correlated modes and MAC number of 0.1 and less defines the uncorrelated modes [15].

Another mode comparison technique is COMAC where for an individual DOF, i , it can be written as [15]:

$$COMAC(i) = \frac{\sum_{l=1}^L |(\varphi_X)_{il} (\varphi_A)_{il}|^2}{\sum_{l=1}^L (\varphi_X)_{il}^2 \cdot \sum_{l=1}^L (\varphi_A)_{il}^2} \quad (2.2)$$

In equation (2.2), l represents the correlated mode pair and L is the total number of correlated mode pairs, i is the mode in concern. Mathematical mode shape

vector is $\{\varphi_A\}$ and the experimental mode shape vector is $\{\varphi_x\}$ [15]. The regions which have low values of COMAC can indicate the areas which have more effect on the discrepancies between the models [15]. The value of 1 for COMAC indicates good correlation for that coordinate; whereas the value of 0 indicates bad correlation for that coordinate [15].

2.2.1. Direct Matrix Methods

In direct matrix methods, structural matrix elements are changed with respect to the mathematical and experimental results [15]. Some advantages related to this group of methods can be listed as [15]:

- Direct matrix methods have non-iterative procedure which provides less solution time.
- Divergence is not a problem with direct matrix methods.
- Resulting mathematical matrices represents the experimental results accurately.

The capability of this kind of methods is to represent the experimental data accurately [15]. For that reason, measurement noise has much more importance than other methods [16]. The representative model comprises the noise coming from different sources which leads to wrong solutions. The measurement noise and other sources of discrepancies must be identified and eliminated from the experimental results before updating procedure [16].

The mathematical procedure needs the mass, stiffness matrices' sizes to be equal. Modal expansion or model data reduction techniques must be applied to these types of methods [15].

Model reduction is a procedure to degrade the degree of freedom of the mathematical model generally to comparison purposes. It is not easy to compare the mathematical model which has far more degrees of freedom than experimental

model [15]. The most of the techniques that are applied to mathematical model to be updated use reduction of the mathematical models. Recently, due to improvements of computer calculations and the reduction of time for the getting the solution from the finite element analysis, the reduction techniques become less necessary [16].

There are two main kinds of model reduction techniques both implemented to spatial models. The spatial model refers to the structures' physical properties defined by mass, stiffness and damping characteristics. Two main types of reduction techniques are [15]:

- The reduction of the model results in the structure that can represent the whole structure by small degrees of freedom.
- The reduction causes the mathematical model to lose the information about related DOFs that were disregarded.

This reduction procedure serves like representing a large model as a coarser model means the reduced model is an estimation of the larger model [15].

Expansion procedure is used to expand the experimental model for comparison and some model update applications. Modal test must be carried to extract the experimental model results. Before carrying out the modal test, some judgments must be made. These are generally [15]:

- The DOF that is measured must be coincided with the mathematical model.
- The number of measured DOFs must be maximized to closely correlate the experimental and mathematical model.

Due to some problems with the modal tests like: limited test time; unavailability to measure some DOFs like rotational ones, the DOFs measured from the tests are generally by far more less than the mathematical model [15].

Other difficulties are also taken into concern. By measuring the less DOFs from modal test, the construction of the mode shape model becomes too hard. There are several ways to expand the measured modes [15]:

- Geometric interpolation using mathematical approaches.
- Mode expansion by referring to the mathematical model structural matrices.
- Mode expansion by referring to the mathematical model's eigendata (eigenvectors, eigenvalues)

All three methods have the aim to build up a transformation matrix that relates the incomplete vector with the complete vector [15].

The most trustworthy technique is assumed as which uses the finite element model to build up the experimental model. Finite element model is used as high order polynomial fit function to estimate the experimental DOFs that are not measured [16].

Finite element models include much more DOF (Degrees of Freedom) than experimental model. Finite element model must be reduced to correlate with the experimental model of the structures. The response is measured from limited measurement locations for experimental model and the frequency range of interest is restrained by the measurement system in modal test. For that reason, a part of the mode shape vector can be constructed from the modal test. There are 4 methods as model reduction techniques [15]:

- Guyan or Static Reduction.
- Dynamic Reduction.
- Improved Reduced System.
- SEREP (System Equivalent Reduction Expansion Process).

Another way of equating the degrees of freedom of the experimental and mathematical models is to expand the eigenvector data which ends up with prediction of the unmeasured mode shape data [17]. The model reduction and modal expansion techniques have some correspondence.

The low order of the measurement degrees of freedom can cause some problems [17]:

- The visualization of the mode shapes cannot be effectively made.
- The unmeasured degrees of freedom are assumed to have zero displacement which is not the real case.

4 methods are investigated in this part of work [15]:

- Geometric interpolation using spline functions
- Expansion using Theoretical Spatial Model – Kidder’s Method
- Expansion using Mathematical Model Mode Shapes
- SEREP Expansion Technique

The details of the finite element model reduction and expansion methods are given in APPENDIX section.

2.2.2. Iterative (Indirect) Methods

Iterative methods give more physically reliable and meaningful results with respect to direct methods [15]. The degree of correlation is defined with the minimization of an objective function [16]. The objective function can be constructed by including the weights of the eigenvalue and eigenvector differences [16]. Forming the objective function, the method starts to work iteratively to make the difference decrease. Large amount of parameters can be updated at the same time and there is an opportunity to build up an objective function with different weightings to different response values [16]. For example,

generally the eigenfrequency values are generally close to each other between mathematical and experimental data but the eigenvectors may differ so much due to errors in accelerometers or measurement noise [16]. For that reason, initial correlation must be done before updating procedure. The compared mode shapes must belong to the same mode. Visual check is not sufficient for mode shape correlation [15]. An appropriate correlation method like MAC [15], COMAC [15] must be applied to mode shapes of mathematical and experimental mode shape results. The flexibility of application of iterative methods does not make this kind of method be easily and correctly update the mathematical model [15]. The engineering insight gains importance prior to the application of the chosen algorithm. The difference of the responses defined in the objective function is generally nonlinear function of the parameters [16]. Nonlinearity needs an iterative procedure to be solved in this application [16].

In the iterative procedure, the mathematical modal data must be processed in each loop. For example, after updating the required parameters, the updated mathematical must be processed again to extract the eigendata which will be used in the following iteration. The change of the parameters in the iteration loop shows the convergent or divergent behavior of the procedure. If the difference between the parameters is getting closer and closer, the mathematical model will represent the experimental model in more accurate way [15]. The diverging amount of difference of the parameters gives the engineer the idea that there may be a convergence problem [15].

The reference data which is the experimental data can be modal data or response function data. There are some techniques that can be applied to both of the experimental results. Choosing the response types to be correlated, the vector of the measured quantities is constructed. For example, for modal results the vector may consist of the eigenvalues and mode shape vectors.

There are some problems with correlating the mathematical and the corresponding experimental counterpart. The eigenfrequency and the mode shape must be related to the same mode in mathematical and experimental models [15]. For example, considering the close modes with simple beam, the order of the torsional and bending modes can change due to the wrong estimation of the parameters [15]. Mode shapes must be paired correctly prior to the updating procedure. Scaling problem must be also taken into consideration. Mathematical eigenvectors are generally mass normalized and also maximum displacement normalization can be done [15]. The measured mode shape vector is generally mass normalized. Due to the difference between the mathematical and experimental mass scatter, there must be a scale between the mathematical and experimental eigenvectors [15]. Allemang and Brown [18] introduced a modal scale factor (MSF) that must be multiplied with the measured mode shape vector;

$$MSF = \frac{\{\varphi_i\}^T \{\varphi_{mi}\}}{\{\varphi_{mi}\}^T \{\varphi_{mi}\}} \quad (2.3)$$

where $\{\varphi\}$ represents the mode shape vector and m denotes the measured mode, i is the mode in concern.

The iterative methods generally use Taylor series expansion of the modal data [16]. Assuming the linearization and neglecting the 2nd order terms in the expansion, the vector equation can be written as follows [16]:

$$\delta\{z\} = \{S_j\}\delta\{\theta\}, \quad (2.4)$$

where $\delta\{z\} = \{z_m\} - \{z_j\}$ is the difference between the measured output and mathematical results which must be evaluated in each iteration, $\delta\{\theta\} = \{\theta\} - \{\theta_j\}$ is the difference between the initial and the following estimate for the parameters,

$\{S_j\}$ is the sensitivity matrix, and $\{\theta\}$ is the vector that must be updated in each iteration. Assuming the updating procedure is based on the modal results, the sensitivity matrix defines the first order derivatives of eigenfrequencies and mode shapes with respect to the design parameters [16]. Sensitivity matrix must also be evaluated in each iteration which is responsible for taking role the most time consuming part of the updating procedures [16]. The time elapsed to converge the results can be decreased by modifying the sensitivity calculation options.

In direct methods, full system matrices are changed to satisfy the test results [15]. The difference and the advantageous aspect of the indirect methods is the ability to modify the individual elements of the system matrices [16]. Assuming the number of the elements that are needed to be updated is N, the following equations related with mass and stiffness matrices can be written as [15],

$$[\Delta M] = \sum_{j=1}^N p_j [m_j] \quad (2.5)$$

$$[\Delta K] = \sum_{j=1}^N q_j [k_j] \quad (2.6)$$

In equations (2.5) and (2.6), p_j and q_j terms represents the updating parameters; $[m_j]$, $[k_j]$ matrices are mass and stiffness matrix for the j^{th} element, N is the total number of elements; $[\Delta M]$ and $[\Delta K]$ are change in the mass and stiffness matrix [15].

CHAPTER 3

SELECTION OF THE APPROPRIATE METHOD FOR LARGE ORDER FINITE ELEMENT MODELS WITH CASE STUDIES

3.1 CASE STUDIES ON SIX DOF SPRING MASS SYSTEM

The system that is to be analyzed must be well identified and known. For that purpose, the system is selected from literature named as Kabe's system to check the correctness of the updated results. Results were obtained via code generated in Matlab. The spring mass system is used to understand the effectiveness of direct updating techniques and indirect updating techniques. Applying Direct Matrix Method and Error Matrix Method, the MAC plots before and after updating procedure are given as results. Besides the MAC plots, FRF plots before and after the updating procedure are shown as reference results. The mass spring system which is used in the updating procedures is given in Figure 1.

The construction of the code was made via Matlab. Direct Matrix Method and Error Matrix methods were selected as candidates for Direct Model Updating Methods. Inverse Eigensensitivity Method was used as iterative method to see the effectiveness and stability of the method. Response Function Method (RFM) was not applied to mass spring system because the application of the method to real case structures is limited and difficult which uses frequency response functions as a basis objective function. Considering the sensitivity of the frequency response functions with respect to the measurement and environment noise, the RFM method is eliminated from the iterative methods. Due to the requirement of the developed algorithm to be applied to real life aerospace structures, the Inverse Eigensensitivity Method (IEM) was selected as iterative method which is

advantageous over RFM by considering the sensitivity to measurement noise and the ability of the commercial finite element programs like Nastran to calculate eigenvalue, eigenvector sensitivity values.

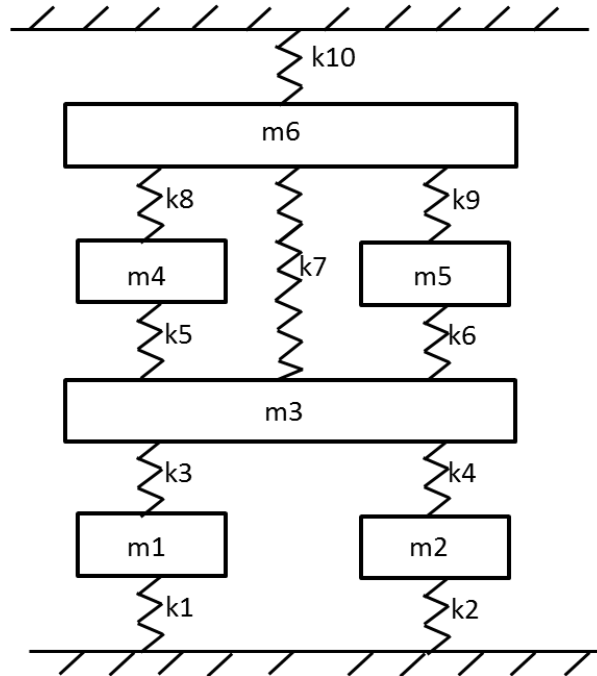


Figure 1. Reference Spring Mass System

The mathematical model mass and stiffness values are chosen arbitrarily to clearly identify the effectiveness of the algorithms developed. The difference between the mathematical values and experimental model values is listed in Table 1.

Table 1. Parameter Values for Experimental Model and Mathematical Model

Parameter	Analytical Model Values	Experimental Model Values	Error Percentage(%)
m1	2 (kg)	1.8 (kg)	11.1
m2	2.5 (kg)	2.4 (kg)	4.2
m3	1.1 (kg)	1.6 (kg)	31.3
m4	1.2 (kg)	1.2 (kg)	0.0
m5	1.5 (kg)	1.1 (kg)	36.4
m6	1 (kg)	0.9 (kg)	11.1
k1	1100 (N/m)	1500 (N/m)	26.7
k2	1000 (N/m)	1600 (N/m)	37.5
k3	1250 (N/m)	1400 (N/m)	10.7
k4	5000 (N/m)	6500 (N/m)	23.1
k5	1400 (N/m)	1300 (N/m)	7.7
k6	1100 (N/m)	1500 (N/m)	26.7
k7	2000 (N/m)	1300 (N/m)	53.8
k8	1000 (N/m)	400 (N/m)	150.0
k9	3000 (N/m)	2200 (N/m)	36.4
k10	3000 (N/m)	3800 (N/m)	21.1

3.1.1. Results for Update by Direct Matrix Method

In this method, the stiffness and mass matrices are updated in a consecutive manner. Before application of the algorithm, the size of the matrices must be same. Basically, it is applied to undamped system and modifies the mass matrix of the structure. After modification of the mass matrix, the stiffness matrix is updated to satisfy the experimental results. The drawback of the method is that it needs the mode shape vector for the mathematical and experimental model for all degrees of freedom. To satisfy this requirement, appropriate expansion technique must be applied to experimental mode shape data.

As previously explained, the modified mass matrix is given as follows [16],

$$[\Delta M] = [M_A][\varphi_X][m_A]^{-1}(I - [m_A])[m_A]^{-1}[\varphi_X]^T[M_A] \quad (3.1)$$

In equation (3.1), the $[m_A]$ term equals to,

$$[m_A]_{m \times m} = [\varphi_X]_{m \times N}^T [M_A]_{N \times N} [\varphi_X]_{N \times m} \quad (3.2)$$

In equation (3.2), [M] and [K] are mass and stiffness matrices, subscript ‘A’ indicates mathematical, whereas subscript ‘X’ indicates the experimental data, φ is mode shape vector and [I] is the identity matrix. In equation (3.2), m refers to the number of modes identified from the modal test and N is total number of degrees of freedom. After finding the $[\Delta M]$ value and putting it into the updated stiffness matrix, the following equation is derived:

$$\begin{aligned} [\Delta K] = & [M_A][\varphi_X][\varphi_X]^T [K_A][\varphi_X][\varphi_X]^T [M_A] \\ & + [M_A][\varphi_X][w_X^2][\varphi_X]^T [M_A] - [K_A][\varphi_X][\varphi_X]^T [M_A] \\ & - [M_A][\varphi_X][\varphi_X]^T [K_A] \end{aligned} \quad (3.3)$$

The solution derived for updated mass and stiffness matrices is not a single solution. There are several possible matrices to satisfy the given equations. The modified mass and stiffness matrices are only numerical solutions not the meaningful ones in physical aspect.

As the first case, it is assumed that all degree of freedoms are measured. This case is formed to figure out the importance the number of measured degrees of freedom. The MAC plot is constructed to clearly analyze the mode shape of the system. In the 2nd case, it is assumed that there is no measurement from 6th degree of freedom. In the 3rd case, it is assumed that there is no measurement from 5th and 6th degree of freedom. The cases were tabulated as below in Table 2. The results are arranged due to given name for the cases.

Table 2. The Case Definitions for Direct Matrix Updating Method

Case Numbers	Assumptions Done for the Cases
Case 1	All DOFs are measured
Case 2	Only 6 th DOF is not measured
Case 3	5 th and 6 th DOFs are not measured

The method given in the Appendix which is called Kidder's Method or Inverse Guyan Reduction is used to equate the matrix sizes for using in the subsequent mathematical formulations. The incomplete elements of the measured eigenvectors are estimated by the help of Kidder's Method.

MAC plots before and after updating procedure were given to analyze the mode shapes. The maximum number in MAC plot is 1 which means there is a % 100 correlation between the mathematical and experimental model and 0 means no correlation between mathematical and experimental model. In addition to the MAC plots, the MAC numbers were given to see the accurate number on the diagonal of the MAC matrix. The MAC plots with numbers, FRF plots for selected degree of freedom for Case1, Case2 and Case 3 were given respectively in Figures 2 through 16. The diagonal terms must be above 0.8 [16] for the correlated modes which are given in Tables 3 through 8. The MAC numbers that were plotted in Figure 2 are listed in Table 3.

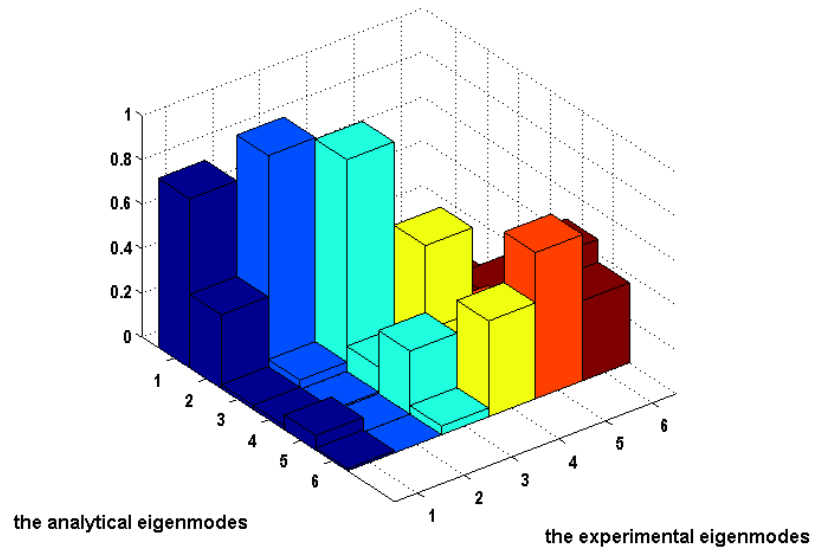


Figure 2. MAC Plot before Updating for Case 1

Table 3. The MAC Numbers before Updating for Case-1 that Belong to Figure 2

CASE 1- MAC NUMBERS	Experimental Model					
Mathematical Model	0.76	0	0	0	0	0.02
	0.33	0.97	0.03	0.02	0.05	0
	0.02	0.05	0.96	0.02	0	0.11
	0.02	0.01	0.12	0.59	0.15	0.07
	0.07	0	0.28	0.2	0.1	0.46
	0.01	0	0.04	0.43	0.66	0.36

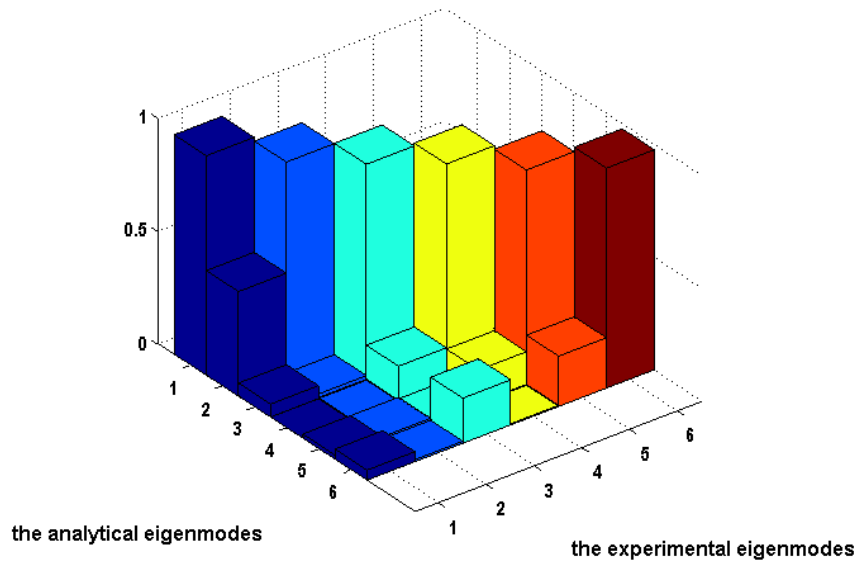


Figure 3. MAC Plot after Updating for Case 1

Table 4. The MAC Numbers before Updating for Case-1 that Belong to

Figure 3

CASE 1- MAC NUMBERS	Experimental Model					
	Mathematical Model	0.97	0.41	0.04	0	0.01
0.46		0.95	0.02	0	0.01	0.01
0.06		0.02	0.95	0.14	0.01	0.23
0		0	0.15	0.97	0.16	0.01
0.02		0.02	0.01	0.15	0.95	0.27
0.04		0.01	0.2	0.01	0.22	0.97

Plotting MAC plots for Case 1, the FRF results are plotted for 6th degree of freedom (Figure 6). First of all, the experimental and mathematical FRF results are plotted in Figure 4. Afterwards, updated FRF result was added to the plot in Figure 5.

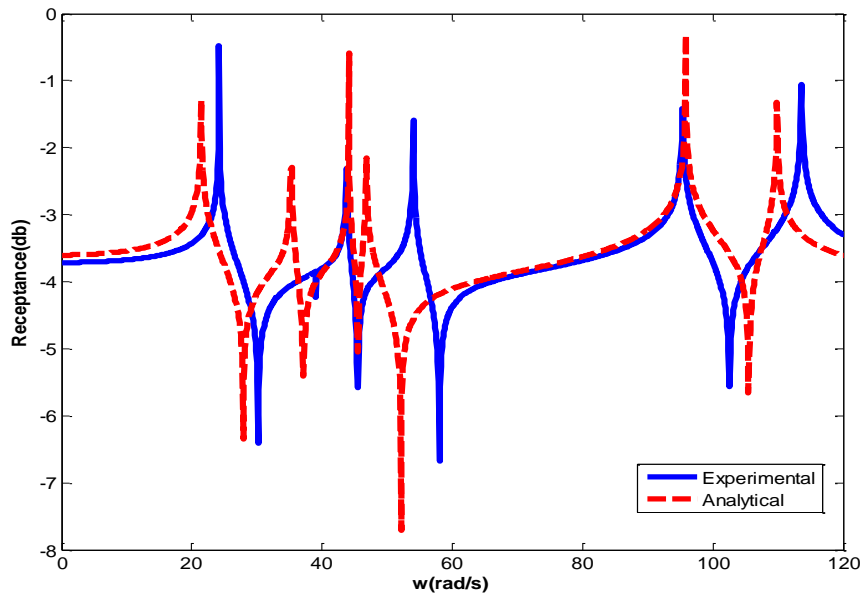


Figure 4. The Semi Log Point FRF Plot of the 6th DOF for Experimental and Mathematical Model for Case 1

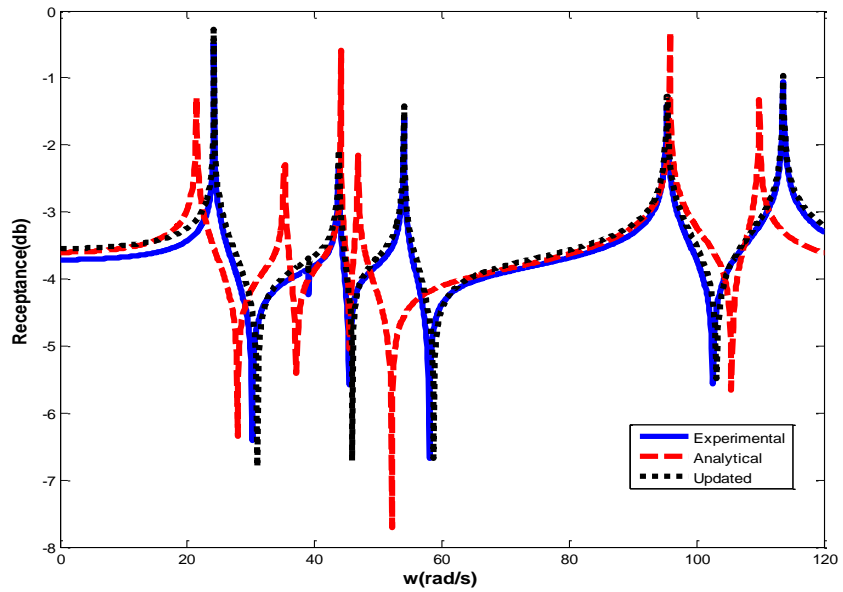


Figure 5. The Semi Log Point FRF Plot of the 6th DOF for Experimental, Mathematical and Updated Model for Case 1

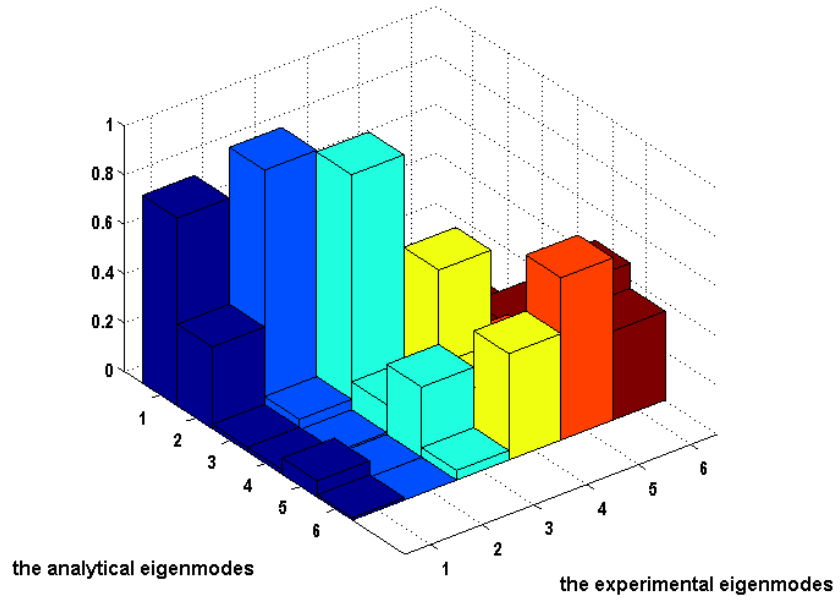


Figure 6. MAC Plot before Updating for Case 2

The MAC numbers that were plotted in Figure 6 are listed in Table 5.

Table 5. The MAC Numbers before Updating for Case-2 that Belong to Figure 6

CASE 2- MAC NUMBERS	Experimental Model					
Mathematical Model	0.76	0	0	0	0	0.02
	0.33	0.97	0.03	0.02	0.05	0
	0.02	0.05	0.96	0.02	0	0.11
	0.02	0.01	0.12	0.59	0.15	0.07
	0.07	0	0.28	0.2	0.1	0.46
	0.01	0	0.04	0.43	0.66	0.36

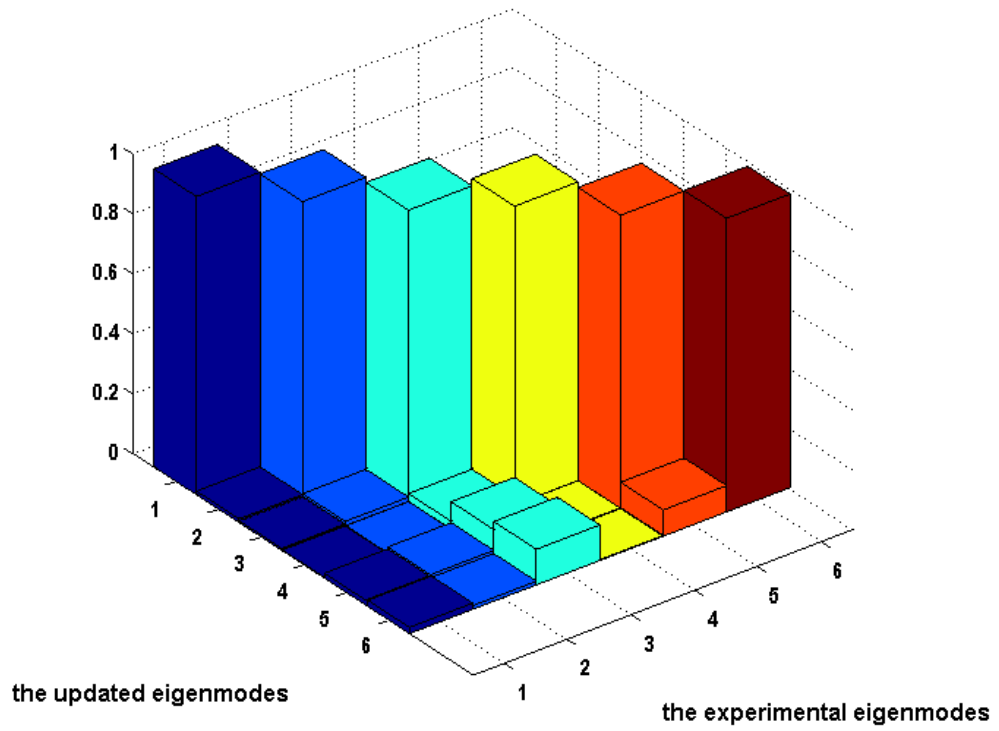


Figure 7. MAC Plot after Updating for Case 2

Table 6. The MAC Numbers after Updating for Case-2 that Belong to Figure 7

CASE 2- MAC NUMBERS	Experimental Model					
	1	2	3	4	5	6
Mathematical Model	1	0.01	0.01	0	0.02	0.02
	0.01	0.99	0.02	0	0.03	0.01
	0.01	0.02	0.97	0.03	0.1	0.1
	0	0	0.03	1	0	0
	0.02	0.02	0.09	0	0.98	0.07
	0.02	0.01	0.12	0	0.09	0.98

Giving MAC plots for Case 2, the FRF results are plotted for 5th degree of freedom. First of all, the experimental and mathematical FRF results are plotted in

Figure 8. Afterwards, updated FRF result is added to the plot in Figure 9 and Figure 10.

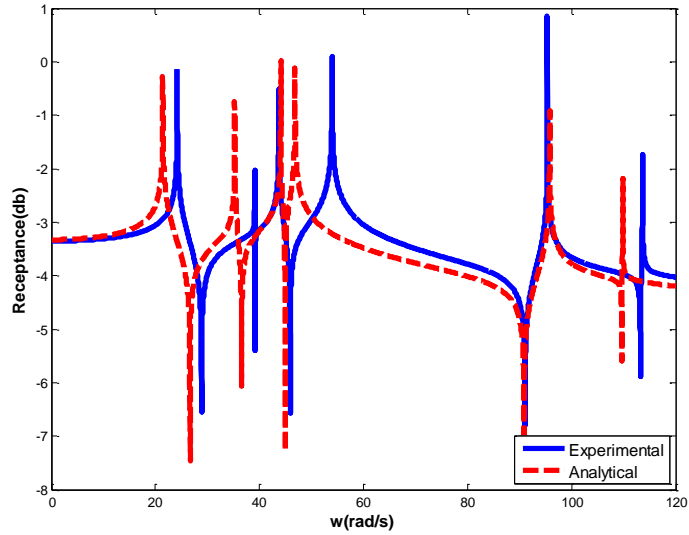


Figure 8. The Semi Log Point FRF Plot of the 5th DOF for Experimental and Mathematical Model for Case 2

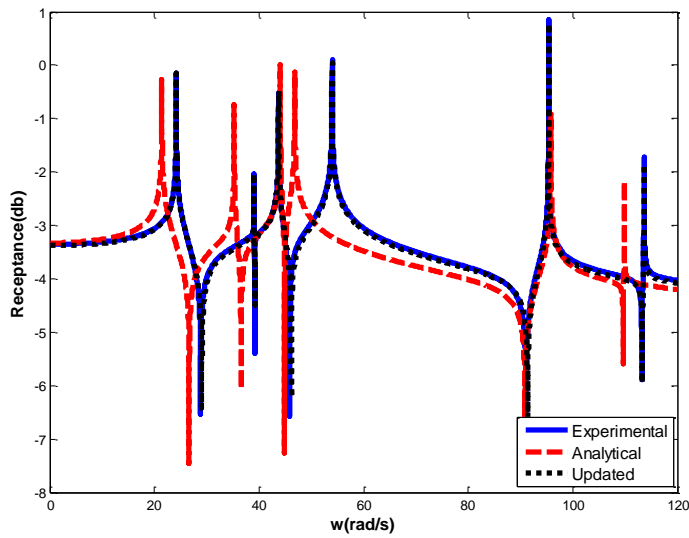


Figure 9. The Semi Log Point FRF Plot of the 5th DOF for Experimental, Mathematical and Updated Model for Case 2

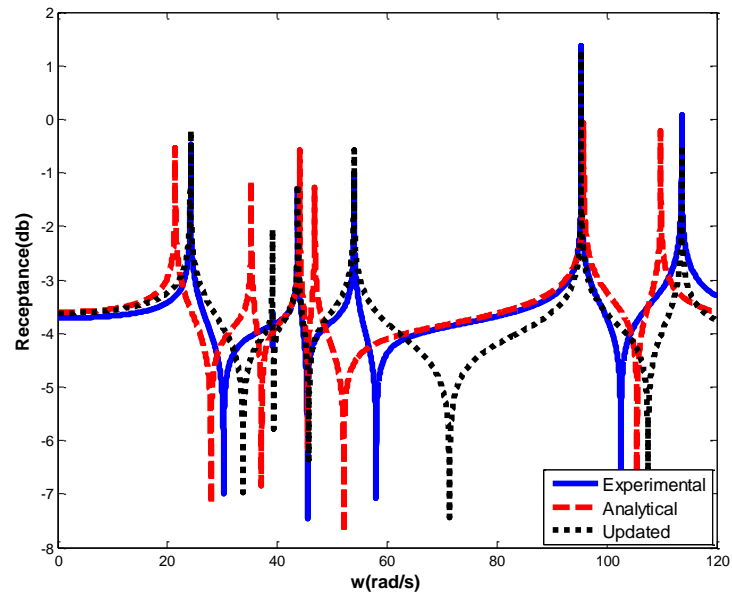


Figure 10. The Semi Log Point FRF Plot of the 6th DOF for Experimental, Mathematical and Updated Model for Case 2

As seen clearly in Figure 10, the updated FRF graph for 6th degree of freedom is different from the experimental results. The reason for that difference is not to take measurement data from 6th degree of freedom.

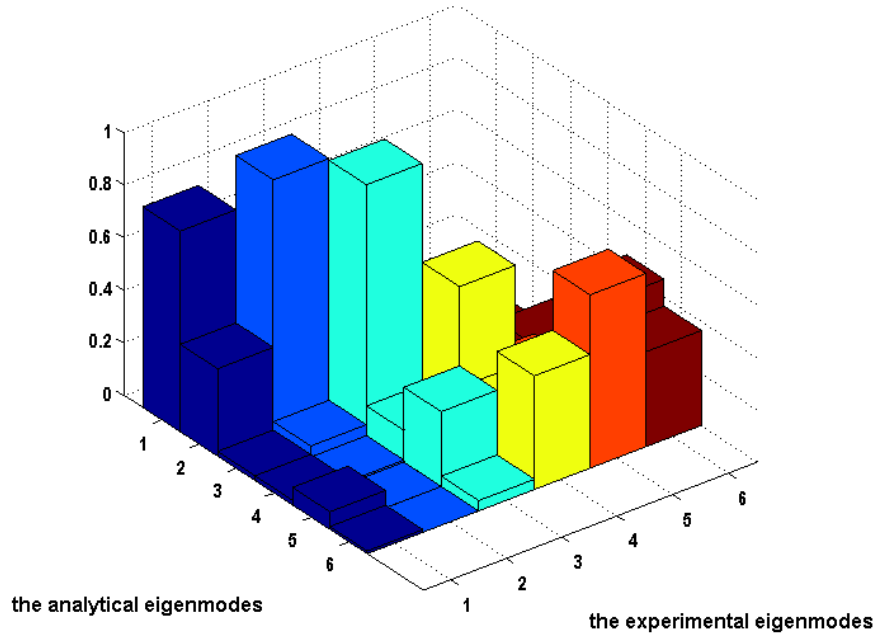


Figure 11. MAC Plot before Updating for Case 3

Table 7. The MAC Numbers before Updating for Case-3 that Belong to Figure 11

CASE 3- MAC NUMBERS	Experimental Model					
	Mathematical Model	0.76	0	0	0	0
0.33		0.97	0.03	0.02	0.05	0
0.02		0.05	0.96	0.02	0	0.11
0.02		0.01	0.12	0.59	0.15	0.07
0.07		0	0.28	0.2	0.1	0.46
0.01		0	0.04	0.43	0.66	0.36

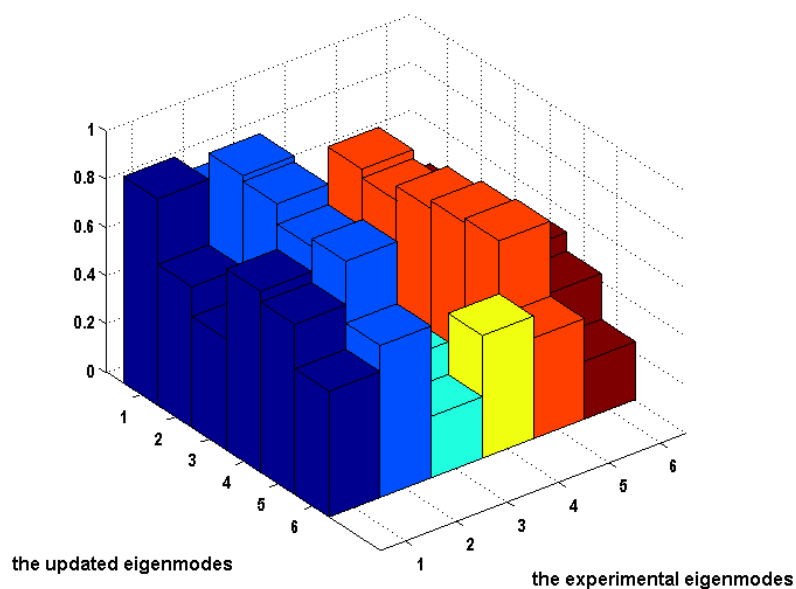


Figure 12. MAC Plot after Updating for Case 3

Table 8. The MAC Numbers after Updating for Case-3 that Belong to Figure 12

CASE 3- MAC NUMBERS	Experimental Model					
	Mathematical Model	0.86	0.78	0.25	0.06	0.65
0.58		0.96	0.38	0.05	0.62	0.36
0.46		0.94	0.58	0.05	0.68	0.31
0.75		0.85	0.3	0.05	0.71	0.51
0.71		0.89	0.39	0.05	0.73	0.43
0.52		0.63	0.25	0.51	0.42	0.24

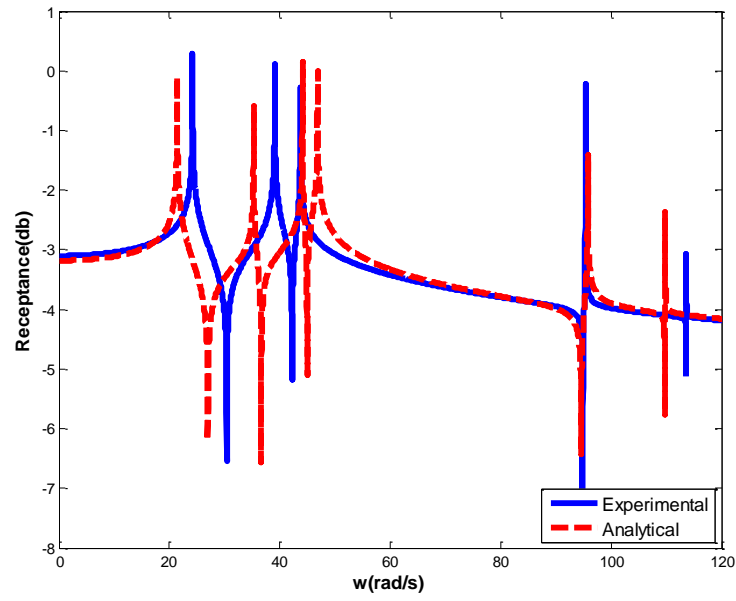


Figure 13. The Semi Log Point FRF Plot of the 4th DOF for Experimental and Mathematical Model for Case 3

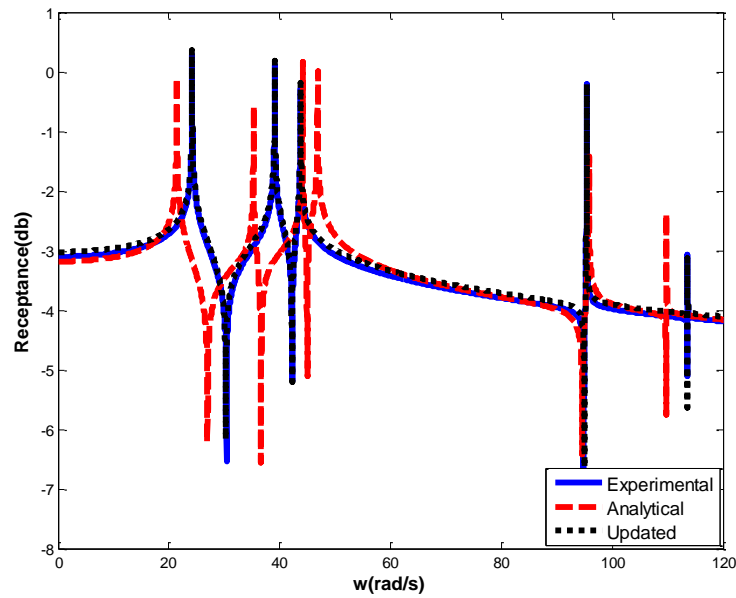


Figure 14. The Semi Log Point FRF Plot of the 4th DOF for Experimental, Mathematical and Updated Model for Case 3

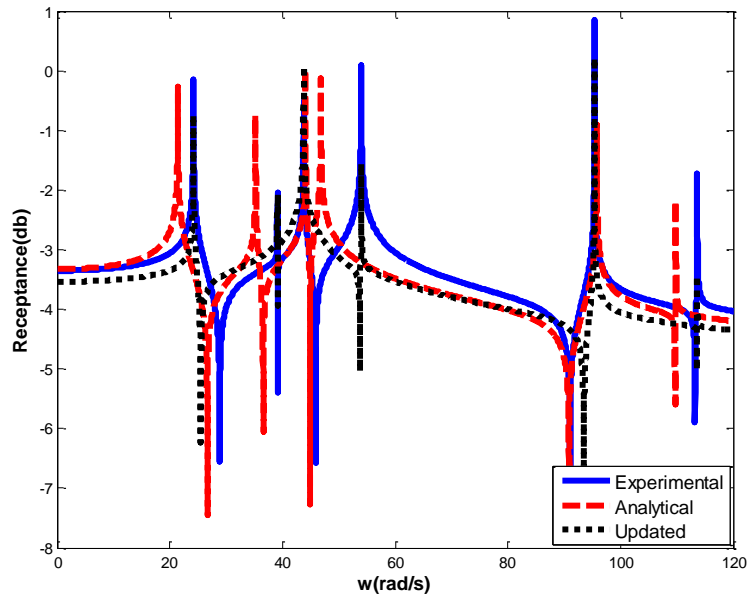


Figure 15. The Semi Log Point FRF Plot of the 5th DOF for Experimental, Mathematical and Updated Model for Case 3

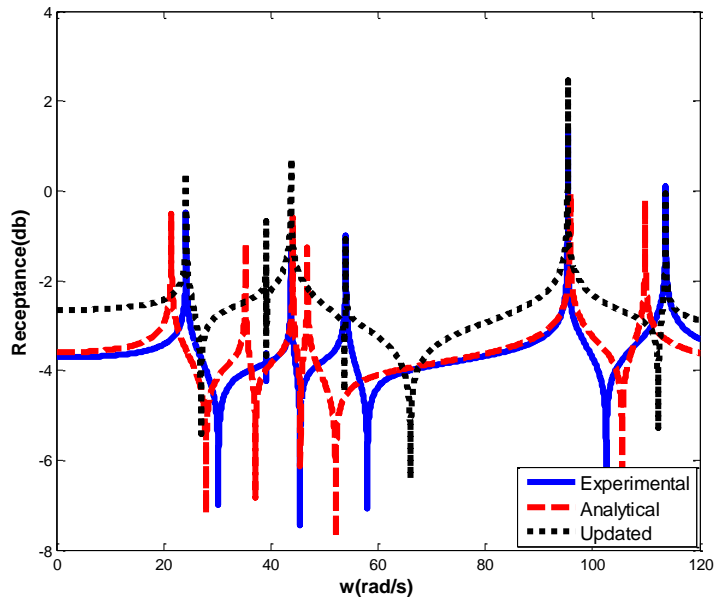


Figure 16. The Semi Log Point FRF Plot of the 6th DOF for Experimental, Mathematical and Updated Model for Case 3

As seen clearly in Figure 15 and Figure 16, the updated FRF graphs for 5th and 6th degrees of freedom are different from the experimental results. The reason for that difference is not to take measurement data from 5th and 6th degrees of freedom.

Direct Matrix Updating Method has the capability to update the model when all degrees of freedom can be measured [15]. However, this option is impossible in real life applications. The other disadvantage of the method, the full system matrices of the mathematical model must be extracted to be used in the iterative formulations [15]. To be able to extract the system matrices of large finite element models is a long procedure and taking the inverse of large sized matrices increase the error and solution time [16].

The results of experimental and mathematical models are the same when all degrees of freedom are measured. But as seen from Figure 10, Figure 15, Figure 16, FRF plots for measured degrees of freedom were different from experimental results. There is a big deviation between the updated and experimental results except for the region of resonance frequencies. Using the expansion process to estimate the eigenvector of unmeasured degrees of freedom the error percentage of the algorithm increases. MAC numbers are lower than 0.8 in Case 3 for 3rd, 4th, 5th and 6th degrees of freedom. As a consequence, Direct Matrix Method is applicable only to simple models if great deal of degrees of freedom are measured which is nearly impossible in real life finite element models.

3.1.2. Results for Update by Error Matrix Method

The Error Matrix Method is used as 2nd Direct Method to update the mass spring system. The aim of this method is to modify the elements of the mass and stiffness matrices [15]. Referring 'X' to experimental and 'A' to mathematical model, the error matrices are defined as following [15]:

$$[\Delta M] = [M_x] - [M_A] \quad (3.4)$$

$$[\Delta K] = [K_x] - [K_A] \quad (3.5)$$

,where $[M]$ and $[K]$ are mass and stiffness matrices, X denotes to experimental and A denotes to mathematical matrices. The problem of the above equations, (3.4) and (3.5) is to find the structural matrices of the experimental model. Considering the transformation from modal properties to spatial properties, the mass and stiffness matrices for experimental model can be constructed as [15]:

$$[M] = [\varphi]^{-T} [\varphi]^{-1} \quad (3.6)$$

$$[K] = [\varphi]^{-T} [w_r^2] [\varphi]^{-1} \quad (3.7)$$

where φ is mode shape vector, w_r is the natural frequency of r^{th} mode shape, K is stiffness matrix and M is mass matrix.

To able to find the mass and stiffness matrices for experimental model for all degrees of freedom, the mode shapes and eigenfrequencies must be extracted for all degrees of freedom which is nearly impossible in real applications. The method makes a prediction for the updated mass and stiffness matrices by distributing the effect of the known modes to the unknown degrees of freedom [15]. Experimental stiffness matrix can be written as [15],

$$[K_x]^{-1} = ([I] + [K_A][\Delta K])^{-1} [K_A]^{-1} \quad (3.8)$$

where $[I]$ is the identity matrix. Using Binomial Theorem and writing the above equation by neglecting the second and higher order terms, the following equation can be derived as [15];

$$[K_x]^{-1} \approx [K_A]^{-1} - [K_A]^{-1} [\Delta K] [K_A]^{-1} + ([K_A]^{-1} [\Delta K])^2 [K_A]^{-1} + \dots \quad (3.9)$$

Rewriting the equation (3.9), $[\Delta K]$ is defined as [15]:

$$[\Delta K] \approx [K_A] \left([K_A]^{-1} - [K_X]^{-1} \right) [K_A] \quad (3.10)$$

$$[\Delta K] \approx [K_A] \left([\varphi_A] [w_{Ar}^2]^{-1} [\varphi_A]^T - [\varphi_X] [w_{Xr}^2]^{-1} [\varphi_X]^T \right) [K_A] \quad (3.11)$$

Writing the equation for stiffness matrix, the same procedure can be applied to mass matrix. Using equation (3.6) and the estimation which is given for the stiffness matrix, $[\Delta M]$ can be written as [15]:

$$[\Delta M] = [M_A] \left([\varphi_A] [\varphi_A]^T - [\varphi_X] [\varphi_X]^T \right) [M_A] \quad (3.12)$$

The assumption is made that all degrees of freedom are measured. As clearly explained in this section, the Error Matrix method is based on the linearization and neglecting the higher order terms [15]. For that reason, it is impossible to estimate the experimental results accurately even if all degrees of freedom were measured. Applying the developed algorithm by Matlab, the MAC plots and FRF graphs for 6th degree of freedom is given as results. The MAC numbers before updating that are plotted in Figure 17 are listed in Table 9. The MAC numbers after updating that are plotted in Figure 18 are listed in Table 10. First of all, the experimental and mathematical FRF results are plotted in Figure 19. Afterwards, updated FRF result is added to the plot in Figure 20.

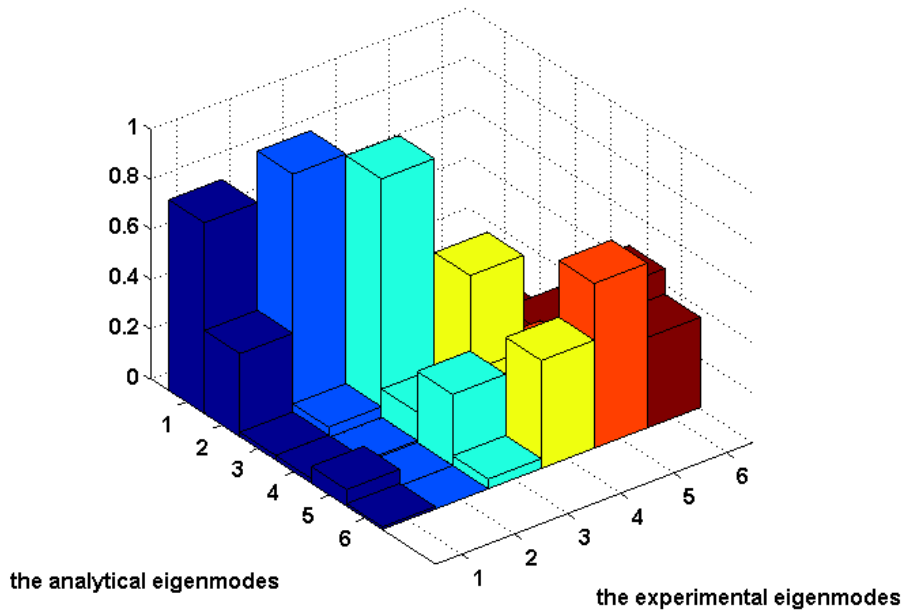


Figure 17. MAC Plot before Updating

Table 9. The MAC Numbers before Updating that Belong to Figure 17

MAC NUMBERS	Experimental Model					
	Mathematical Model	0.76	0	0	0	0
0.33		0.97	0.03	0.02	0.05	0
0.02		0.05	0.96	0.02	0	0.11
0.02		0.01	0.12	0.59	0.15	0.07
0.07		0	0.28	0.2	0.1	0.46
0.01		0	0.04	0.43	0.66	0.36

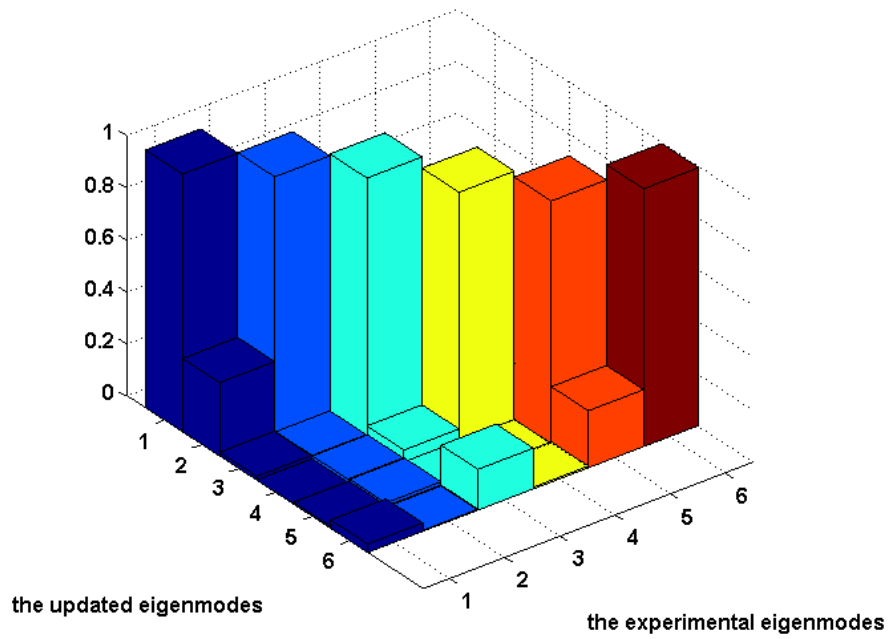


Figure 18. MAC Plot after Updating

Table 10. The MAC Numbers before Updating that Belong to Figure 18

MAC NUMBERS	Experimental Model					
Mathematical Model	0.99	0.19	0.01	0	0	0.02
	0.28	0.99	0.01	0	0	0.03
	0.01	0.01	1	0.1	0.02	0.12
	0	0.01	0.05	0.95	0.21	0.02
	0.01	0.02	0	0	0.93	0.12
	0.03	0	0.16	0.01	0.22	0.99

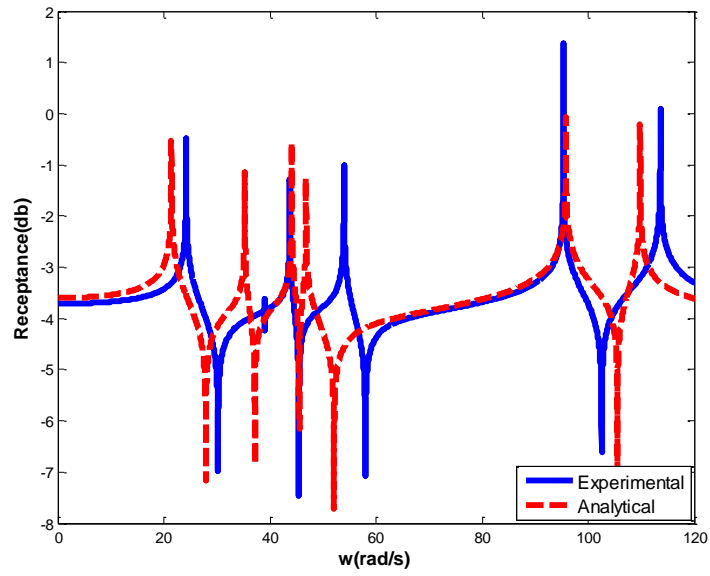


Figure 19. The Semi Log Point FRF Plot of the 6th DOF for Experimental and Mathematical Model

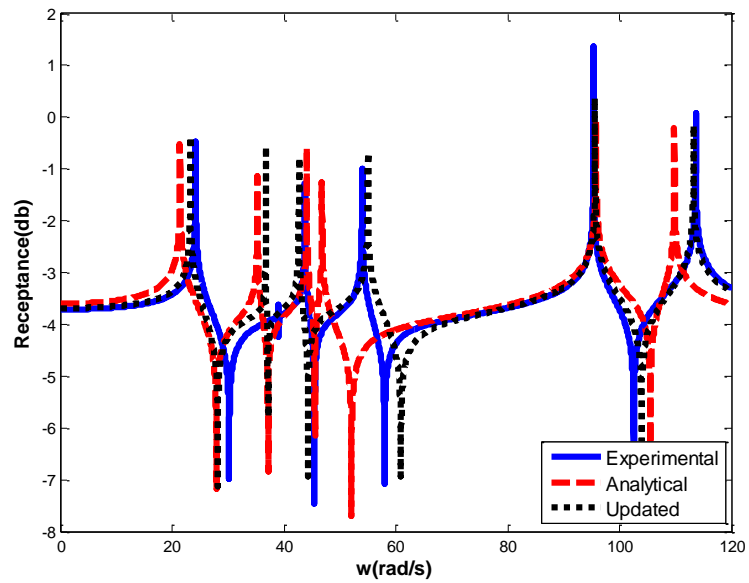


Figure 20. The Semi Log Point FRF Plot of the 6th DOF for Experimental, Mathematical and Updated Model

Even if all the degrees of freedom are measured, there is a deviation between results. For that reason, other cases for the unmeasured degrees of freedom are skipped. As previously mentioned, the deviation between the experimental and mathematical results arises from the linearization of the theory of Error Matrix Method [15].

3.1.3. Results for Update by Inverse Eigensensitivity Method (IEM)

Spring mass system is also updated with IEM. IEM is sensitivity based iterative method. Model updating methods related to sensitivity calculation use basically Taylor Series Expansion of modal results [16]. Experimental modal results can be formulized by using mathematical eigenvectors and eigenvalues [15]. The experimental modal results can be written as a Taylor expansion in terms of model updating parameters about mathematical solution as given in Eqs. (3.13) and (3.14) [16] as follows;

$$\lambda_r^X = \lambda_r^A + \sum_{s=1}^L \frac{\partial \lambda_r^A}{\partial p_s} \Delta p_s + 0(\Delta p_s^2) + \dots, \quad (3.13)$$

$$\{\phi_X\}_r = \{\phi_A\}_r + \sum_{s=1}^L \frac{\partial \{\phi_A\}_r}{\partial p_s} \Delta p_s + 0(\Delta p_s^2) + \dots, \quad (3.14)$$

where subscript X indicates experimental result, subscript r indicates the r^{th} mode, p_s is the s^{th} design parameter, Δp_s is defined as the change in the s^{th} design parameter and L is the total number of design parameters, λ_r and $\{\phi\}_r$ show the eigenvalue and mode shape to the r^{th} mode, respectively. Sensitivity matrix involves first order derivatives of the modal results with respect to model updating parameters. Disregarding the effect of second and higher order terms, Eqs. (3.13) and (3.14) can be written in an iterative matrix form as follows [16]:

$$\{\Delta z_j\} = [S_j] \cdot \{\Delta p\} \quad (3.15)$$

where $\{\Delta z_j\}$ is the difference between the experimental and mathematical modal results at the j^{th} iteration, $\{\Delta p\}$ is the amount of change in the design parameters at the j^{th} iteration and $[S_j]$ is the sensitivity matrix at the j^{th} iteration. Accepting the updating procedure is based on the modal results, the sensitivity matrix describes the first order partial derivatives of natural frequencies and mode shapes with respect to the design parameters as given in equations (3.13) and (3.14). It should be noted that sensitivity matrix should be calculated at each iteration which is the most time consuming part of the updating procedure. Especially for large order systems, overall updating time can be reduced considerably if the computational time spent for the calculation of the sensitivity matrix is decreased. Eq. (3.15) can be written explicitly as follows [16]:

$$\begin{Bmatrix} \Delta \lambda_1 \\ \{\Delta \phi\}_1 \\ \vdots \\ \Delta \lambda_m \\ \{\Delta \phi\}_m \end{Bmatrix}_j = \begin{bmatrix} \frac{\partial \lambda_{A1}}{\partial p_1} & \frac{\partial \lambda_{A1}}{\partial p_2} & \dots & \frac{\partial \lambda_{A1}}{\partial p_L} \\ \frac{\partial \{\phi_A\}_1}{\partial p_1} & \frac{\partial \{\phi_A\}_1}{\partial p_2} & \dots & \frac{\partial \{\phi_A\}_1}{\partial p_L} \\ \vdots & \vdots & \ddots & \vdots \\ \frac{\partial \lambda_{Am}}{\partial p_1} & \frac{\partial \lambda_{Am}}{\partial p_2} & \dots & \frac{\partial \lambda_{Am}}{\partial p_L} \\ \frac{\partial \{\phi_A\}_m}{\partial p_1} & \frac{\partial \{\phi_A\}_m}{\partial p_2} & \dots & \frac{\partial \{\phi_A\}_m}{\partial p_L} \end{bmatrix}_j \cdot \begin{Bmatrix} \Delta p_1 \\ \Delta p_2 \\ \vdots \\ \Delta p_L \end{Bmatrix}, \quad (3.16)$$

where subscript j describes the terms that should be evaluated by using the design parameter values at the j^{th} iteration. In Eq. (3.16), size of vector $\{\Delta p\}$ is $m(n+1) \times 1$, size of the sensitivity matrix is $m(n+1) \times L$ and size of vector $\{\Delta z_j\}$ is $(L \times 1)$, where n is the number of degrees of freedom obtained from the modal test, m designates the number of modes included in the updating algorithm and L is

the number of design parameters to be updated. It is achievable to have an over determined problem if the number of design parameters to be updated is less than the number of equations [16]. The parameters can be identified with the following formulation [16]:

$$\{\Delta p_{j+1}\} = [S_j]^+ \{\Delta z_j\}, \quad (3.17)$$

where $[S_j]^+$ is the pseudo-inverse of the sensitivity matrix at the j^{th} iteration. Using Eq. (3.17) values of the design parameters at the next iteration step can be acquired as follows:

$$\{p_{j+1}\} = \{p_j\} + \{\Delta p_{j+1}\}. \quad (3.18)$$

The flexibility of this method is the advantageous aspect over other type of methods. By applying this method, there are some options to be selected that effects the time elapsed to reach convergence criteria. These options were listed as:

- The number of modes that is included in the algorithm can be selected.
- The number of the measured coordinates that is included in the algorithm can be selected.
- Mode frequency or mode shape vector sensitivity can be selected which will be used in updating procedure. Mode shape sensitivity calculation needs much more time than mode frequency sensitivity calculation [15]. For that reason, the selected sensitivity matrix is constructed with engineering insight.

The details for more and less measurement points than the number of parameters conditions are given in APPENDIX section.

There are lots of parameter set options that can be updated with Inverse Eigensensitivity Method (IEM). In given mass spring example, the mass values are assumed to be constant as generally the case. Stiffness terms are identified to be updated by IEM. The following stiffness terms are selected in the algorithm to be updated: k_1 , k_2 , k_3 and k_4 . The number of parameter to be updated is 4. As an experimental result: 2nd; 3rd and 4th mode shapes are assumed to be measured from 1st, 2nd and 3rd degrees of freedom. The erroneous values of stiffness terms that need correction are given below in Table 11. IEM is used to see the effectiveness of the code over the direct methods and to search the capability of application to large order finite element models. IEM has the flexibility that gives an option to choose the parameter sets which have the dominant effect on the dynamic responses.

Table 11. The Erroneous Values of the Parameters

Parameter	Erroneous Values(N/m)	Experimental Model Values(N/m)	Error Percentage (%)
k1	1100	1500	26.7
k2	1000	1600	37.5
k3	1250	1400	10.7
k4	5000	6500	23.1

A custom code for IEM was developed in Matlab environment. As a result of IEM: the eigenvalues before and after updating(Figure 21, Figure 22); MAC plots before and after updating(Figure 23, Figure 24); the change of parameters with the iteration sequence(Figure 29); FRF plots(Figure 30 and Figure 31 for 6th degree of freedom are given.

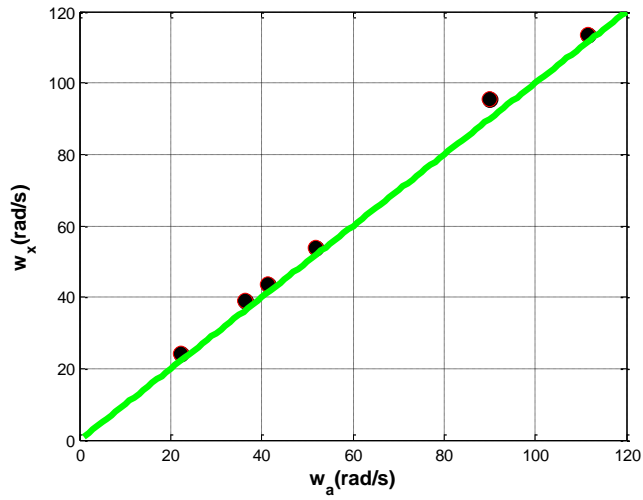


Figure 21. The Natural Frequencies of the Experimental and Mathematical Models before Updating

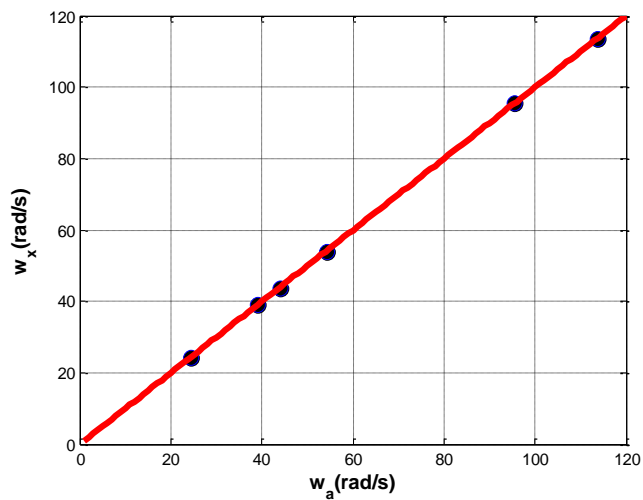


Figure 22. The Natural Frequencies of the Experimental and Mathematical Models after Updating

The comparison of the natural frequency values of the experimental and mathematical models before and after updating was given in Figure 21 and Figure 22 respectively. The method visualizes the natural frequency values of experimental and mathematical models by referencing the line which has the

angle with the positive X axis 45° [15]. If the point which denotes natural frequency is on the line, the natural frequencies have the same value. If not, the natural frequency values are different from each other. As seen in Figure 21, the natural frequency values are different from each other. It can be observed by identify the points that do not lie on the line of 45° . But in Figure 22, the points lie on the line of 45° which means the natural frequencies overlap.

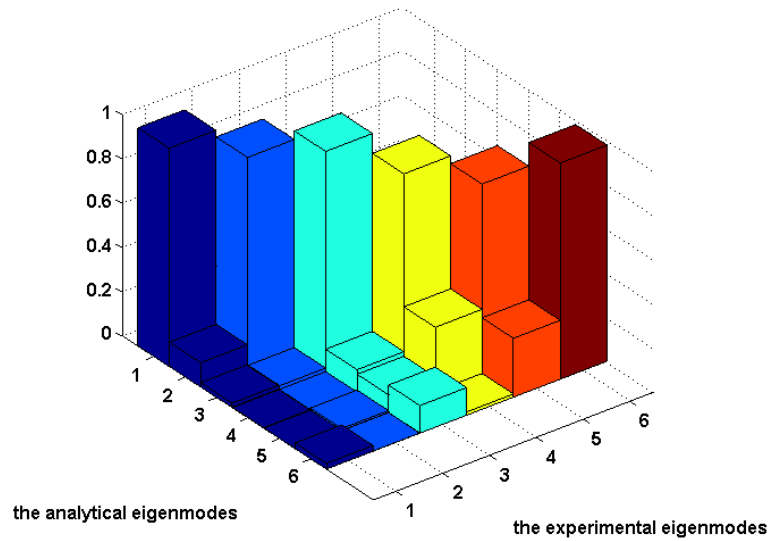


Figure 23. MAC Plot of the Experimental and Mathematical Models before Updating

Table 12. The MAC Numbers before Updating that Belong to Figure 23

MAC NUMBERS	Experimental Model					
Mathematical Model	0.99	0.37	0.02	0	0.01	0.02
	0.11	0.96	0	0.01	0.01	0.05
	0.02	0.02	0.99	0.05	0.01	0.13
	0	0	0.1	0.9	0	0
	0	0.01	0.08	0.3	0.87	0.03
	0.03	0	0.12	0.01	0.27	0.98

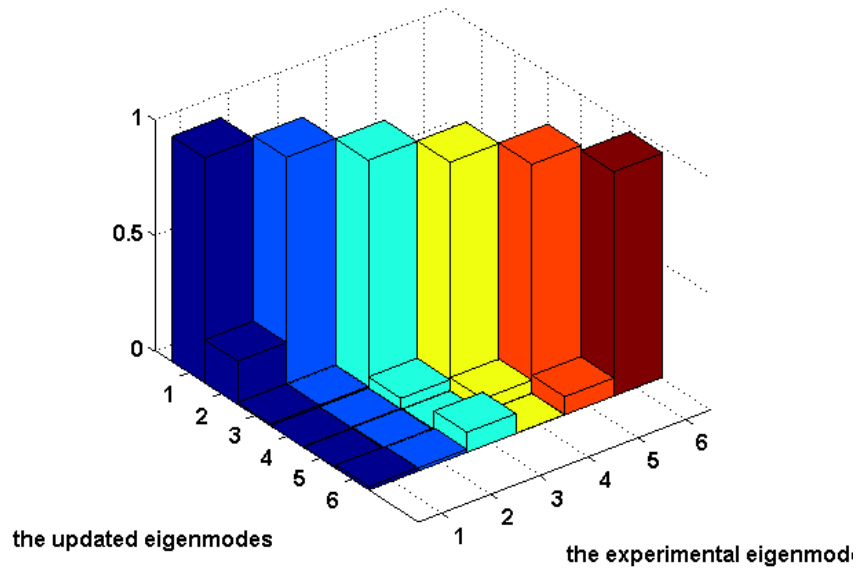


Figure 24. MAC Plot of the Experimental and Mathematical Models after Updating

Table 13. The MAC Numbers after Updating that Belong to Figure 24

MAC NUMBERS	Experimental Model					
	Mathematical Model	0.97	0.14	0.01	0	0
0.19		0.99	0.01	0	0.01	0.01
0.01		0.01	0.99	0.05	0.01	0.09
0		0	0.05	0.99	0.04	0
0		0.01	0	0.06	0.99	0.13
0.02		0.01	0.09	0	0.08	0.97

The change of design parameters with the iterations are plotted in Figure 25, Figure 26, Figure 27 and Figure 28.

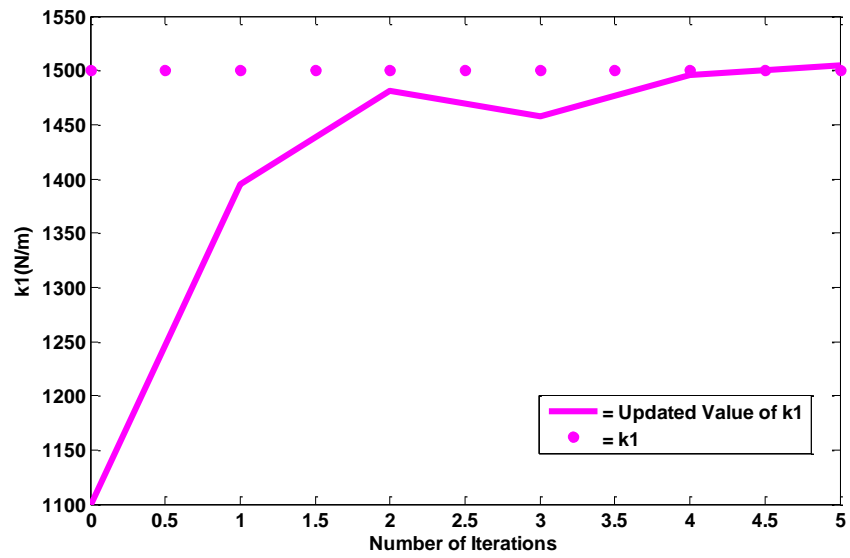


Figure 25. The Convergence of Erroneous Parameter k_1

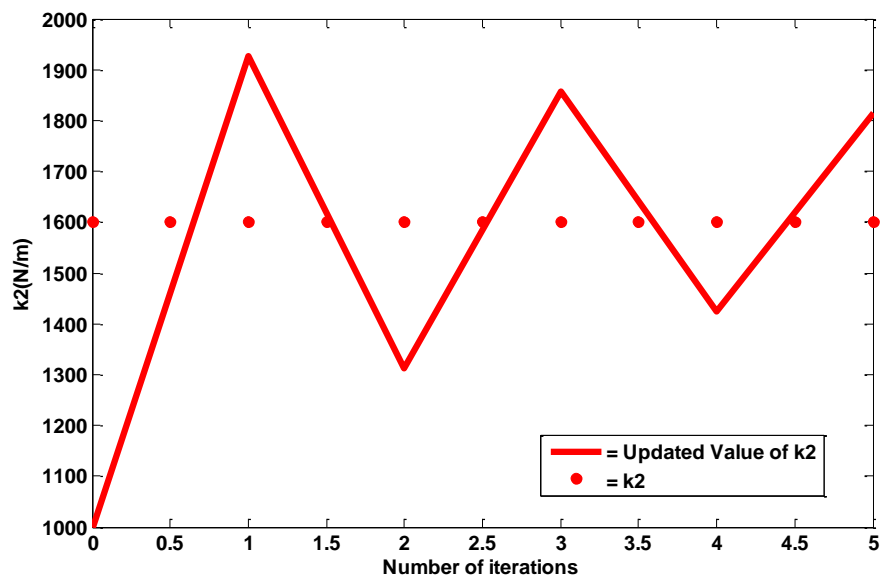


Figure 26. The Convergence of Erroneous Parameter k_2

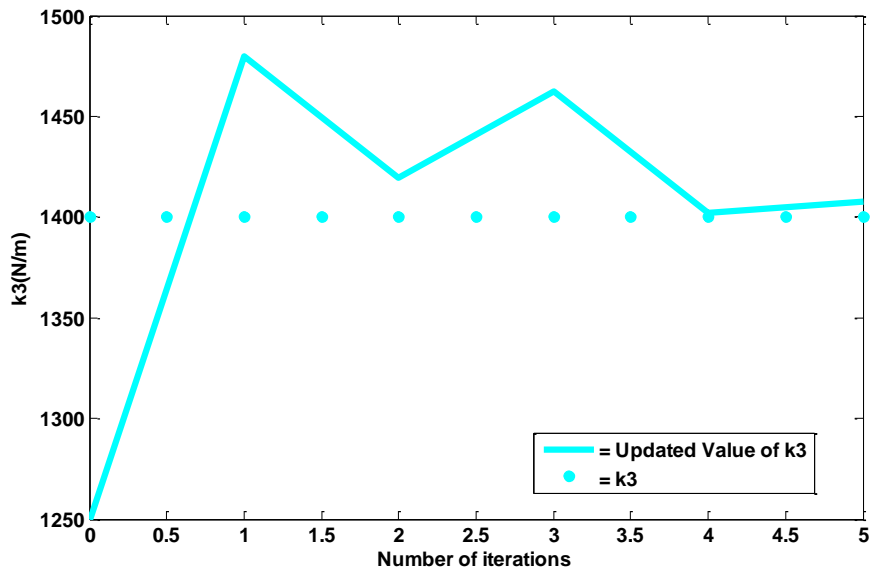


Figure 27. The Convergence of Erroneous Parameter k_3

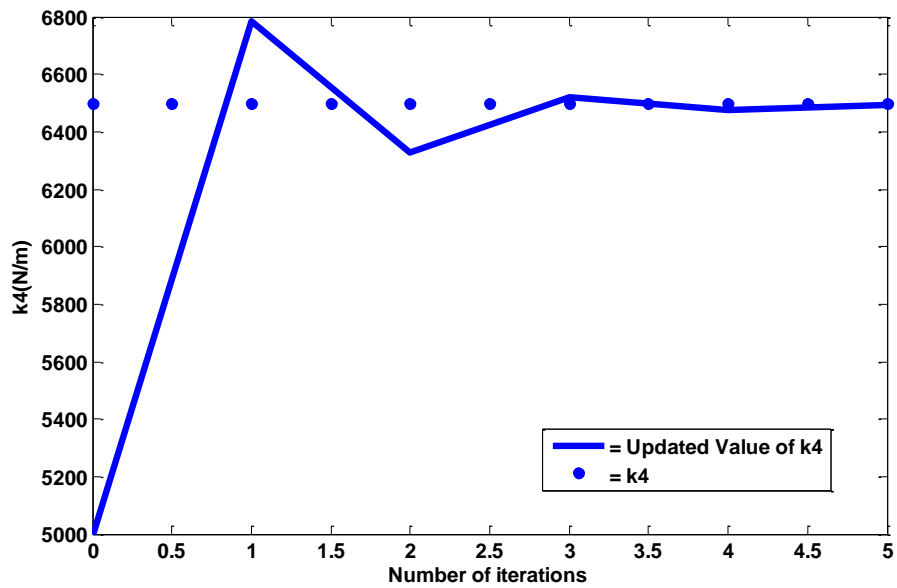


Figure 28. The Convergence of Erroneous Parameter k_4

Giving the convergence of parameters with respect to the number of iterations, the convergence of all parameters is given as below in Figure 29.

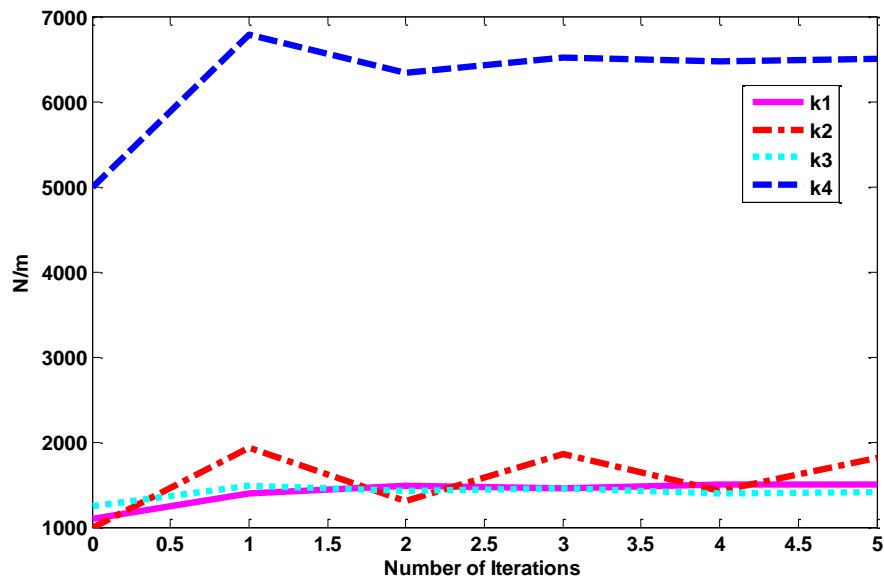


Figure 29. The Convergence of Parameters With Respect to Number of Iterations

The convergence criterion is constructed by considering the difference in eigenvalues and eigenvectors of experimental and mathematical models with checking the MAC values. Convergence is reached after 6 iterations. As previously given in Figure 22 for natural frequency values and the diagonal elements given in

Table 13 for eigenvectors of experimental and mathematical models, it is decided that the correlation is very accurate by considering the modal results. After assuring the convergence of parameters, the FRF plot for 6th degree of freedom is plotted in Figure 30 before and after updating in Figure 31 to correlate the response functions of the experimental and mathematical models.

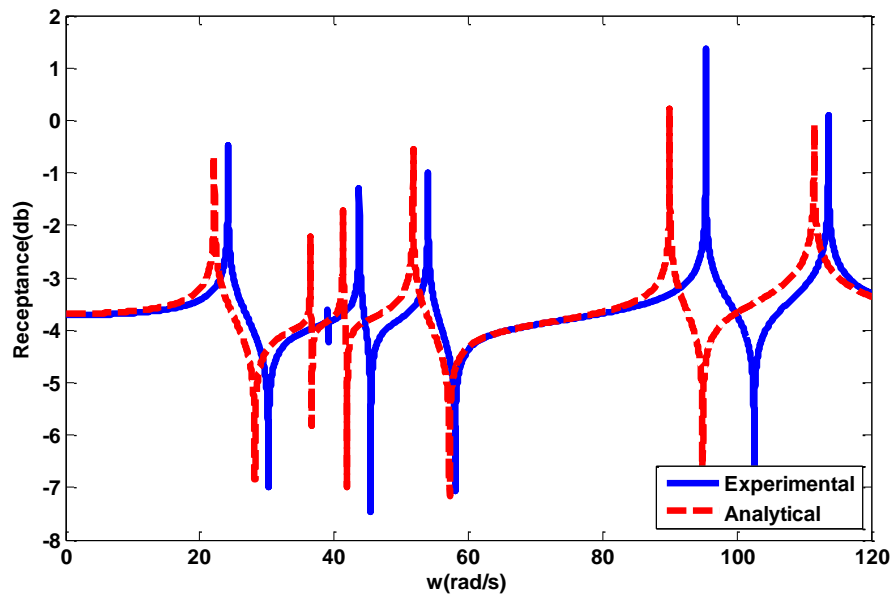


Figure 30. The Semi Log Point FRF Plot of the 6th DOF for Experimental and Mathematical Model

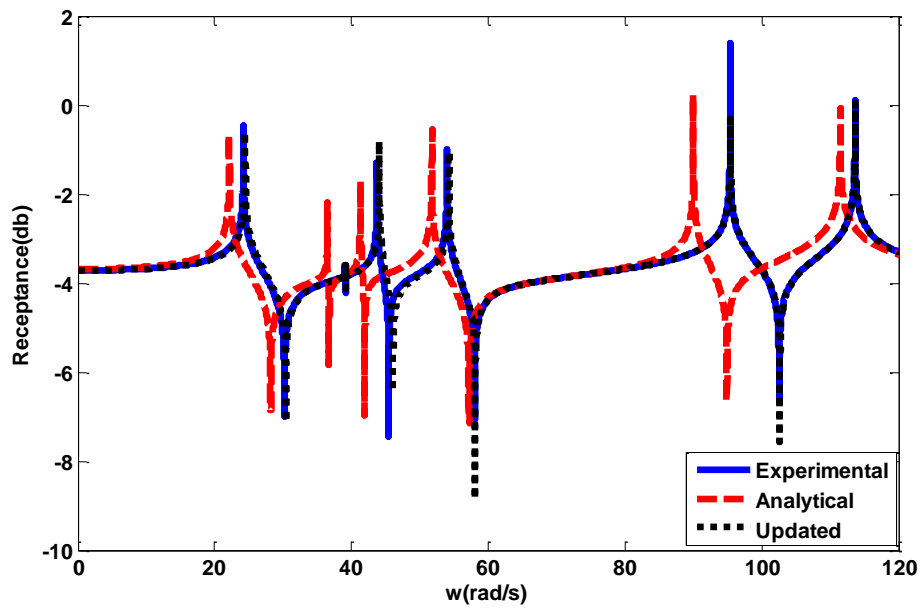


Figure 31. The Semi Log Point FRF Plot of the 6th DOF for Experimental, Mathematical and Updated Model

Inverse Eigensensitivity Method worked effectively with the spring mass system example. 6 iterations are required for convergence of the modal results. Parameters have behavior to converge the experimental values. Some of the parameters have not convergent behavior but the required convergence criterion is not based on the amount of deviation of the mathematical parameters from experimental values. The modal results of the updated model must be close enough to represent the experimental model. Besides the representation of the modal results, FRF of the updated model is nearly the same as the experimental FRF plot given in Figure 31.

CHAPTER 4

DEVELOPED ALGORITHM AND FLOWCHART

Obtaining the results with the direct methods and iterative method, it is concluded that the iterative methods have many advantages over direct methods concerning the application to large order finite element models. Response function methods and modal based methods can be used with large order finite elements. Response function methods use frequency response functions as the objective function. Modal based methods use eigenfrequency and eigenvector values of the experimental model as the reference data to be converged.

The measurement and environment noise can degrade the quality of the frequency response function data. Frequency response function is thoroughly sensitive to the excitation location and technique. Modal results (eigenvalues, natural frequencies, modal damping coefficients) are not sensitive to measurement noise. In addition to disadvantage of response function method, extraction of the FRF from large order finite element model is time consuming procedure with respect to the normal mode analysis. For these reasons, the response function method is eliminated to be used with the large order finite elements. In the reference paper introduced by Göge and Link [10], the method that uses the eigenvalue and eigenvector sensitivity value has more convergent behavior than the method that uses the eigenvalue and frequency response function sensitivity values. To visualize the selection of the updating method, a chart is developed which is given Figure 32.

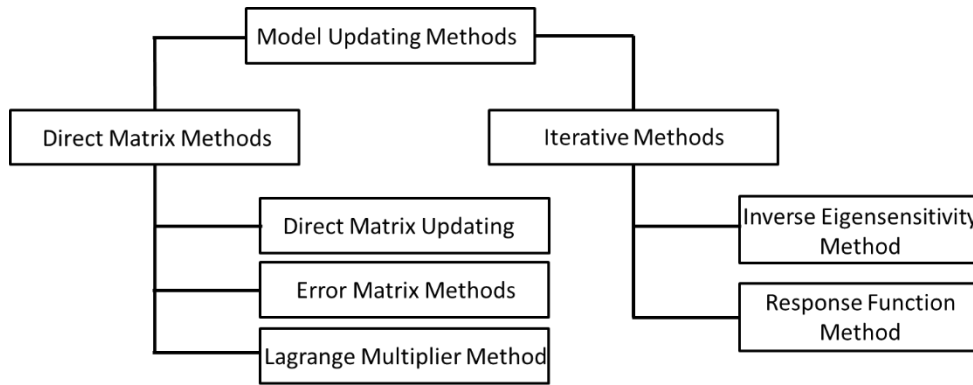


Figure 32. The Model Updating Methods

As a summary, the direct methods are eliminated because of the non-applicability to large order finite elements and the difficulty in coping with the taking inverse of structural matrices. Afterwards, beyond the iterative methods response function methods have some characteristic properties which make these methods sensitive to measurement noise. Verifying the effectiveness of the Inverse Eigensensitivity Method that is applied to spring mass structure given in Section 3.1.3, inverse eigensensitivity method is selected to use with large order finite element models.

Modal based methods are more effective considering the flexibility to select the result sets to be used in procedure. One of the most crucial advantages of the method is its capability of selecting the eigenvalues and eigenvectors from the full set of results extracted through modal test [16]. Number of modes introduced into the analysis, number of measured coordinates and utilizing eigenvalues, eigenvectors or both in the analysis effects the computational time significantly; hence, they should be taken into account before an updating procedure. It should be noted that calculation of eigenvector sensitivities requires more time compared the eigenvalue sensitivities [16].

In application of the Inverse Eigensensitivity Method, sensitivity calculations and normal modes analysis are accomplished using the commercial FE software Nastran. Two different control criteria are used in the updating algorithm. In the first control criteria, the difference between experimental and mathematical model

results is inspected in each iteration and if this value reduces below a predefined error tolerance, algorithm ends which can be summarized as follows:

$$\{P\}^j = \left\{ \begin{array}{c} \Delta\lambda_1 \\ \{\Delta\phi_1\} \\ \vdots \\ \Delta\lambda_m \\ \{\Delta\phi_m\} \end{array} \right\}^j \leq e_1. \quad (4.1)$$

where subscript j describes the terms that should be evaluated by using the design parameter values at the j^{th} iteration, e_1 is the acceptable error limit value for the difference between experimental and mathematical modal results, λ is the eigenvalue and ϕ is the eigenvector. In the second control criteria, the rate of decrease of the error defined in the first criteria is checked. If this decrease is less than a predefined tolerance value, the sensitivity matrix is not calculated for the next iteration. The second criterion can be summarized as follows:

$$\frac{|\{P\}^j - \{P\}^{j-1}|}{L} \leq e_2, \quad (4.2)$$

where e_2 is a limiting value for the decrease in error and L is the number of design parameters. The 2nd control criterion causes to save time in updating procedure with eliminating the calculation of sensitivity step. The goal is to decrease the time needed to update large order finite element models which may need much time to calculate the sensitivity of the modal results with respect to the parameters.

The flowchart of the developed in-house computational code which uses Matlab and Nastran simultaneously is given in Figure 33. Pre-analysis starts with the selection of the design parameters and modal results which are needed to be updated. Normal modes analysis is ran with the option to calculate the sensitivities of the selected modal results with respect to the parameters. As a

following step, Inverse Eigensensitivity Method algorithm is applied to obtain the change in parameters by using modal results of finite element model, sensitivity values and experimental results. Subsequently, the 1st control criterion is checked if the difference between the results of finite element model and experiment is small enough. If the value is in the range of a limit, procedure is stopped. If the value is not in the range of a limit, procedure is continued with the checking of the 2nd control criterion and loop is repeated until 1st criterion is met.

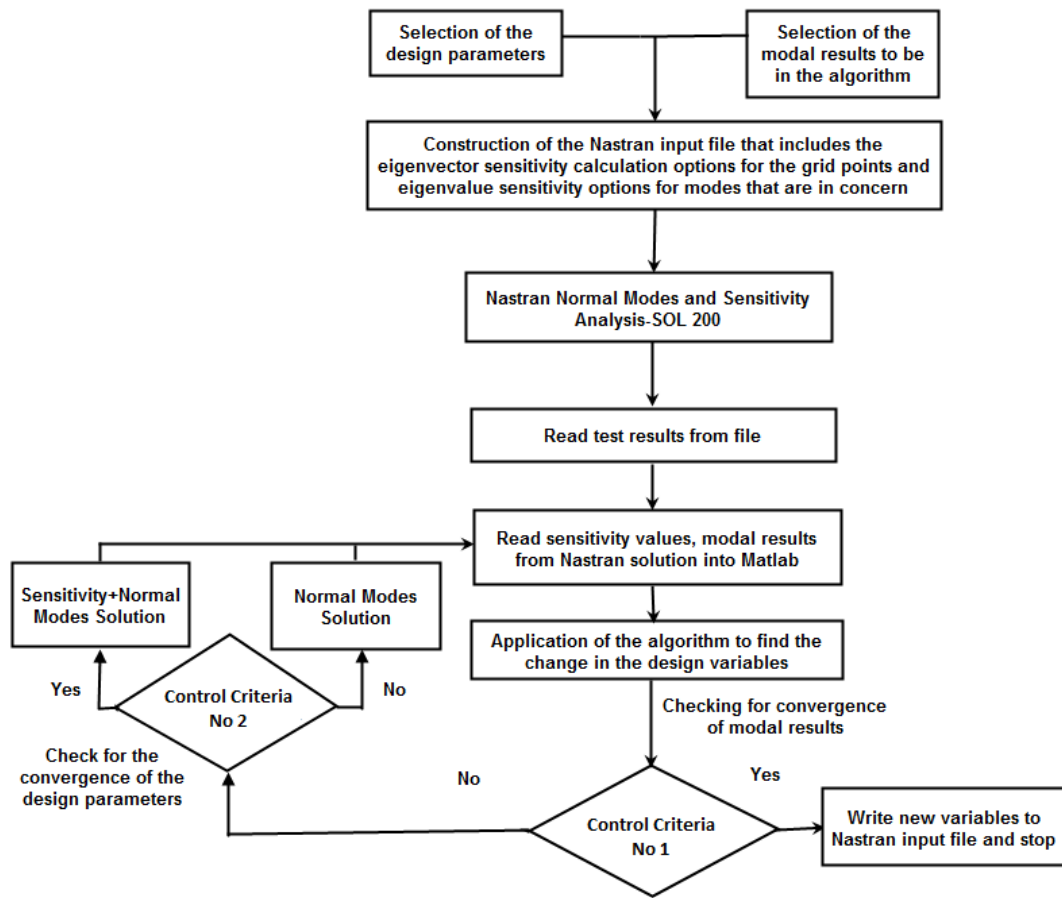


Figure 33. Flowchart of the developed algorithm

CHAPTER 5

APPLICATION OF THE DEVELOPED ALGORITHM TO GARTEUR MODEL AND MISSILE LAUNCHER

5.1 CASE STUDY ON A SCALED AIRCRAFT MODEL USING THE DEVELOPED ALGORITHM WITH INVERSE EIGENSENSITIVITY METHOD

Deciding the appropriate method that can be applied to real structures, the developed algorithm was carried on the test structure that was designed by GARTEUR (Group for Aeronautical Research and Technology in Europe). The geometry of the aircraft model is given in Figure 34. The dimensions given are in millimeters.

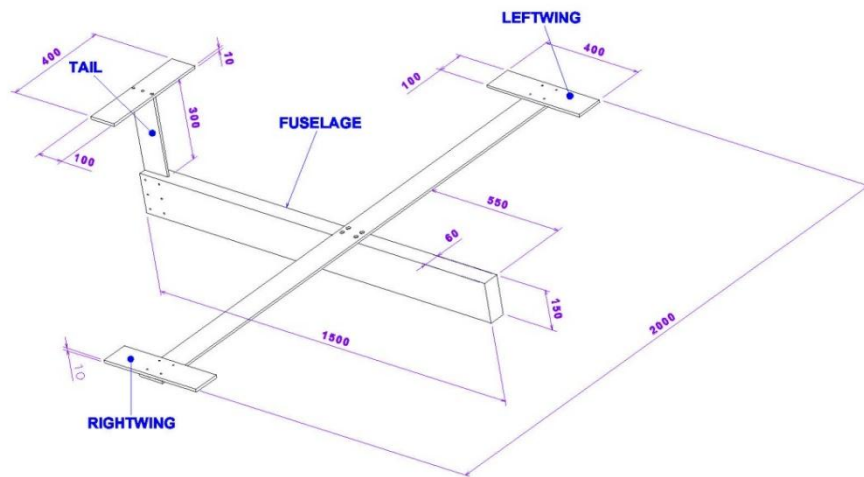


Figure 34. Geometry of the aircraft model

The test structure was produced based on geometry in Figure 34. The connection of the aluminum parts was made with bolts. The test structure was hung with elastic cords to the test frame. The test structure was excited by a shaker produced by MB Dynamics. The shaker can deliver up to force of 500 N and give 38 mm stroke peak to peak. The excitation point was selected to excite the modes of the structure after observing the finite element solution for normal modes. The excitation point was identified in such way that the external moment was applied with respect to the mass center of the structure [15]. The test configuration with the direction of the applied force by the shaker was shown in Figure 35.

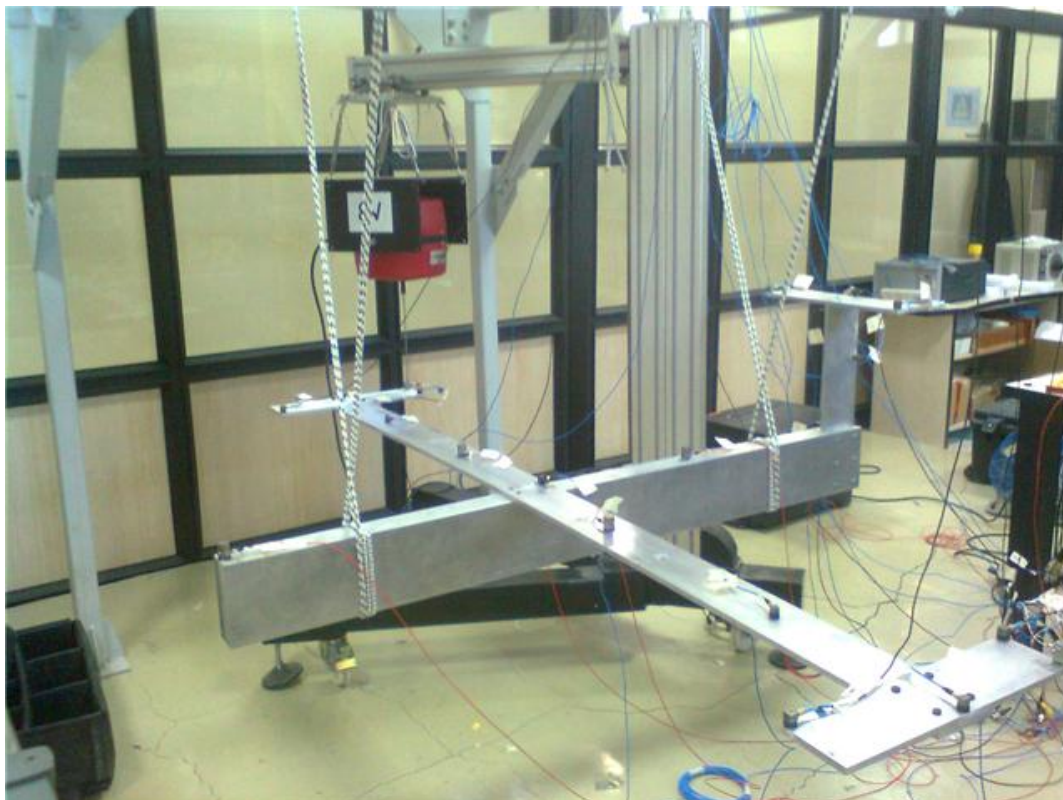


Figure 35. The Test Configuration for the GARTEUR Aircraft Model

Test was carried out based on the number of 40 measurements. Completing the modal test, the modal parameter identification procedure was followed. The steps of that procedure are:

- Modal Data Selection,
- Extraction the mode shapes

The rigid body modes were observed around 2 Hz. There is an option to select the FRF from the full set of FRFs. The measurements from accelerometers can be erroneous and needed to be excluded from the modal parameter identification process. After the selection step, the sum FRF plot was obtained.

Subsequent to the modal data selection step, the modal identification procedure was carried out. It has 3 parts to be completed. In the first part, the frequency band is selected to be processed. In the second part, the stabilization procedure is accomplished with the selected model number. Model number includes the number of mode shapes that can represent the sum FRF plot of the real structure. In the 3rd part, the mode shapes can be visualized.

Defining the frequency band for the model identification process, the stabilization procedure must be made. For that aim, the stabilization diagram was constructed in this step before the selection of the stable poles. Stable pole is s type pole in frequency in a range %1, damping ratio %5 and mode vector in a range %2 with respect to a pole of preceding model order. 3 stable poles can give an opinion about a real mode.

The symbols in the stabilization diagram are based on the agreement of frequency, damping ratios and mode vectors between the poles of the sequential model orders. Based on the given details about the stabilization diagram, the stable poles were selected.

Table 14. The Natural Frequency and Damping Ratios for the Calculated Modes in the Selected Frequency Range

Mode number	Natural Frequency(Hz)	Damping Ratio (%)
Mode 1	5.51	0.42
Mode 2	15.74	0.31
Mode 3	34.75	0.3
Mode 4	36.17	0.47
Mode 5	44.2	0.09
Mode 6	52	0.16
Mode 7	55	0.07
Mode 8	58.87	0.31
Mode 9	63.8	0.16

Aircraft finite element model was constructed with 8 noded linear elements which is called HEX8 in Nastran. The connection points were modeled as if they were the same structure. The elements in the connection regions were constructed with common nodes. It provided opportunity not to model contact algorithm in the finite element modeling. The full model was divided into 5 subparts as given in Figure 36. Each subpart has its own property identity number which is used to update each property value separately.

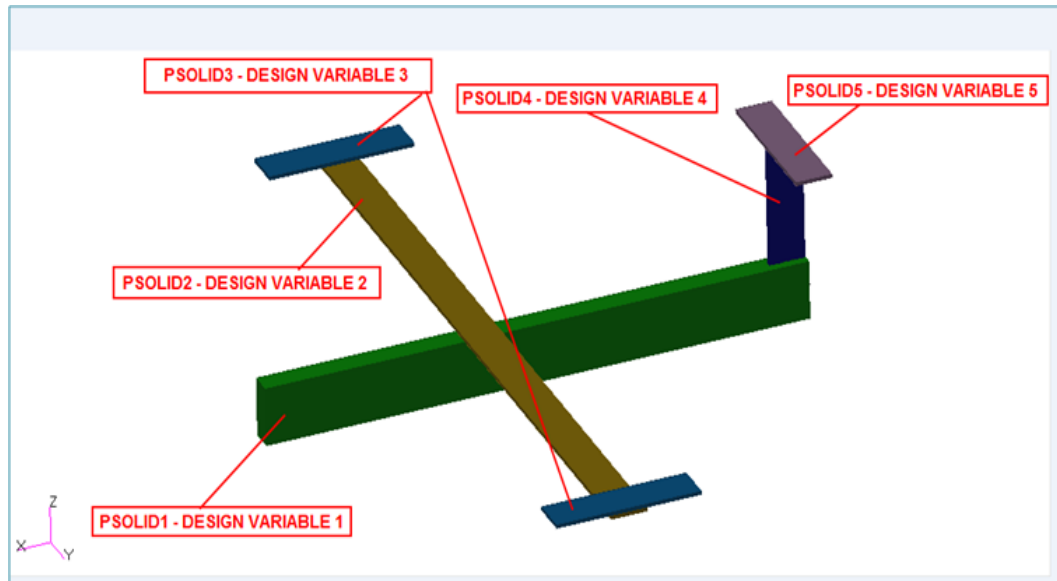


Figure 36. The Properties Identity Numbers of Aircraft Model

The finite element model consists of 20540 HEX8 elements and 29028 nodes. The total degree of freedom of the model is 168848. The finite element model is shown in Figure 37. The design parameters were selected as Young's modulus and density. By using both of the design variables, the updating procedure was carried out. It is more logical to use Young's modulus values because by changing the density values, the location of the mass center may deviate and there is a need of another control loop in the algorithm which causes the solution time to increase.

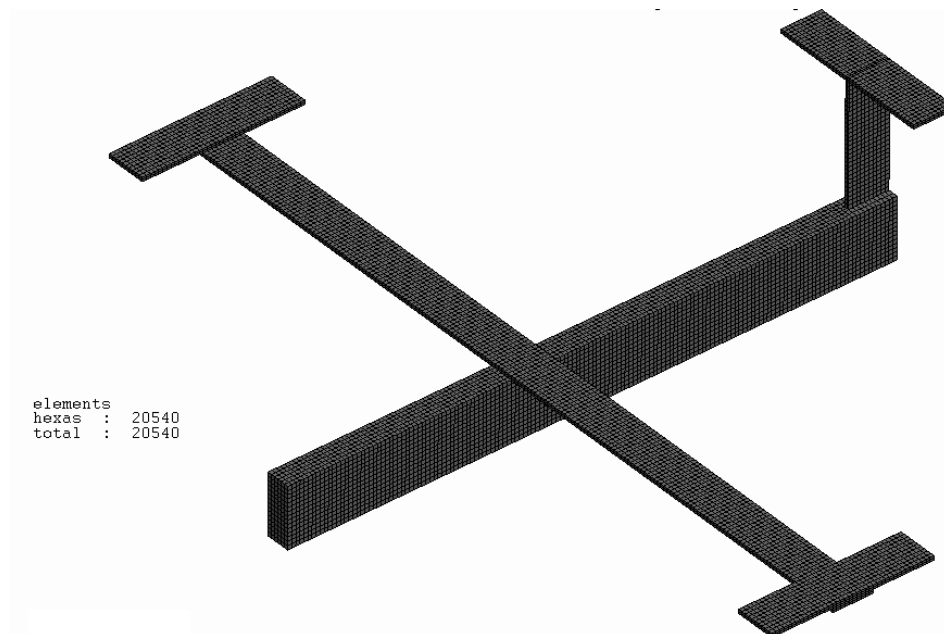


Figure 37. The Finite Element Model of the Aircraft Model

Owing to the few number of design variables, it was evaluated that there was no need to make sensitivity analysis. 5 set of design variables was selected to be a volunteer in updating algorithm. The eigenvectors were checked for correlation. For finite element solution, the eigenvectors were extracted from 5 grid points given in Figure 38. The coordinates were identified after the investigation of the mode shapes of the structure. These points had the potential to move more than the other locations by regarding the first 6 mode shapes. To be able to visualize the initial correlation of the mode shapes, the maximum displacement was maximized in mathematical and experimental solutions. After that procedure, the MAC plot was constructed to quantify the correlation of models. Developed code that checks the initial correlation, reads the mode shapes and plots the 3D MAC plot for visualization purposes. For the grid points defined, the mode shapes in X, Y, Z axes were taken in concern with respect to the global reference frame.

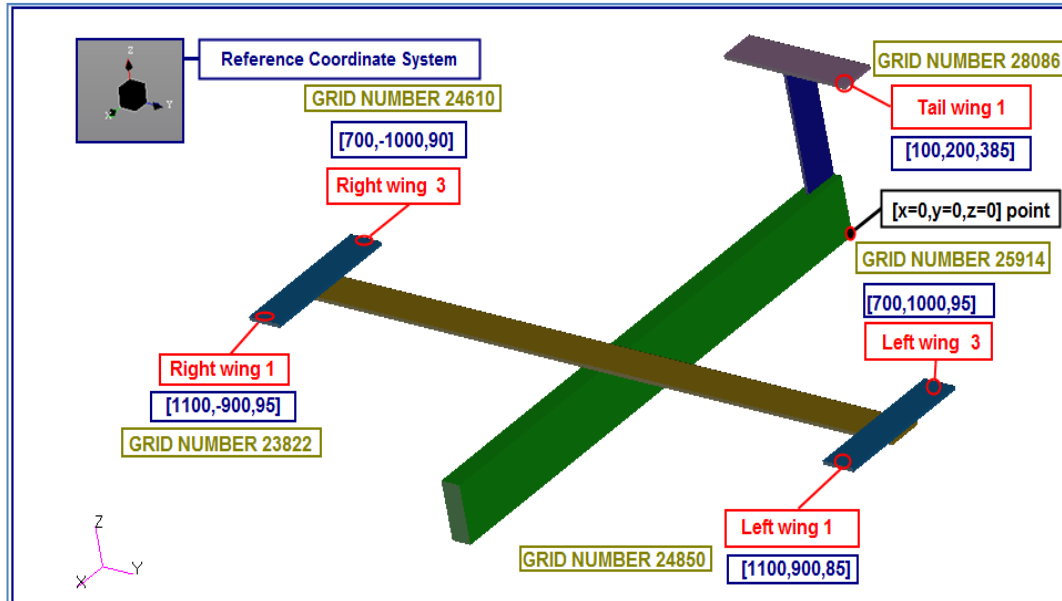


Figure 38. The Coordinates and Grid Numbers of Nodes that the Eigenvectors Are Extracted From

The MAC plot before updating procedure is shown in and the MAC numbers are given in Figure 39. As clearly seen from Table 16, the diagonal numbers of the MAC matrix are above 0.75 except for the 4th mode. The updating procedure was applied to the Young's Modulus values for each of the property of solids that was previously given in Figure 38. The structural material property of aluminum that was used as parts of the aircraft model is given in Table 15.

Table 15. The Material Properties of Al 7071-T6

Al 6061-T6 Material Properties		
Young's modulus(MPa)	Poisson's Ratio	Density(kg/m ³)
71700	0.3	2810

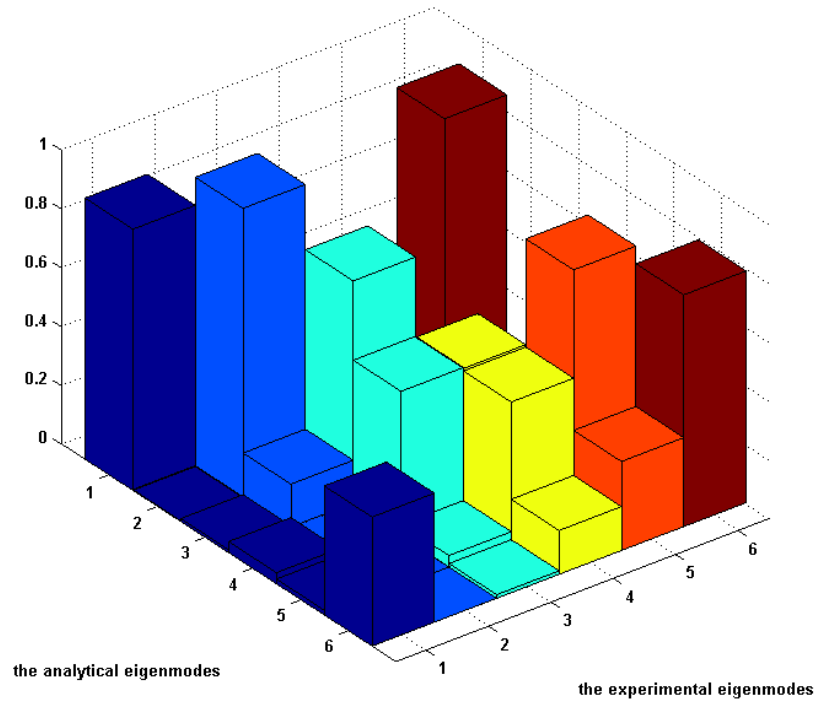


Figure 39. The MAC Plot for the Aircraft Model before Updating

Table 16. The MAC Matrix for the Aircraft Model before Updating

MAC NUMBERS	Experimental Model					
	Mathematical Model	0.89	0	0	0	0
0		0.98	0.05	0.01	0.01	0
0.01		0.15	0.76	0.02	0.05	0.03
0.04		0.01	0.49	0.49	0.09	0.08
0.02		0	0.04	0.48	0.85	0.08
0.44		0	0.01	0.15	0.3	0.79

The initial values of the natural frequencies of the experimental and mathematical models with the difference in percentage are given in Table 17.

Table 17. The Natural Frequencies for Experimental and Mathematical Models before Updating

	Natural Frequencies from Mathematical (Finite Element)Model (Hz)	Natural Frequencies Extracted From Modal Test(Hz)	%Difference
1st Mode	6	5.5	9.2
2nd Mode	16.7	15.7	6
3rd Mode	39	34.8	12.3
4th Mode	40.6	36.2	12.2
5th Mode	41	38	7.9
6th Mode	46.9	44.2	6.2

The visual representation of the comparison of the natural frequencies is given in Figure 40 with the positive 45° line to identify the difference.

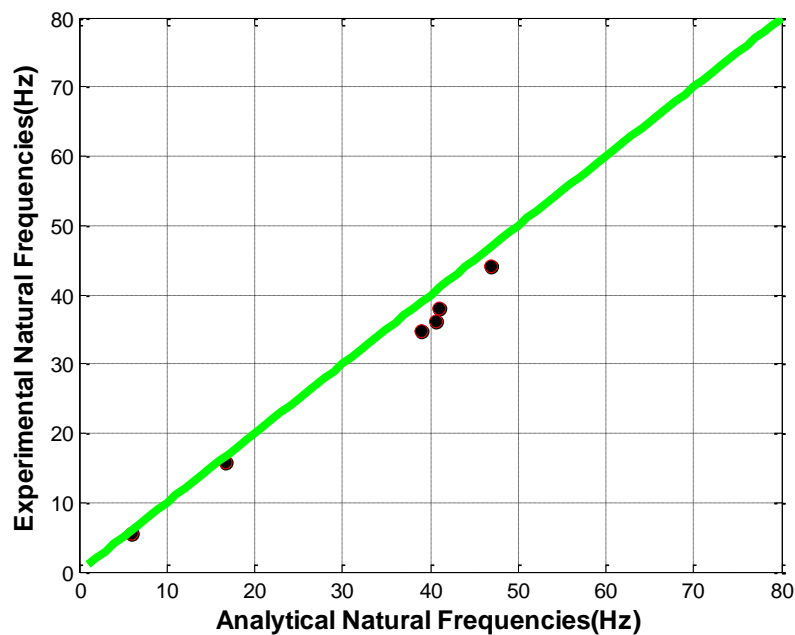


Figure 40. The Comparison of the Natural Frequencies before Updating

Visual representation of the first 6 mode shapes of the aircraft model that was extracted from Nastran SOL 103 solution is shown in Figure 41.

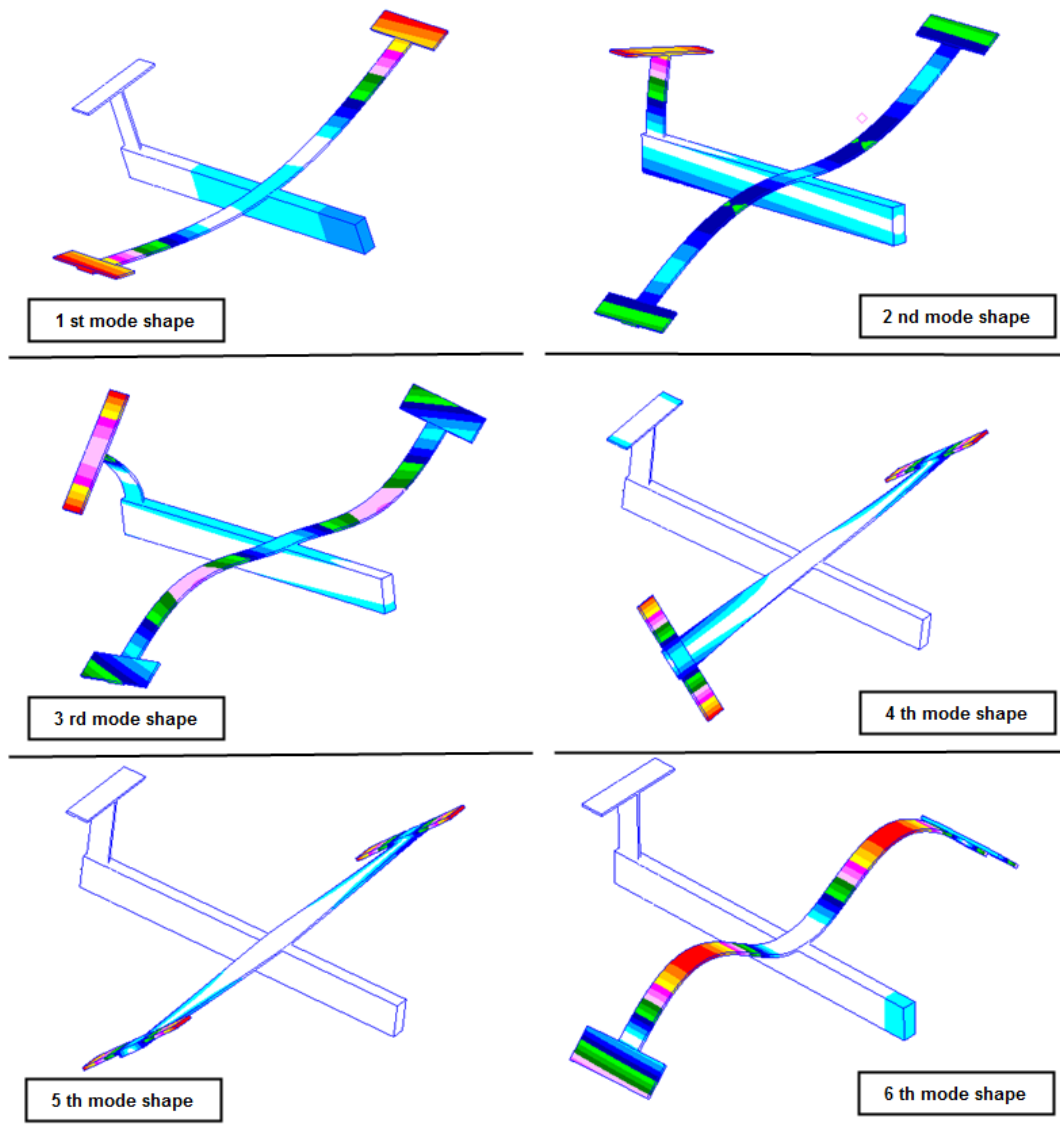


Figure 41. Visual representation of the mode shapes extracted from Nastran

The developed algorithm was applied to mathematical model of the aircraft to see the effectiveness and flexibility of the inverse eigensensitivity method. The initial parameters that used in the updating procedure were selected to take the first 6 natural frequencies and 1st mode shape into account. For that reason, the mode shapes were not supposed to be well correlated with the test results with respect to

the initial configuration of the mathematical model. The change of design parameters with respect to the iteration number is shown in

Table 18. The convergence of parameters was not observed because the mathematical and experimental models were well correlated with each other. For that reason, the behavior of the convergence was not observed in a similar manner that seen in six DOF mass spring system example. The design objective was selected to decrease the difference in the first 2 natural frequencies. The change of parameters is demonstrated individually with respect to the iteration number in Figure 42, Figure 43, Figure 44, Figure 45 and Figure 46.

Table 18. The Change of Design Variables with respect to the Iteration Number

		Value of Design Parameters with Iteration Number			
		Initial Mathematical Model Values	1	2	3
Design Parameters	Design Parameter No 1	71000	70290	70992	71702
	Design Parameter No 2	71000	71710	82064	65989
	Design Parameter No 3	71000	70290	69587	70282
	Design Parameter No 4	71000	70290	69587	68891
	Design Parameter No 5	71000	71710	70992	70282

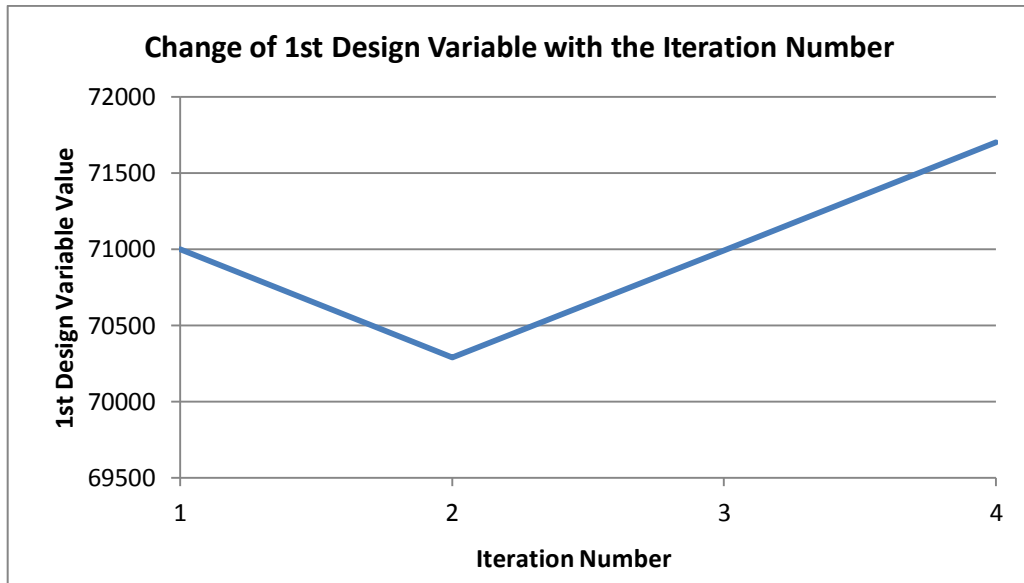


Figure 42. Change of 1st Design Parameter with the iterations

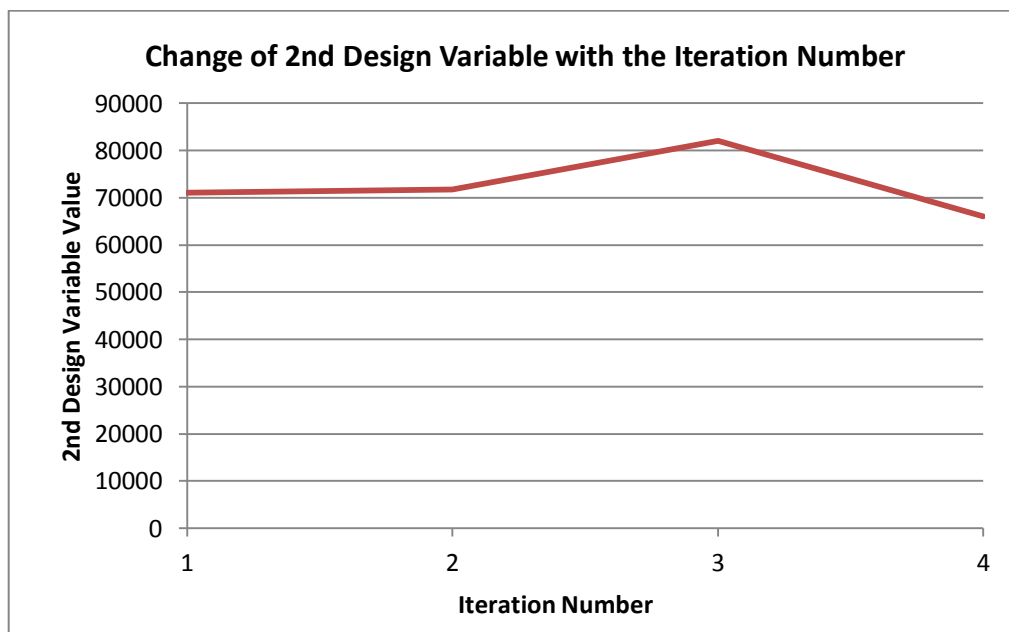


Figure 43. Change of 2nd Design Parameter with the iterations

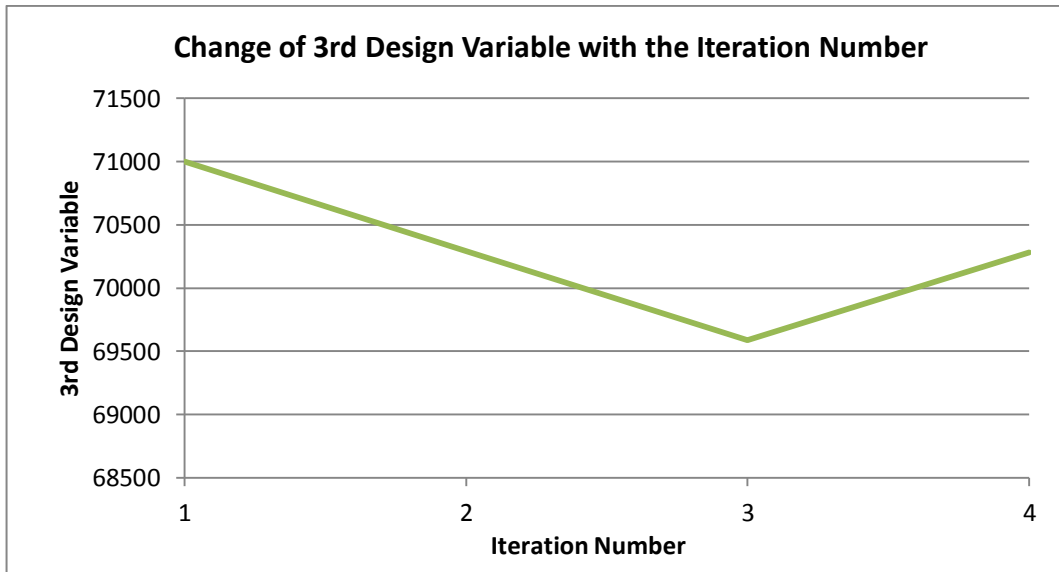


Figure 44. Change of 3rd Design Parameter with the iterations

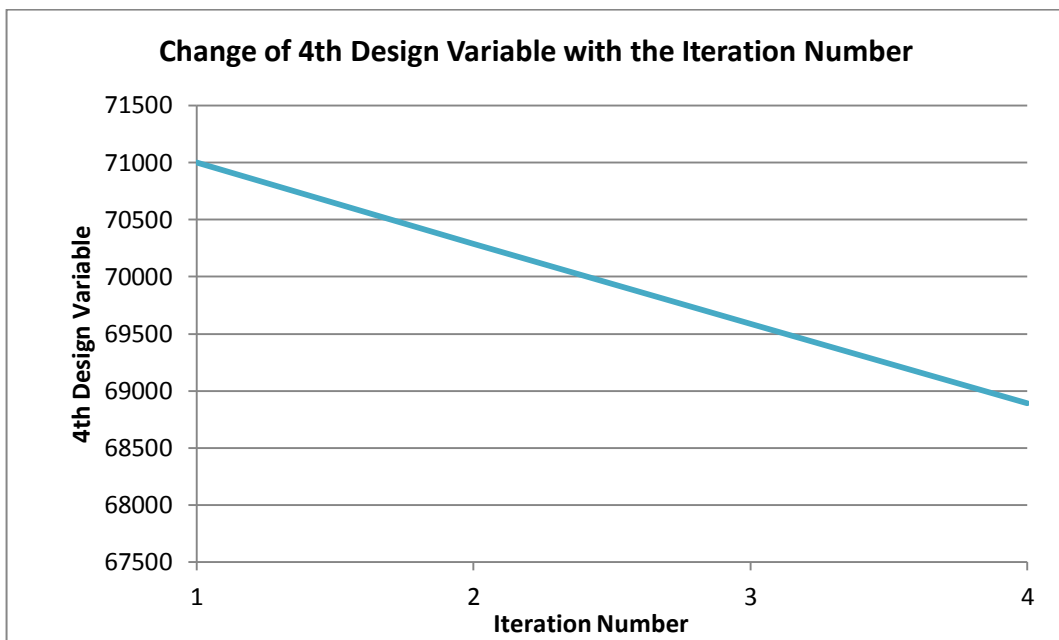


Figure 45. Change of 4th Design Parameter with the iterations

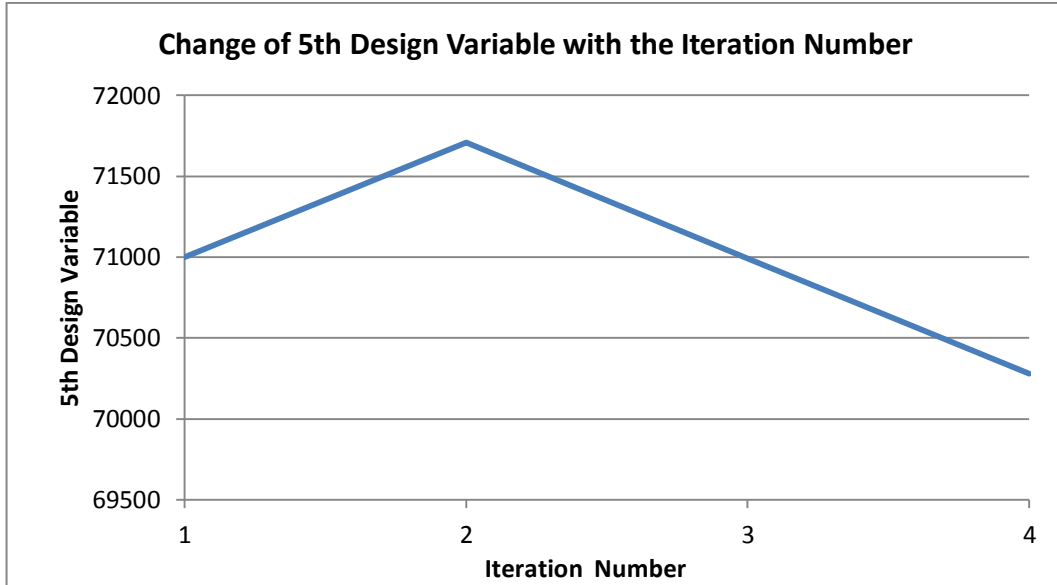


Figure 46. Change of 5th Design Parameter with the iterations

The natural frequency values of the mathematical and experimental models are given below in Table 19 after updating procedure. It was observed that first 6 natural frequencies were converged to the test counterparts. The mode shapes were checked if for the correlation of the experimental and mathematical results. Before and after updating procedure, the mode correlation was needed to be observed. In both cases, the first 6 mode shapes of the experimental and mathematical model were checked to verify the sequence of modes did not change. The change of sequence of modes was caused by the closely spaced natural frequencies and double modes. The aircraft model is symmetrical model and convenient to have double modes. For that reason, the change of sequence of modes was controlled before and after the updating procedure. Developed algorithm worked with the aim of decreasing the amount of difference for the first 2 natural frequencies and minimized the objective function. The convergence was reached in 3 iterations which totally lasted 416 seconds. The MAC plot is given in Figure 47 and the corresponding MAC numbers are listed in Table 20.

Table 19. The Natural Frequencies for Experimental and Mathematical Models after Updating

	Natural Frequencies of Mathematical Model (Hz)	Natural Frequencies Extracted From Modal Test(Hz)	%Difference
1st Mode	5.6	5.5	1.6
2nd Mode	15.8	15.7	0.4
3rd Mode	36	34.8	3.6
4th Mode	38.3	36.2	5.9
5th Mode	38.4	38	1
6th Mode	44.3	44.2	0.2

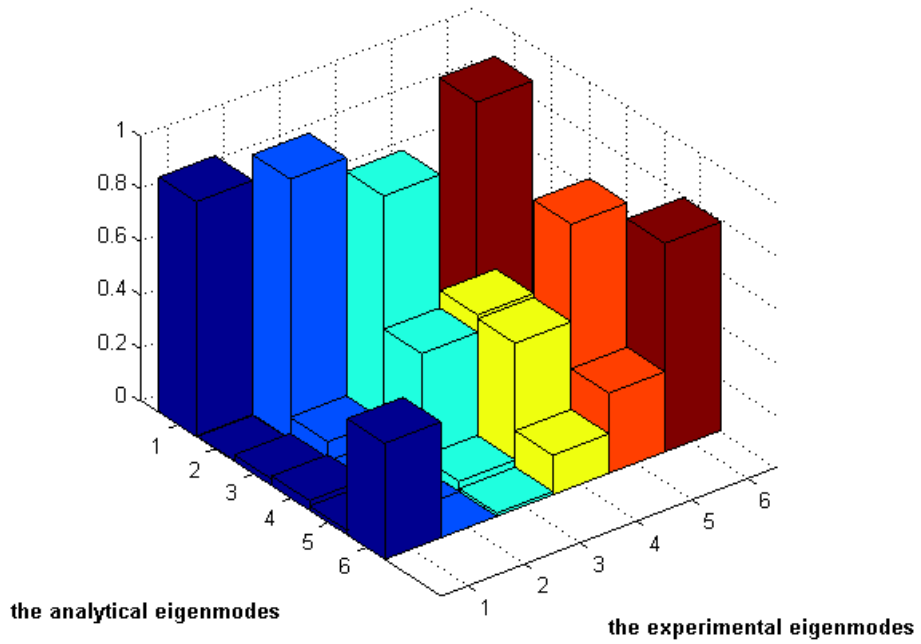


Figure 47. The MAC Plot for the first 6 Mode Shapes After Updating Procedure

Table 20. The MAC Matrix for the Aircraft Model after Updating

MAC NUMBERS	Experimental Model					
Mathematical Model	0.89	0	0	0	0	0.86
	0	0.98	0.05	0.01	0.01	0
	0.02	0.08	0.93	0.14	0.08	0.06
	0.04	0.01	0.43	0.49	0.09	0.08
	0.02	0	0.04	0.48	0.85	0.08
	0.44	0	0.01	0.15	0.3	0.79

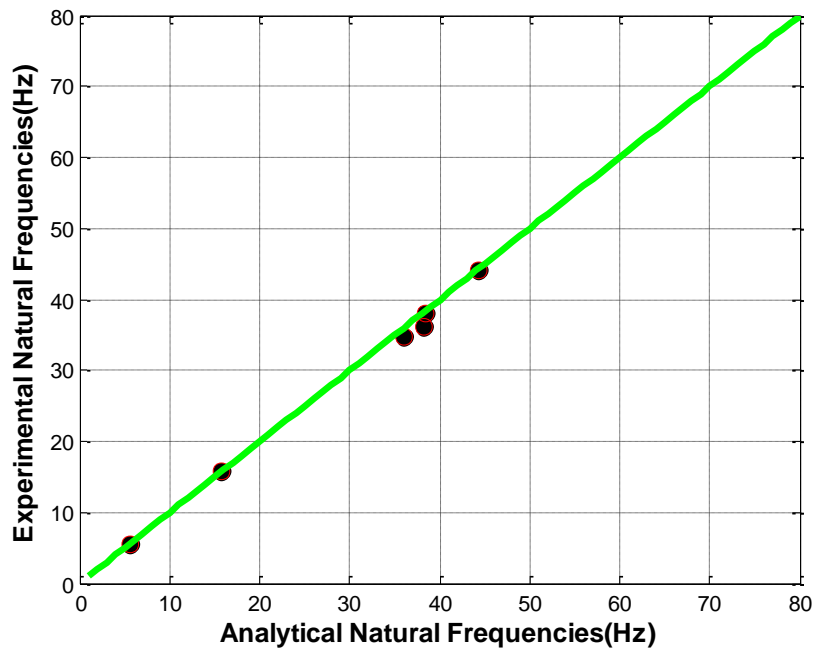


Figure 48. The Comparison of the Experimental and Mathematical Natural Frequency Values After Updating Procedure

As clearly seen from the Table 20, the MAC number of the 3rd mode increased after updating while others did not change anymore. Because the objective function is constructed to decrease the difference in natural frequency values. The visual representation of the comparison of the natural frequencies is given in

Figure 48. Additionally, the percentage of difference between the experimental and mathematical natural frequencies was observed to decrease. Defining the objective function to decrease the first 2 natural frequencies, the algorithm worked to minimize that amount. The percentage of difference decreased from %9.2 to %1.6 for the 1st mode and from %6 to %0.4 for the 2nd mode. To clearly visualize the improvement of the natural frequency values, the table is given below in Table 21.

Table 21. The Comparison of the Natural Frequencies of Mathematical and Experimental Models

	Natural Frequencies of Mathematical Model before Updating(Hz)	Natural Frequencies of Mathematical Model after Updating(Hz)	Natural Frequencies Extracted From Modal Test(Hz)	%Difference before Updating	%Difference after Updating
1st Mode	6	5.6	5.5	9.2	1.6
2nd Mode	16.7	15.8	15.7	6	0.4
3rd Mode	39	36	34.8	12.3	3.6
4th Mode	40.6	38.3	36.2	12.2	5.9
5th Mode	41	38.4	38	7.9	1
6th Mode	46.9	44.3	44.2	6.2	0.2

5.2 CASE STUDY ON A LAUNCHER OF A GUIDED MISSILE USING THE DEVELOPED ALGORITHM WITH INVERSE EIGENSENSITIVITY METHOD

In this part, Inverse Eigensensitivity Method is applied to finite element model of a missile launcher which is demonstrated in Figure 52. To obtain the modal parameters of the missile launcher, modal tests are carried out. Missile launcher finite element model consists of 8 noded linear solid elements, HEX8, 10 noded quadratic linear solid elements, TET10, 4 noded linear shell elements, QUAD4 and 3 noded linear shell elements, TRIA3, in Nastran. There are total number of

373630 elements, 964396 nodes and 5786376 degrees of freedom in the finite element model.

Sensitivity study is carried out to identify the dominant set of parameters on modal results. Parameter sets are grouped and effective parameter sets are selected according to the sensitivity calculations. Totally, 10 parameter sets are investigated with respect to their effects on first 3 natural frequency values and most effective parameter sets are obtained to be used in updating algorithm. Normalized sensitivity values are given consecutively in Figure 49, Figure 50 and Figure 51. Finite element model is divided into subgroups. The selected subgroups are given in Figure 53. Each subpart has its own property identity number which can be updated separately. Initially, the developed code is run with the default settings (Case I); whereas, in order to observe the effectiveness of the method developed, the same model is run by calculating the sensitivities in all iterations (Case II). Model updating parameters were selected as Young's Modulus of each subpart. Eigenvectors are extracted from the 26 grid points. Coordinates of the grid points are selected such that they are coincident with measurement locations in experiment. These points have the potential to move more than the other locations taking into account the first 6 mode shapes obtained from FE analysis. For proper comparison of the mathematical and experimental mode shapes, each mode shape vector is normalized with respect to its element with maximum amplitude. In addition to this, MAC matrix is calculated to quantify the correlation between the mathematical and experimental modes.

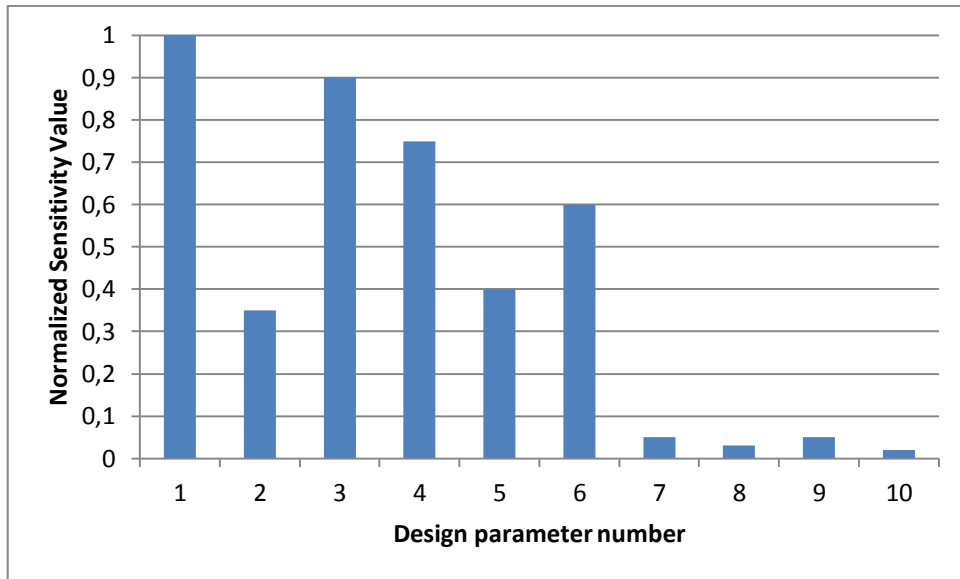


Figure 49. Normalized Sensitivity Values for 1st Natural Frequency

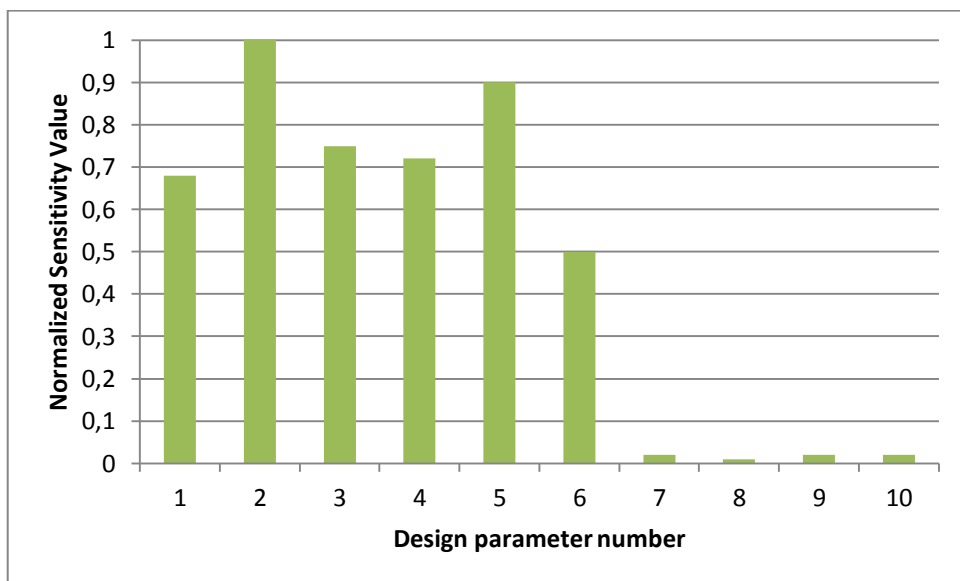


Figure 50. Normalized Sensitivity Values for 2nd Natural Frequency

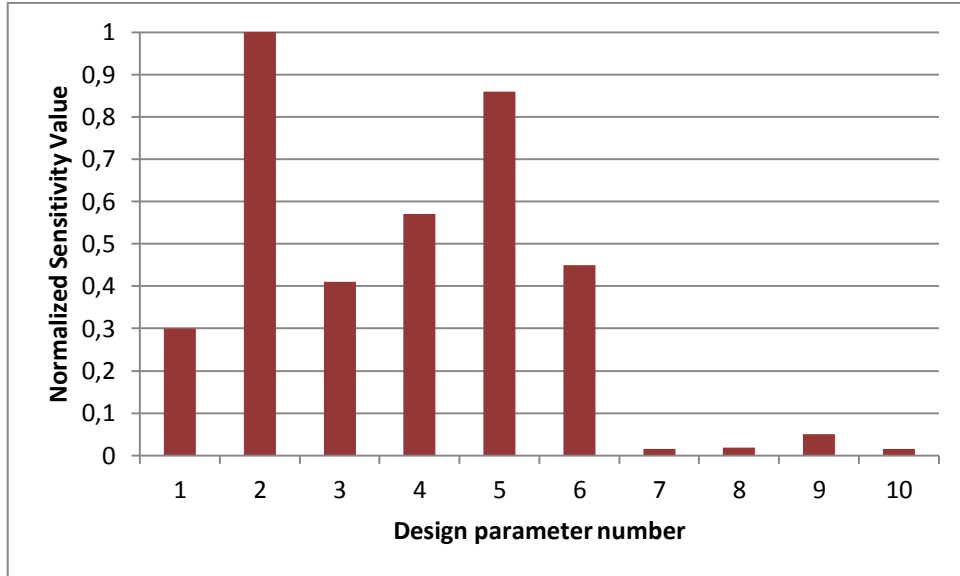


Figure 51. Normalized Sensitivity Values for 3rd Natural Frequency



Figure 52. Missile Launcher

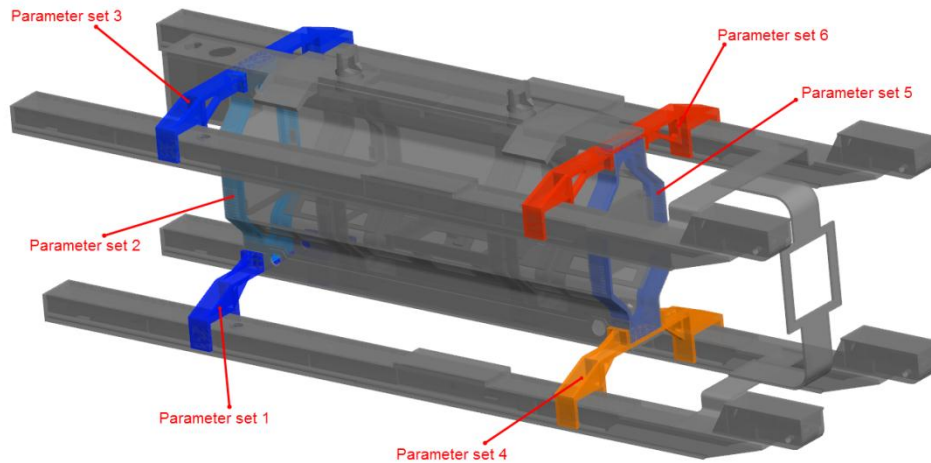


Figure 53. Parameter Sets Defined In Updating Algorithm

Initial correlation between the experimental and mathematical mode shapes is shown in Figure 54 by using the MAC plot, which is summarized in Table 22. It is observed that except the first mode, initially experimental modes are correlated with the different mode number. First 3 natural frequencies and first 3 mode shape are used in updating procedure and updating objective function is constructed to decrease the difference in the first 3 natural frequencies and increase the MAC number values.

The updating procedure is applied by considering Young's Modulus of each subpart shown in Figure 53 as the updating variable. Initially, Young's modulus value is assumed as 71000 MPa for all subparts. Density and Poisson's ratio for each subpart is taken as 2810 kg/m³ and 0.3, respectively.

Natural frequencies and MAC values before and after updating are compared with the experimental one in Table 23. It is observed that the percent difference between the experimental and updated mathematical natural frequencies is decreased prominently. The percent difference decreased from 6.1% to 1.6% for the first mode; from 5.1% to 1.2% for the second mode and from 3.2% to 1.5%

for the third mode for Case I and from 6.1% to 1.5% for the first mode; from 5.1% to 1.2% for the second mode and from 3.2% to 1.4% for the third mode for Case II. Time elapsed to reach convergence is reduced %25 in Case I. Change of design variables is shown in Figure 55 and Figure 56.

Table 22. MAC Matrix for the Missile Launcher Model before Updating

		Experimental Model					
		1 st Mode	2 nd Mode	3 rd Mode	4 th Mode	5 th Mode	6 th Mode
Mathematical Model	1 st Mode	0.969	0.041	0.000	0.000	0.000	0.000
	2 nd Mode	0.956	0.001	0.001	0.000	0.000	0.001
	3 rd Mode	0.000	0.245	0.034	0.007	0.001	0.001
	4 th Mode	0.022	0.705	0.061	0.001	0.001	0.003
	5 th Mode	0.002	0.163	0.860	0.062	0.016	0.003
	6 th Mode	0.008	0.001	0.003	0.003	0.002	0.018
	7 th Mode	0.003	0.000	0.007	0.871	0.112	0.123
	8 th Mode	0.003	0.001	0.018	0.389	0.941	0.000
	9 th Mode	0.005	0.000	0.001	0.286	0.036	0.828

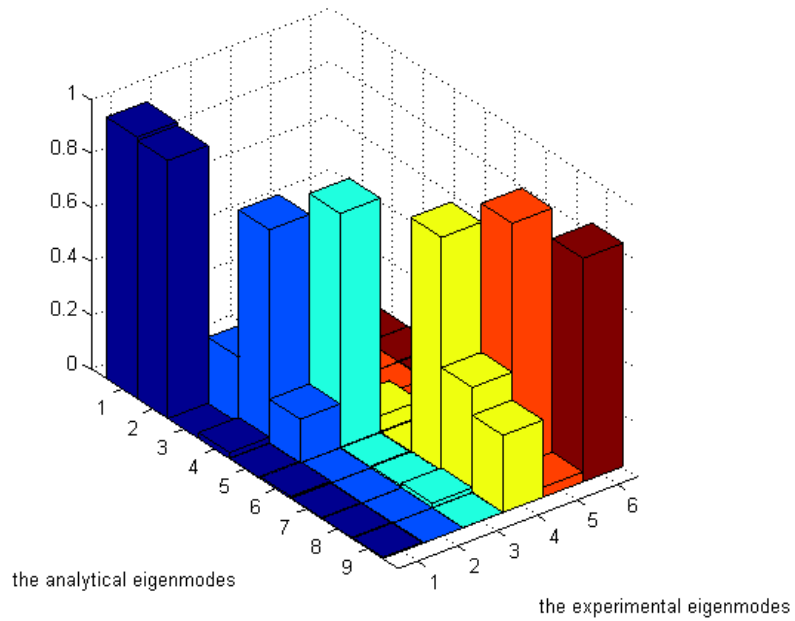


Figure 54. MAC Plot before Updating

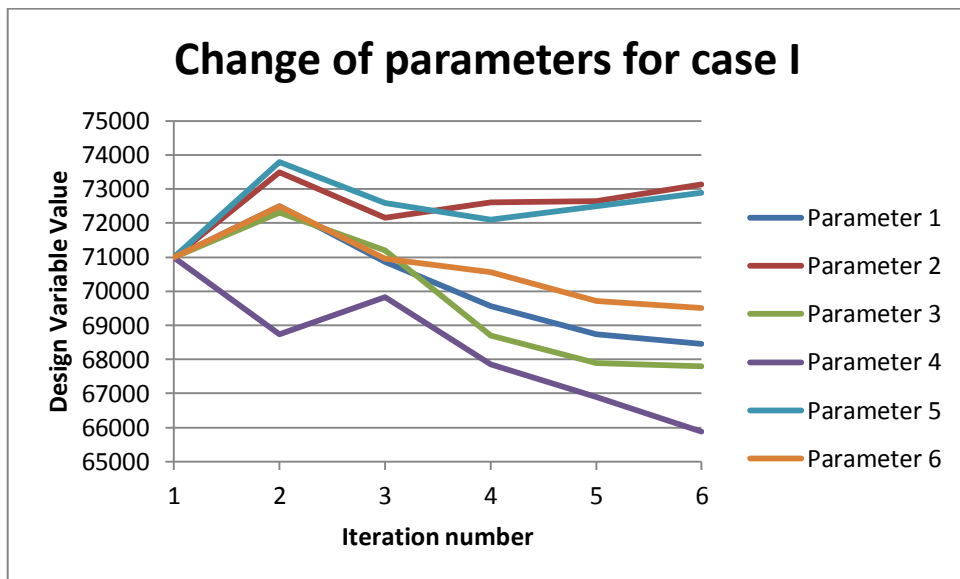


Figure 55. Change of Design Variable for Case I

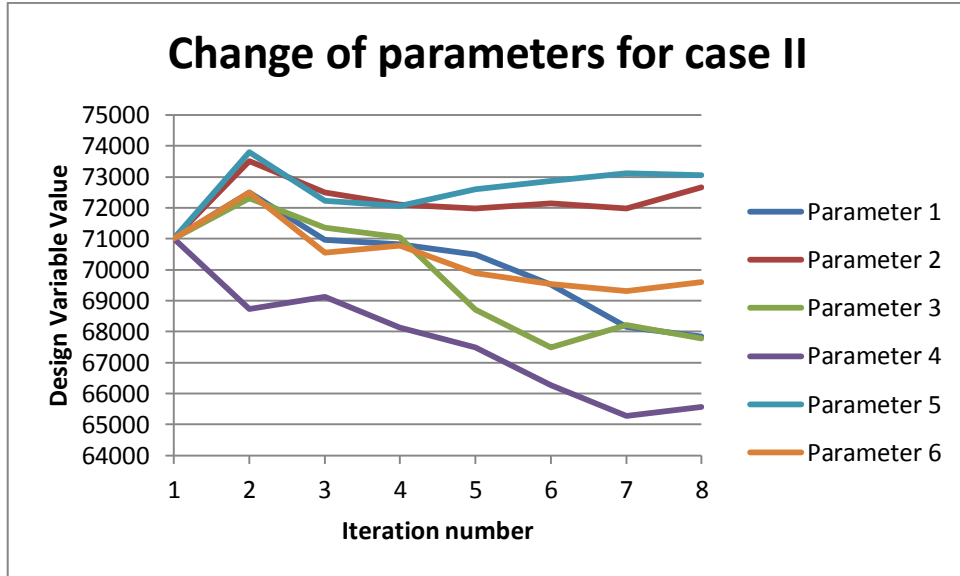


Figure 56. Change of Design Variable for Case II

Table 23. Comparison of the Natural Frequencies and MAC Values

		Natural frequency values		MAC values		Time elapsed(s)
		%Difference before Updating	%Difference after Updating	MAC Value before Updating	MAC Value after Updating	
Case I	1 st Mode	6.1	1.6	0.95	0.96	4120
	2 nd Mode	5.1	1.2	0.7	0.82	
	3 rd Mode	3.2	1.5	0.86	0.87	
Case II	1 st Mode	6.1	1.5	0.95	0.95	5520
	2 nd Mode	5.1	1.2	0.7	0.84	
	3 rd Mode	3.2	1.5	0.86	0.87	

CHAPTER 6

CASE STUDY ON VIBRATION TEST FIXTURE USING FEMTOOLS SOFTWARE

Completing the model updating of simple and large order finite element models, it is concluded to apply model update technique to a vibration test fixture by using commercial software Femtools. It has more capabilities to work with different finite element software and it can handle many different kinds of parameter sets simultaneously. It is also aimed in this thesis work to gain know-how, insight and application of a commercial finite element updating software in addition to developing custom procedures to do model updating work. Femtools uses finite difference method which computes the sensitivity values based on the differential method. It decreases the calculation time for sensitivity matrix and structural matrices in each iteration loop. The fixture is a previously designed test system fixture used to measure the complex modulus of viscoelastic materials [20]. The procedure uses two DOF driving point FRF method which takes 1st natural frequency of test fixture into account. That's why the natural frequency values of the test fixture must be high enough not to extract erroneous results for viscoelastic material. Modal analysis is carried by using Lanczos method within Abaqus software and modal parameters are extracted with commercial code, LMS software. In finite element model of the fixture, concrete and base plate are added to structure to obtain more precise modal results as shown in Figure 57. Concrete block is modeled 250mm wider than the base plate in width; whereas 100mm wider than the base plate in length. The thickness of concrete block is not known exactly. It is the most important discrepancy reason of modal results between mathematical and test model. As an initial assumption, thickness of concrete block is taken as 100mm. Sand under the concrete block is modeled as elastic

foundation in finite element analysis. Side interaction of concrete is assumed as more rigid than the bottom interaction with soil. Because, there is a layer consists of concrete and soil around the lateral surface of concrete block. The stiffness values are assumed 10^{-2}N/mm^3 for side surfaces of concrete and 10^{-1} N/mm^3 for bottom surface. Young's modulus of concrete is taken to be 30000 MPa. The number of nodes is 487021 and the number of elements 193934 for finite element model of fixture. First 3 natural frequency values and mode shapes are given in Figure 58.

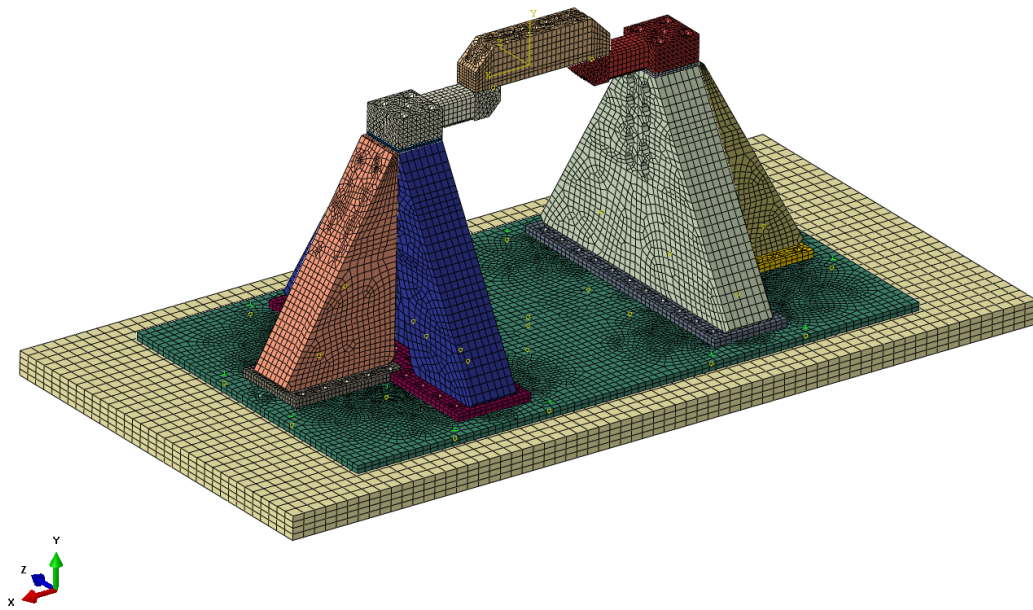
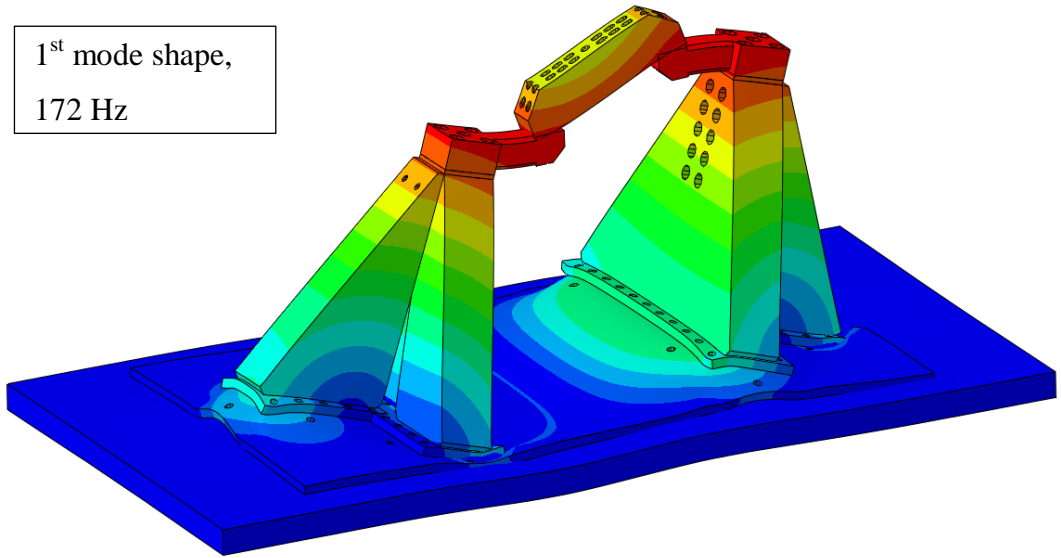
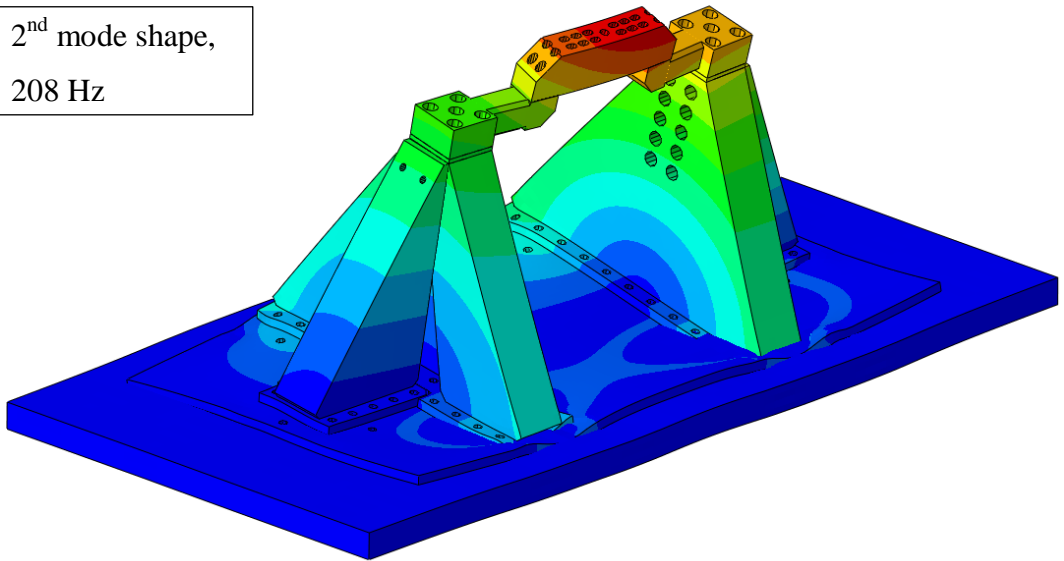


Figure 57. Finite Element Model of Fixture

1st mode shape,
172 Hz



2nd mode shape,
208 Hz



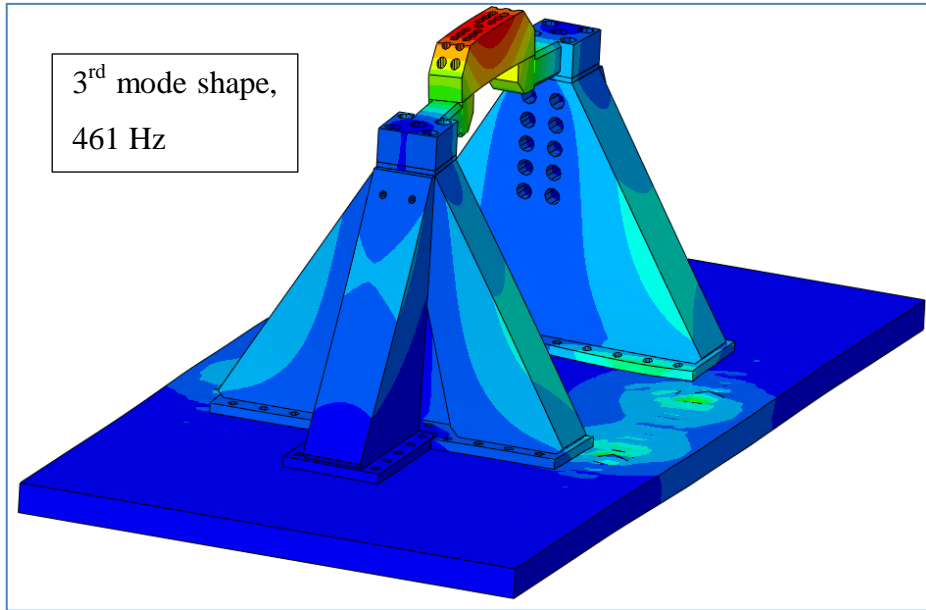


Figure 58. Results of modal analysis of fixture

Modal test is carried with 30 three axis accelerometers as shown in Figure 59. The excitation is made through impact hammer onto 10 locations and 16 directions as given in Figure 60. Impact hammer and modal test configuration are shown in Figure 61 and Figure 62, respectively. The bandwidth of the measurement is 1024Hz and the time of measurement is 4s for each impact. Measurement directions for the accelerometers are given in Figure 63. Driving-point FRF functions are shown Figure 64 and modal frequency values are identified. Modal frequency values are listed in Table 24. The CAD Model of the test fixture is shown in Figure 65.



Figure 61. Impact hammer with plastic tip



Figure 62. Modal test configuration of test fixture

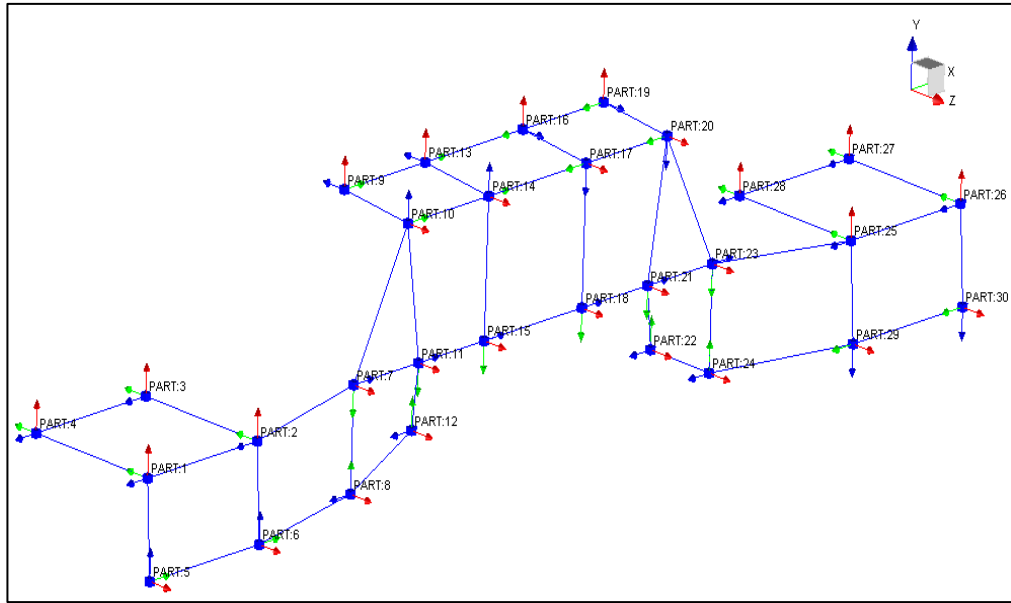


Figure 63. Measurement directions of test fixture

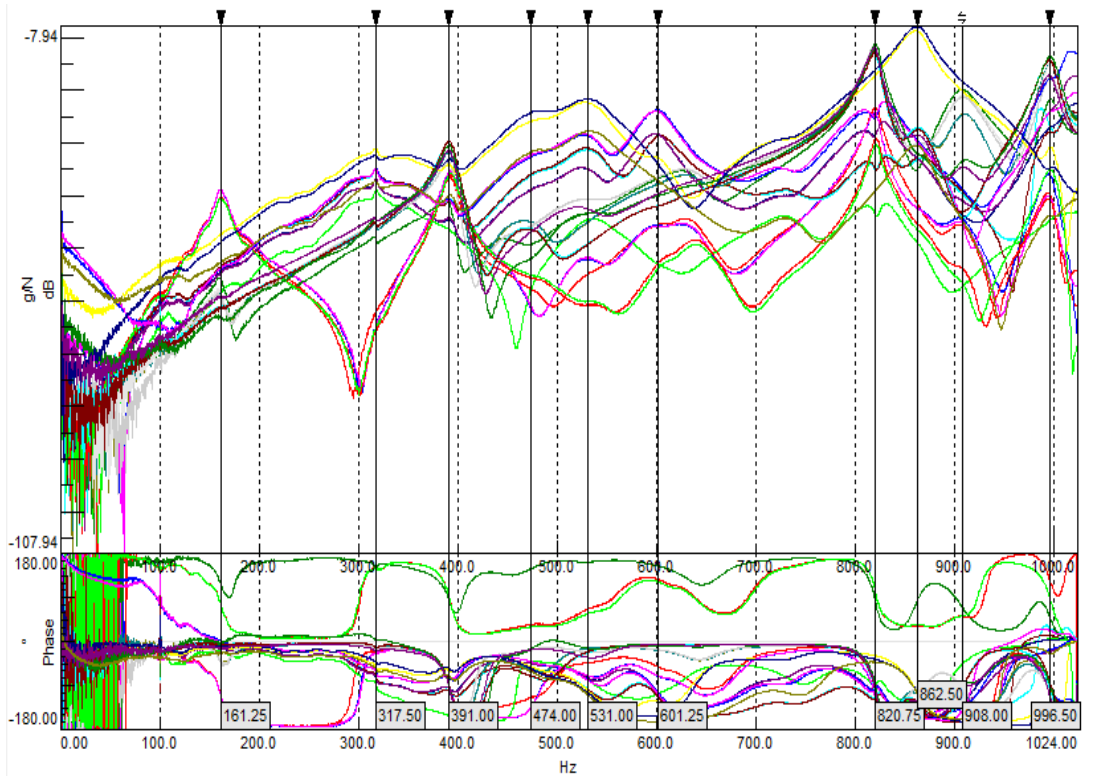


Figure 64. Driving-point FRF functions

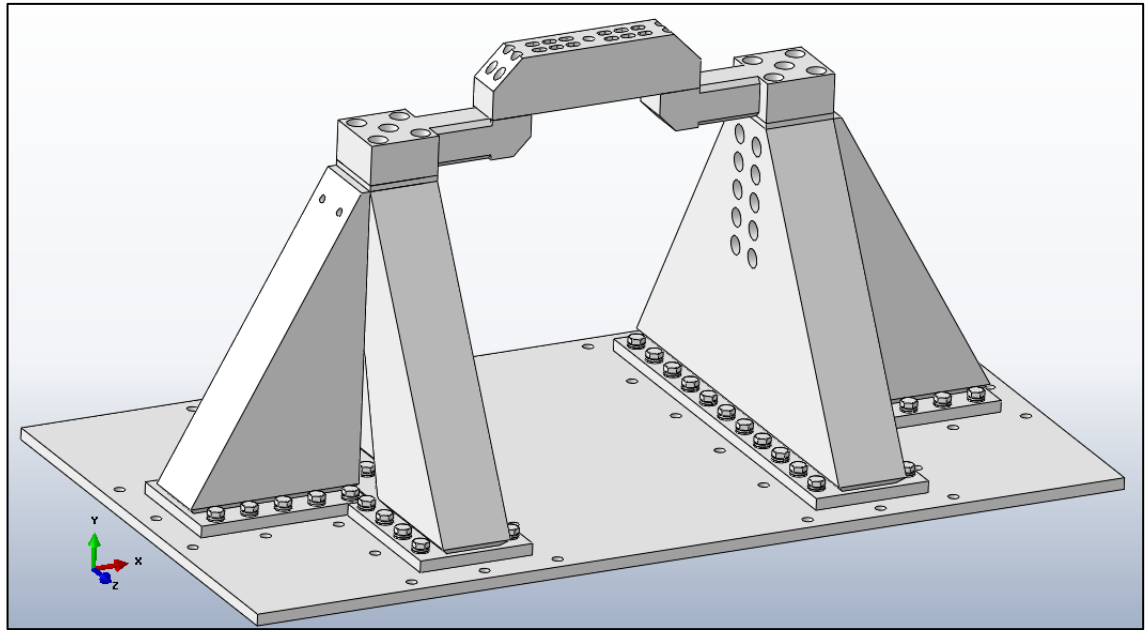


Figure 65. CAD Model of Fixture

Table 24. Modal Frequency Values Extracted from Modal Test

Mode Number	Natural frequency(Hz)
1	162.8
2	317.6
3	393.2
4	439.9
5	474.2
6	479.6
7	530.3
8	601.9
9	629.4
10	823.4
11	862.8
12	904.2

Due to the low correlation of modal results of finite element and test model of fixture, model updating procedure is applied to model. Effective parameters are

investigated by sensitivity analysis on modal results and they are included in updating process. The design parameters and the result of the sensitivity analysis are shown in Figure 66 and Figure 67. According to the sensitivity analysis, 5 parameter sets are selected. The response set in sensitivity analysis includes first 9 natural frequency and MAC numbers as shown in Figure 67. Parameter 1, 2, 3, 5 and 13 are used in updating procedure. Parameters 1, 2 and 3 are the stiffness values of the base in 3 global directions. Parameters 5 and 13 are the stiffness values of the side hole extensions which are made of steel. Initial parameter values are listed in Table 25. 6 iterations are needed to reach convergence. The change of parameters is demonstrated individually with respect to the iteration number in Figure 68 and Figure 69. Femtools interface is shown in Figure 70 and Figure 71. First 3 natural frequencies and first 3 mode shape are used in updating procedure and updating objective function is constructed to decrease the difference in the first 3 natural frequencies and increase the MAC number values. Finishing the model updating procedure, 1st mode frequency difference is decreased from %6 to %2; 2nd mode frequency difference is decreased from %34 to %2 and 3rd mode frequency difference is decreased from %17 to %2. It is also obtained that MAC values are increased up to %84 for 1st mode; %86 for 2nd mode; %89 for 3rd mode. Natural frequencies and MAC values before and after updating are compared with the experimental one in Table 26 and Table 27.

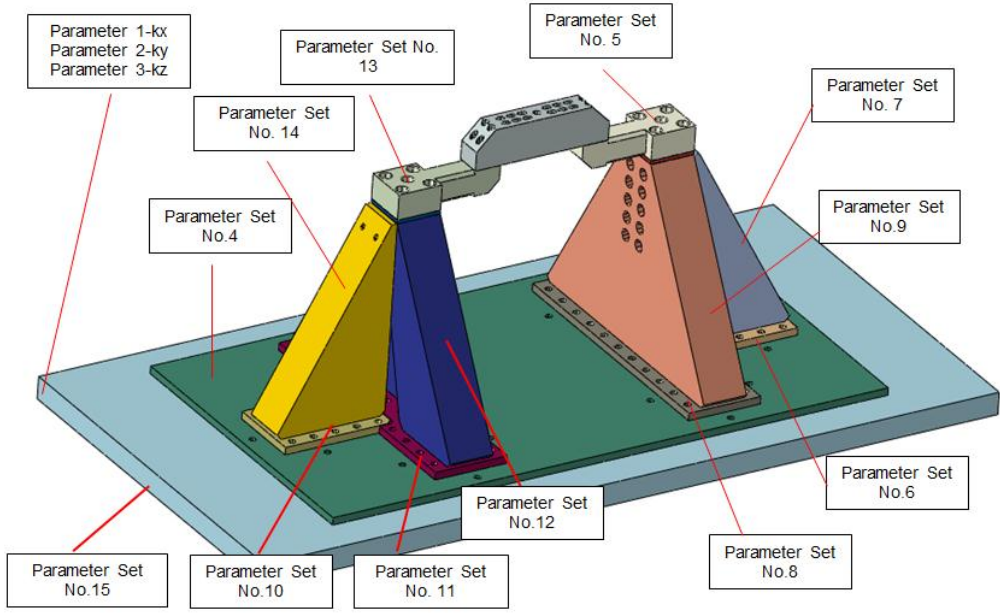


Figure 66. Design Parameters

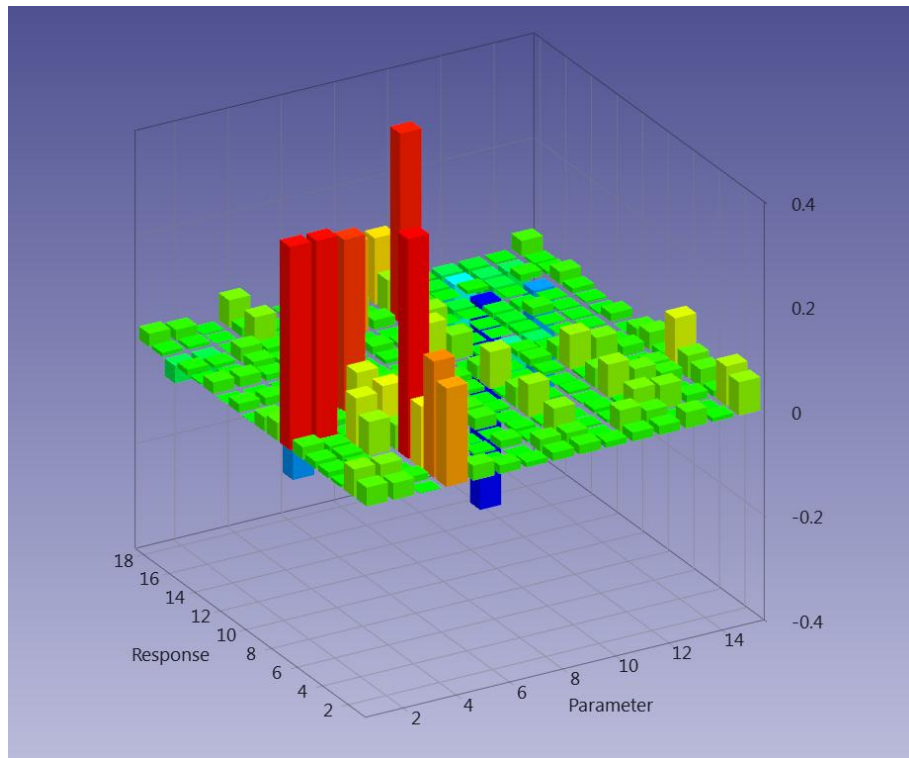


Figure 67. Design Sensitivity Graph

Table 25: Initial Design Parameter Values

Parameters	Parameter Number	Values
K _x (N/mm)	Parameter 1	5000
K _y (N/mm)	Parameter 2	45000
K _z (N/mm)	Parameter 3	5000
E(MPa)	Parameter 4	205000
E(Mpa)	Parameter 5	205000

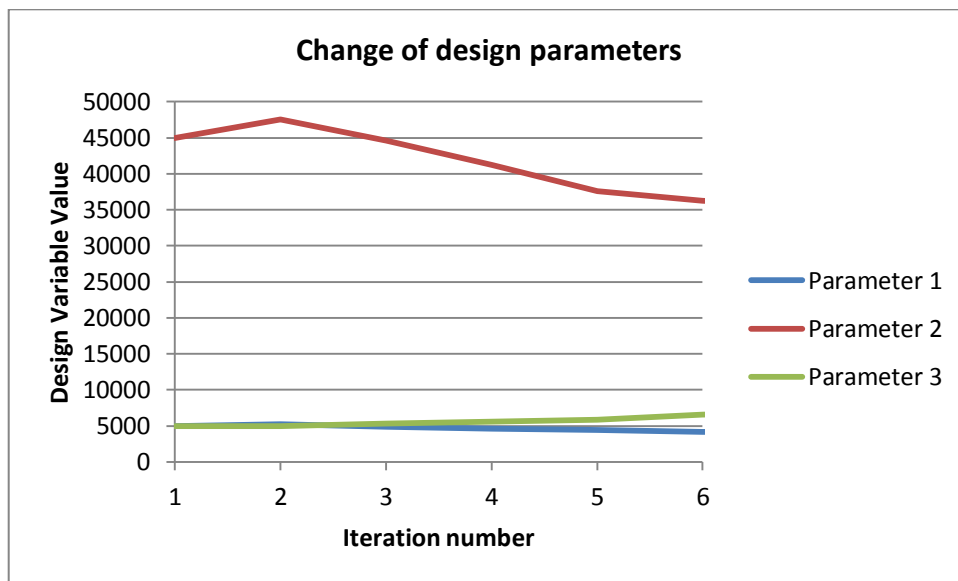


Figure 68. Change of design parameters 1, 2 and 3

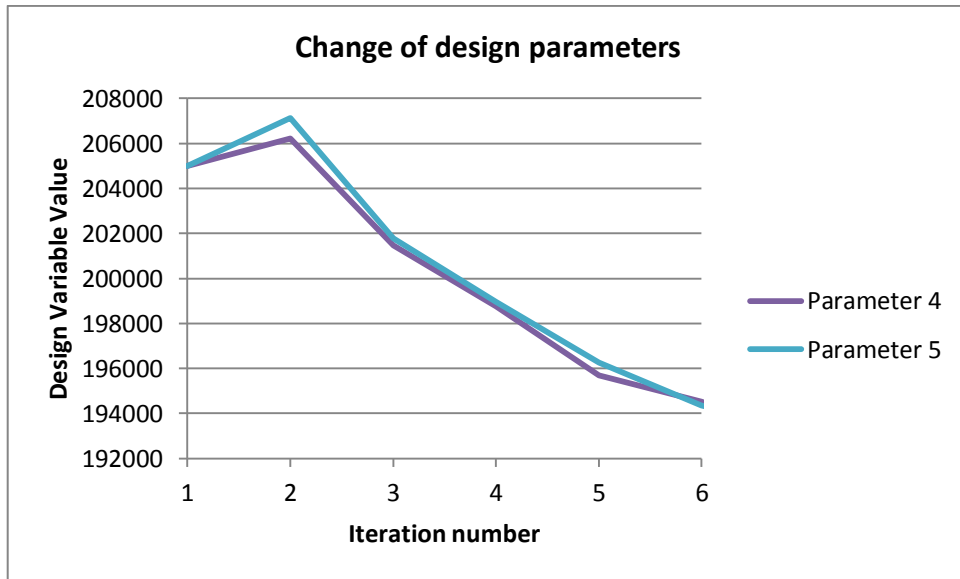


Figure 69. Change of design parameters 4, 5

Table 26: Modal Results before Updating

	Before Updating			
	Frequency(Hz)		% Values	
	Test results	Analysis results	Frequency diff. (%)	MAC values (%)
1st mode	162	172	6.2	70
2nd mode	317	208	34.4	84
3rd mode	393	461	17.3	76

Table 27: Modal Results after Updating

	After Updating			
	Frequency(Hz)		% Values	
	Test results	Analysis results	Frequency diff. (%)	MAC values (%)
1st mode	162	165	1.9	84
2nd mode	317	312	1.6	86
3rd mode	393	400	1.8	89

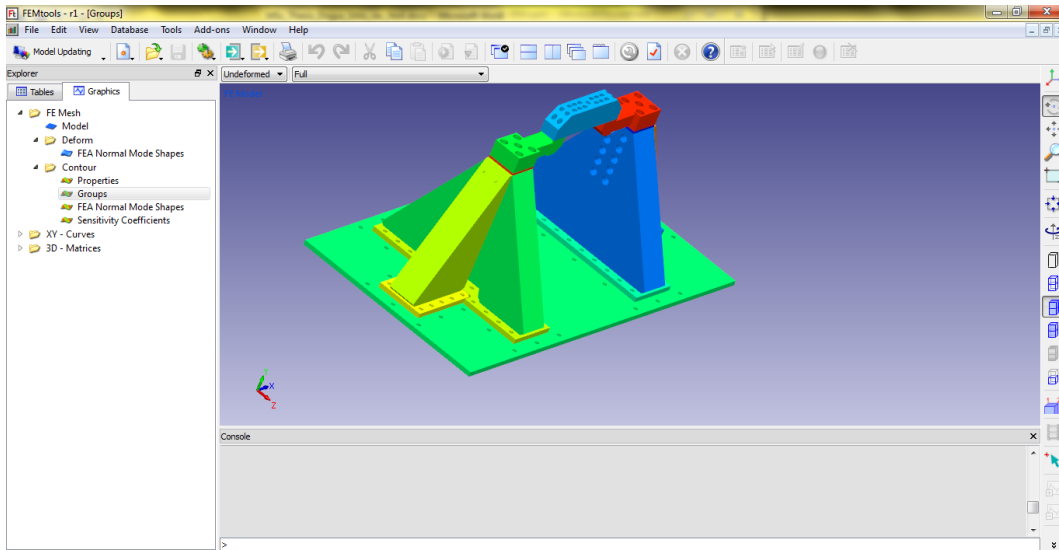


Figure 70. Femtools interface-1

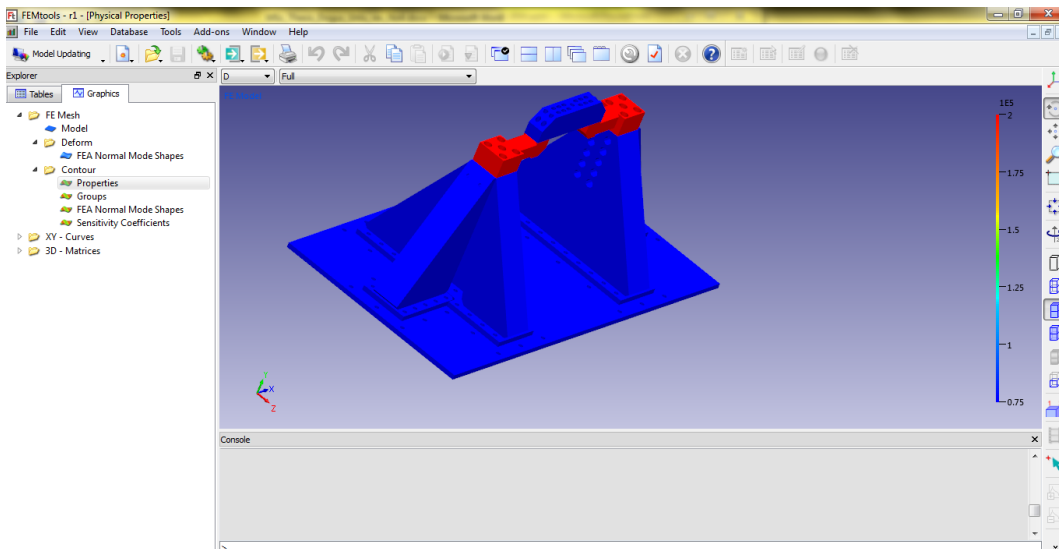


Figure 71. Femtools interface-2

CHAPTER 7

RESULTS AND DISCUSSION

Background information is investigated about model updating theory and it is concluded that iterative methods are suitable for large order finite element models after testing the direct and iterative methods on simple, well known mass-spring system. In that analysis, direct methods have divergent behavior with less number of measurements DOF than the total number of DOF of the system. Direct methods are not appropriate for large order finite element models due to requirement of measuring all DOF of the system.

Eliminating the direct methods for large order finite element models, Inverse Eigensensitivity Method is selected as candidate over Response Function Method. It can effectively be used with the large order finite element models. Whereas; RFM (Response Function Method) have high sensitivity to measurement noise and it can cause erroneous calculations of sensitivity matrices.

An in-house computer code is developed in Matlab in order to perform model updating by using Inverse Eigensensitivity Method. The developed computer code uses commercial finite element software as a solver from where the modal results and sensitivities are obtained. To reduce the computational time, sensitivity matrix calculations are only executed when a specific error slope criterion is met. As the 1st application case, the improved code is applied on the GARTEUR structure and considerable improvement is obtained with updating process. The percentage of difference decreased from %9.2 to %1.6 for the natural frequency of 1st mode and from %6 to %0.4 for the natural frequency of 2nd mode.

Completing the application of code to GARTEUR model, large order finite element model of a missile launcher is updated via the improved custom Matlab code. The updating process is carried out taking into account the first 3 natural frequencies and the first 3 eigenvectors in the objective function. The results acquired showed that natural frequencies of the first 3 modes are improved prominently and MAC number of 2nd mode shape is increased. It is concluded that with the developed computer code, it is possible to analyze the sensitivity of the modal results with respect to the parameters of finite element model and large order finite element models can be updated effectively by using the subparts in the finite element model.

A previously designed special vibration test fixture is used as another structure for application of the model updating procedure. Due to the complex parameters of the test fixture and capability of handling many different parameter sets at the same time, commercial model updating software is used. Due to the unknown factors about the test fixture such as base material thickness, foundation stiffness, there is substantial amount of difference between the experimental and mathematical results of test fixture. Finishing the model updating procedure, 1st mode frequency difference is decreased from %6 to %2; 2nd mode frequency difference is decreased from %34 to %2 and 3rd mode frequency difference is decreased from %17 to %2. It is also obtained that MAC values are increased up to %84 for 1st mode; %86 for 2nd mode; %89 for 3rd mode.

In case of a divergent solution with the developed algorithm, there could be two reasons for that problem. First one is about the number of the measured coordinates from the modal test. Number of measured coordinates must be more than the number of design variables to have over determined problem. Another reason is about the parameter selection for updating process. Effective parameters must be selected to have reasonable results at the end of the updating which requires pre-analysis of structure to find the most effective parameter sets on modal results.

As a future work, code can be modified to work with some other commercial finite element software and different effective model update methods, correlation techniques can be added to algorithm to have more useful, generalized model update tool.

REFERENCES

- [1] **Fox, R. L., M. P. Kapoor.**, "Rates Of Change of Eigenvalues and Eigenvectors", *Aiaa Journal* 6.12 (1968): 2426-2429.
- [2] **Link, M. And Santiago, O.F.**, "Updating and Localizing Structural Errors Based On Minimisation of Equation Errors", *International Conference on Spacecraft Structures and Mechanical Testing*, Esa/Estec, Noordwijk, Holland, 1991
- [3] **Lin R.M., Zhu J.**, "Finite element model updating using vibration test data under base excitation", *Journal of Sound and Vibration*, 2007, p.596–613.
- [4] **K.S. Kwon, R.M. Lin**, "Frequency selection method for FRF-based model updating", *Journal of Sound and Vibration*, 278 (2004) 285-306.
- [5] **Schwarz, B., Richardson, M. and Formenti, D.L.**, "FEA model updating using SDM", *Sound Vib.* v41. 18-23.
- [6] **Wu Haishan, Limin Sun.**, "Model Updating By Combining Substructure Energy Functions and Subset Selection". *Dynamics of Civil Structures*, Volume 4 (2011): 63-70.
- [7] **Carvalho, Joao et al.**, "A Direct Method for Model Updating With Incomplete Measured Data and Without Spurious Modes". *Mechanical Systems and Signal Processing* 21.7 (2007): 2715-2731.
- [8] **W. X. Ren, H. B. Chen**, "Finite element model updating in structural dynamics by using the response surface method", *Engineering Structures* 32 (8) (2010) 2455 – 2465.
- [9] **Göge D.**, "Automatic updating of large aircraft models using experimental data from ground vibration testing ", *Aerospace Science and Technology*, Vol. 7, pp 33–45, 2003.
- [10] **Göge D., Link M.**, "Assessment of computational model updating procedures with regard to model validation", *Aerospace Science and Technology*, Vol. 7, pp 47-61, 2003.
- [11] **Schedlinski C.**, "Computational Model Updating of Large Scale Finite Element Models", *International Modal Analysis Conference*, San Antonio, 2000.
- [12] **Schedlinski C., Göge D., Link M.**, "Parameter Identification and validation of large order finite element models for industrial type structures", *Third European Conference on Structural Control*, Vienna, Austria, 12-15 July 2004
- [13] **Sipple Jesse D., Sanayei Masoud**, "Finite element model updating of the UCF grid benchmark using measured frequency response functions", *Mechanical Systems and Signal Processing* 46(2014)179–190

- [14] **Baiyong Gou, Weijie Zhang , Qiuhai Lu , Bo Wang**, "A Successive Selection Method for finite element model updating ", *Mechanical Systems and Signal Processing* 70-71(2016)320–333
- [15] **Ewins, D.**, *Modal testing*. Baldock, England: Research Studies Press, 2000
- [16] **Friswell, M. and Mottershead, J.**, *Finite element model updating in structural dynamics*, Springer.,2011
- [17] **Maia N. M. M., Silva J.M.M.**, *Theoretical and Experimental Modal Analysis*, Research Studies Press, 1998.
- [18] **Allemang, R. J. and Brown, D. L.**, "A correlation coefficient for modal vector analysis" 1st International Modal Analysis Conference, pp. 110-116. 1982.
- [19] **J.C.O'Callahan, P.Li**, "SEREP Expansion", Fourteenth International Modal Analysis Conference, Detroit, Michigan, Feb 1996
- [20] **Erol F.**, *Development of a Test System for Viscoelastic Material Characterization*, Master's Thesis, METU, 2014

APPENDIX

Finite Element Model Reduction and Expansion Techniques

I. Guyan or Static Reduction

In literature, Guyan reduction is also known as static reduction [15]. All structural matrices, force matrix and displacement matrix are partitioned into master and slave degrees of freedom. Master coordinates are needed to be kept and the slave degrees of freedom will be disregarded [15]. By assuming the force is applied only to the master coordinates. Then the following equation can be written [15],

$$\begin{bmatrix} [M_{mm}] & [M_{ms}] \\ [M_{sm}] & [M_{ss}] \end{bmatrix} \begin{Bmatrix} \{\ddot{x}_m\} \\ \{\ddot{x}_s\} \end{Bmatrix} + \begin{bmatrix} [K_{mm}] & [K_{ms}] \\ [K_{sm}] & [K_{ss}] \end{bmatrix} \begin{Bmatrix} \{x_m\} \\ \{x_s\} \end{Bmatrix} = \begin{Bmatrix} \{F_m\} \\ \mathbf{0} \end{Bmatrix} \quad (1)$$

The subscript ‘m’ is related to the master coordinates and the subscript ‘s’ is related to the slave coordinates. M is mass matrix, K is stiffness matrix, x is displacement and \ddot{x} is the acceleration where F_m is applied force to the master coordinate. Based on the assumption that the inertial forces are negligible, the equation (1) is written in a more compact form in terms of stiffness matrices [15],

$$K_{sm}x_m + K_{ss}x_s = 0 \quad (2)$$

The equation above which is referenced by equation number of (2) can be reoriented to disregard the slave coordinates such that [15],

$$\begin{Bmatrix} \{x_m\} \\ \{x_s\} \end{Bmatrix} = \begin{bmatrix} [I] \\ -[K_{ss}]^{-1}[K_{sm}] \end{bmatrix} \{x_m\} = [T_s] \{x_m\} \quad (3)$$

In equation (3), $[T_s]$ designates the transformation vector between the master coordinates and full system coordinates and $[I]$ designates the identity matrix. Then equation (3) can be written in different way as follows [15]:

$$\{x\} = [T_s] \{x_m\} \quad (4)$$

And after taking the transpose of both hand side of the equation (4) [15],

$$\{x\}^T = \{x_m\}^T [T_s]^T \quad (5)$$

By writing the potential and kinetic energy equations in terms of mass, stiffness and displacement vectors as follows[15]:

$$PE = \frac{1}{2} \{x\}^T [K] \{x\} \quad (6)$$

$$KE = \frac{1}{2} \{\dot{x}\}^T [M] \{\dot{x}\} \quad (7)$$

In the above equations, the PE designates the potential energy and KE designates the kinetic energy, x is displacement and \dot{x} is the velocity. After substituting the equations (4) and (5) into equation (6) and (7), the modified formulas can be written as follows [15]:

$$PE = \frac{1}{2} \{x_m\}^T [T_s]^T [K] [T_s] \{x_m\} \quad (8)$$

$$KE = \frac{1}{2} \{\dot{x}_m\}^T [T_s]^T [M] [T_s] \{\dot{x}_p\} \quad (9)$$

In the above equations, the term $[T_s]^T [K] [T_s]$ defines the reduced stiffness matrix and $[T_s]^T [M] [T_s]$ defines the reduced mass matrix. The assumptions and

derivations are only valid for the zero frequency response functions. By increasing the frequency, the inertial terms and mass effects dominates the dynamic behavior [15].

II. Dynamic Reduction

This method was developed to modify the static reduction for a system which there is an effect of the dynamic forces on the system [15]. The transformation equation given in equation (3) was modified to take the inertial effects into account. The inertial forces were added to system matrices at the selected frequency. Reordering and modifying the equation (3), the equation ends up as follows [17];

$$\begin{Bmatrix} \{x_m\} \\ \{x_s\} \end{Bmatrix} = \begin{bmatrix} [I] \\ -([K_{ss}] - \omega^2 [M_{ss}])^{-1} ([K_{sm}] - \omega^2 [M_{sm}]) \end{bmatrix} \{x_m\} = [T_d] \{x_m\} \quad (10)$$

The subscript ‘m’ is related to the master coordinates and the subscript ‘s’ is related to the slave coordinates. M is mass matrix, K is stiffness matrix and x is displacement. Then the reduced mass and stiffness matrices can be written by substituting the equation above [17].

III. Improved Reduced System

Improved Reduction System was proposed by O’Callahan [19] by including the inertial terms to the static condensation formulas.

The equation of motion for the dynamic system in frequency domain was written as [15];

$$\left(\begin{bmatrix} [K_{ss}] & [K_{sm}] \\ [K_{ms}] & [K_{mm}] \end{bmatrix} - \omega^2 \begin{bmatrix} [M_{ss}] & [M_{sm}] \\ [M_{ms}] & [M_{mm}] \end{bmatrix} \right) \begin{Bmatrix} \{x_s\} \\ \{x_m\} \end{Bmatrix} = \begin{Bmatrix} \{0\} \\ \{0\} \end{Bmatrix} \quad (11)$$

The subscript ‘m’ is related to the master coordinates and the subscript ‘s’ is related to the slave coordinates. M is mass matrix, K is stiffness matrix and x is displacement. The equation (11) is valid where w equals to the natural frequencies of the system. By considering the first part of the equality in equation (11), the following formula can be reached [15];

$$\{x_s\} = -\left[[K_{ss}] - w^2[M_{ss}]\right]^{-1} \left[[K_{sm}] - w^2[M_{sm}]\right] \{x_m\} \quad (12)$$

By substituting $[K_{ss}]^{-1}$ term as division and multiplication into the equation (12), the formula can be rewritten as follows [15]:

$$\{x_s\} = -\left[[I] - w^2[K_{ss}]^{-1}[M_{ss}]\right]^{-1} [K_{ss}]^{-1} \left[[K_{sm}] - w^2[M_{sm}]\right] \{x_m\} \quad (13)$$

Using the binomial theorem and writing the dynamic equation balance in frequency domain by the static reduction process [15]:

$$w^2 \{x_m\} = [M_r]^{-1} [K_r] \{x_m\} \quad (14)$$

Where M_r is reduced mass matrix and K_r is reduced stiffness matrix. $K_r = [T_s]^T [K] [T_s]$ and $M_r = [T_s]^T [M] [T_s]$. And using the above formula by substituting into the equation (13), the equation can be written as follows[15]:

$$\{x_s\} = -[K_{ss}]^{-1} \left[[K_{sm}] - \left([M_{sm}] + [K_{ss}]^{-1}[M_{ss}][K_{sm}]\right)[M_r]^{-1}[K_r]\right] \{x_m\} \quad (15)$$

The equation (15) can be written in a more compact form [15],

$$\{x_s\} = \left(T_s + SMT_s M_r^{-1} K_r\right) \{x_m\} \quad (16)$$

In equation (16), T_s is static reduction transformation matrix which equals to $-[K_{ss}]^{-1}[K_{sm}]$.

The transformation matrix for improved reduced system can be written as follows [15]:

$$T_i = T_s + SMT_s M_r^{-1} K_r \quad (17)$$

IV. SEREP(System Equivalent Reduction Expansion Process)

The system equivalent reduction process which was introduced by O'Callahan and Li [19], uses the eigenvectors to relate the master and slave coordinates. The method takes into account the dynamic behavior of the system by keeping the eigenvectors.

The displacement vector can be written by generalized coordinates as follows [15]:

$$\begin{Bmatrix} \{x_s\} \\ \{x_m\} \end{Bmatrix} = \begin{bmatrix} [\varphi_{ss}] & [\varphi_{sm}] \\ [\varphi_{ms}] & [\varphi_{mm}] \end{bmatrix} \begin{Bmatrix} \{u_s\} \\ \{u_m\} \end{Bmatrix} \quad (18)$$

where u term defines the generalized coordinates; the subscript 'm' is related to the master coordinates and the subscript 's' is related to the slave coordinates and $[\varphi]$ denotes mode shape matrix.

The principal displacement equation can be written as follows [15]:

$$\{x_p\} = [\varphi_{ms}] \{u_s\} + [\varphi_{mm}] \{u_m\} \quad (19)$$

where x_p is principal displacement. By rewriting the general equation (18) in more general way and extracting the part belongs to the master coordinates [15],

$$\{x_m\} = [\varphi_m] \{u\} \quad (20)$$

Then after taking the generalized inverse of both sides of the equation (20),

$$\{u\} = [\varphi_m]^+ \{x_m\} \quad (21)$$

The $[\varphi_m]$ matrix has the $(n_p \times m)$ size in which n_p defines the number of primary degrees of freedom and m defines the number of modes considered.

If $n_p > m$, the generalized inverse is formulized as [15]:

$$[\varphi_m]^+ = [\varphi_m^T \quad \varphi_m]^{-1} \varphi_m^T \quad (22)$$

If $n_p < m$, the generalized inverse is formulized as [15]:

$$[\varphi_m]^+ = \varphi_m^T [\varphi_m^T \quad \varphi_m]^{-1} \quad (23)$$

By reusing the general formula for the generalized coordinates [15],

$$\begin{Bmatrix} \{x_s\} \\ \{x_m\} \end{Bmatrix} = \begin{bmatrix} [\varphi_s] \\ [\varphi_m] \end{bmatrix} [\varphi_m]^+ \{x_m\} \quad (24)$$

The transformation matrix for the SEREP can be written as follows [15]:

$$T_{SEREP} = \begin{bmatrix} [\varphi_s] \\ [\varphi_m] \end{bmatrix} [\varphi_m]^+ \quad (25)$$

The SEREP method keeps the eigendata for the master degrees of freedom. It has advantageous aspects over the static condensation method [17]. The method is needed to be chosen where the model is used in a way of application area. The Guyan reduction is advantageous because of its simplicity to be applied [15]. Another reason can be explained as the use of the lower order eigendata in general applications. For that reason, the effect of the dynamic characteristics is generally low in which Guyan reduction process is applied. But in applications that the dynamic behavior is more substantial and the higher order modes are important,

the SEREP method or Improved Reduction System can be applied to the model [15].

I. Expansion using Theoretical Spatial Model – Kidder’s Method

This method is based on the mathematical mass and stiffness matrix by applying the similar procedure given in Guyan reduction method. The generalized eigenvalue problem can be partitioned as follows [17]:

$$\left(\begin{bmatrix} [K_{ss}] & [K_{sm}] \\ [K_{ms}] & [K_{mm}] \end{bmatrix} - w_r^2 \begin{bmatrix} [M_{ss}] & [M_{sm}] \\ [M_{ms}] & [M_{mm}] \end{bmatrix} \right) \begin{Bmatrix} \{\varphi_s\}^r \\ \{\varphi_m\}^r \end{Bmatrix} = \begin{Bmatrix} \{0\} \\ \{0\} \end{Bmatrix} \quad (26)$$

In equation (26), $\{\varphi_m\}^r$ belongs to the eigenvector of the measured degrees of freedom and $\{\varphi_s\}^r$ belongs to the eigenvector of the unmeasured degrees of freedom; $[M]$ belongs to mass matrix and $[K]$ belongs to stiffness matrix and w_r is the natural frequency of r^{th} mode. By writing the 1st row of the equation (26) [17],

$$[[K_{ss}] - w_r^2 [M_{ss}]] \{\varphi_s\}^r = -[[K_{sm}] - w_r^2 [M_{sm}]] \{\varphi_m\}^r \quad (27)$$

Then for the r th slave mode shape vector can be written as [17]:

$$\{\varphi_s\}^r = -[[K_{ss}] - w_r^2 [M_{ss}]]^{-1} [[K_{sm}] - w_r^2 [M_{sm}]] \{\varphi_m\}^r \quad (28)$$

By applying the given formulation, the unmeasured degrees of freedom can be filled out by using the mathematical spatial data [17]. Awareness must be carried out by applying this technique. Because the matrix can be ill conditioned and the inverse procedure can cause erroneous solutions [17]. These problems generally can be solved by using the generalized inverse procedure instead of the direct inversion procedure [17].

II. SEREP Expansion Technique

The method is similar as the reduction procedure given in SEREP reduction. The procedure is based on the assumption that the full displacement vector can be formulated with the modes of the master coordinates [17].

$$\begin{Bmatrix} \{x_s\} \\ \{x_m\} \end{Bmatrix} = \begin{bmatrix} [\varphi_s] \\ [\varphi_m] \end{bmatrix} \{q\} \quad (29)$$

The subscript ‘m’ is related to the master coordinates and the subscript ‘s’ is related to the slave coordinates; $[\varphi]$ denotes mode shape matrix, x is displacement, and q is generalized coordinate vector. By using the row from above equation (29) for the master coordinates [17],

$$\{x_m\} = [\varphi_m] \{q\} \quad (30)$$

Then by using the generalized inverse for the equation (30), the generalized coordinate vector can be derived as follows [17]:

$$\{q\} = [\varphi_m]^+ \{x_m\} \quad (31)$$

The general equation can be rewritten as follows [17]:

$$\{x\} = \begin{bmatrix} [\varphi_s] \\ [\varphi_m] \end{bmatrix} [\varphi_m]^+ \{x_m\} \quad (32)$$

Then the transformation matrix for SEREP expansion can be written as [17],

$$T_{SEREP} = \begin{bmatrix} [\varphi_s] \\ [\varphi_m] \end{bmatrix} [\varphi_m]^+ \quad (33)$$

Measurement Coordinate Numbers in IEM

I. More Measurement Coordinates than the Number of Design Parameters

Assuming the number of equations is more than the number of parameters, the set of equations is over determined. By using the definition of the least square solution and pseudo-inverse, the general equation (3.17) can be written as [16]:

$$\{\delta\theta\} = \left[\{S\}^T \{S\} \right]^{-1} \{S\}^T \{\delta z\} \quad (34)$$

The above equation can be reorganized with respect to the iteration number:

$$\{\theta\}_{j+1} = \{\theta\}_j + \left[\{S\}_j^T \{S\}_j \right]^{-1} \{S\}_j^T \left(\{z\}_m - \{z\}_j \right) \quad (35)$$

Subscript ‘ j ’ indicates the j^{th} iteration, whereas subscript ‘ m ’ indicates the measured quantities extracted from the experiment, S is sensitivity matrix, θ is parameter vector and z is result vector.

By defining the error or difference between the measured results and mathematical results [16]:

$$\varepsilon = \{\delta z\} - \{S\} \{\delta\theta\} \quad (36)$$

The objective function which needs to be minimized can be introduced as [16]:

$$F(\{\delta\theta\}) = \varepsilon^T \varepsilon \quad (37)$$

By using the definition of the error term and inserting the related term in equation (37), the equation is modified as [16]:

$$F(\{\delta\theta\}) = \left\{ \{\delta z\} - S \{\delta\theta\} \right\}^T \left\{ \{\delta z\} - S \{\delta\theta\} \right\} \quad (38)$$

By expanding the equation (38) [16];

$$F(\{\delta\theta\}) = \{\delta z\}^T \{\delta z\} - 2\{\delta\theta\}^T S^T \{\delta z\} + \{\delta\theta\}^T S^T S \{\delta\theta\} \quad (39)$$

The general problem with the given formulation, the equal weight is given to each element of the experimental results. In general, the natural frequency values can be extracted with high accuracy whereas the eigenvectors cannot [16]. The eigenvectors extracted from modal test contain more error with respect to the natural frequency values of the test structure [16]. For that reason, weighting matrix must be introduced to the general formula:

$$F(\{\delta\theta\}) = \{\varepsilon\}^T [W_{\varepsilon\varepsilon}] \{\varepsilon\} \quad (40)$$

The $[W_{\varepsilon\varepsilon}]$ term defines the weighting matrix which is diagonal [16]. Its elements are the reciprocals of the variance of the experimental results. By reorienting the given equations including the weighting matrix, equation (34) and (35) can be written as [16]:

$$\{\delta\theta\} = \left[\{S\}^T [W_{\varepsilon\varepsilon}] \{S\} \right]^{-1} \{S\}^T [W_{\varepsilon\varepsilon}] \{\delta z\} \quad (41)$$

$$\{\theta\}_{j+1} = \{\theta\}_j + \left[\{S\}_j^T [W_{\varepsilon\varepsilon}] \{S\}_j \right]^{-1} \{S\}_j^T [W_{\varepsilon\varepsilon}] (\{z\}_m - \{z\}_j) \quad (42)$$

By assuming the matrix $\left[\{S\}^T [W_{\varepsilon\varepsilon}] \{S\} \right]$ is square and full rank, the set of equations can be solved. There may be some problems with the solution of the equations. The design parameter set solution given in equation (34) and (41) may be ill conditioned [16]. There are 2 reasons for the ill condition equations. First, the chosen set of design parameters has really low effect on the measurements. The second reason is that the set of parameters can have same kind of effects on the results [16].

II. Less Measurement Coordinates than the Number of Design Parameters

In many real case problems, the number of measurement coordinates is less than the number design parameters. The resulting equation set is under determined which means the number of unknowns is greater than the number of equations [16]. Infinite numbers of solutions satisfy the equations. Singular Value Decomposition or Moore-Penrose inverse for under determined equations can be used to solve these types of equations [16].

By using Lagrange Multiplier technique, the general equation can be written as [16]:

$$\{\delta\theta\} = \{S\}^T \left[\{S\} \{S\}^T \right]^{-1} \{\delta z\} \quad (43)$$

or by including the iteration subscripts:

$$\{\theta\}_{j+1} = \{\theta\}_j + \{S\}_j^T \left[\{S\}_j \{S\}_j^T \right]^{-1} \left(\{z\}_m - \{z\}_j \right) \quad (44)$$

in which, subscript ‘ j ’ indicates the j^{th} iteration, whereas subscript ‘ m ’ indicates the measured quantities extracted from the experiment, S is sensitivity matrix, θ is parameter vector and z is result vector.

Different sets of design parameters have the effect on the dynamic properties of the structure. The amount of change in the design parameters can differ. For example, Young’s Moduli and shell thickness have really different values in magnitudes. For that reason, the normalization procedure must be carried out not to perform any numerical instabilities [16].

Another weighting matrix can be taken into account to reflect the real structure. Weighting matrix $[W_{\theta\theta}]$ was introduced to add the estimation errors into account in the finite element model [16]. For instance, the stiffness of the bolts cannot be

accurately estimated with respect to the density of a material. It is constructed as diagonal matrix whose elements are the reciprocals of variances of the parameters [16].

Assuming that all the parameters have the equal error in the finite element model is a simple way of calculating the weighting matrices. Introducing the weighting matrix into the general equation, the following equation can be written [16]:

$$\{\theta\}_{j+1} = \{\theta\}_j + [W_{\theta\theta}]^{-1} \{S\}_j^T \left[\{S\}_j [W_{\theta\theta}]^{-1} \{S\}_j^T \right]^{-1} \left(\{z\}_m - \{z\}_j \right) \quad (45)$$

Adding the effect of the errors in the measurements by using the weighting matrix for the measurements, the objective function can be oriented as [16]:

$$F(\{\delta\theta\}) = \{\varepsilon\}^T [W_{\varepsilon\varepsilon}] \{\varepsilon\} + \{\delta\theta\}^T [W_{\theta\theta}] \{\delta\theta\} \quad (46)$$

Putting the required terms and expanding the formula gives [16]:

$$F(\{\delta\theta\}) = \{\delta z\}^T [W_{\varepsilon\varepsilon}] \{\delta z\} - 2\{\delta\theta\}^T S^T [W_{\varepsilon\varepsilon}] \{\delta z\} + \dots \dots \{\delta\theta\}^T \left[S^T [W_{\varepsilon\varepsilon}] S + [W_{\theta\theta}] \right] \{\delta\theta\} \quad (47)$$

Minimizing the above penalty function with respect to term $\{\delta\theta\}$ results in the parameter change as [16]:

$$\{\delta\theta\} = \left[S^T [W_{\varepsilon\varepsilon}] S + [W_{\theta\theta}] \right]^{-1} S^T [W_{\varepsilon\varepsilon}] \{\delta z\} \quad (48)$$

Inserting the indices of iterative procedure:

$$\{\theta\}_{j+1} = \{\theta\}_j + \left[S_j^T [W_{\varepsilon\varepsilon}] S_j + [W_{\theta\theta}] \right]^{-1} S_j^T [W_{\varepsilon\varepsilon}] \left(\{z\}_m - \{z\}_j \right) \quad (49)$$

As another approach, the weighting was done to the initial estimates of the parameters [16]. This approach can result in quantification of the error between

the last converged parameter set and initial values rather than difference in each iteration [16].

The objective function which is to be minimized is organized as:

$$F(\{\delta\theta\}) = \{\varepsilon\}^T [W_{\varepsilon\varepsilon}] \{\varepsilon\} + (\{\theta\} - \{\theta\}_0)^T [W_{\theta\theta}] (\{\theta\} - \{\theta\}_0) \quad (50)$$

$$F(\{\delta\theta\}) = \{\varepsilon\}^T [W_{\varepsilon\varepsilon}] \{\varepsilon\} + \dots \dots \left(\{\delta\theta\} + (\{\theta\}_j - \{\theta\}_0) \right)^T [W_{\theta\theta}] \left(\{\delta\theta\} + (\{\theta\}_j - \{\theta\}_0) \right) \quad (51)$$

In above equation (50) and (51), term $\{\theta\}_0$ belongs to the initial parameter.

By minimizing the penalty function after some mathematical manipulations, the equation can be reached given as below [16]:

$$\{\delta\theta\} = \left[\{\mathcal{S}\}^T [W_{\varepsilon\varepsilon}] \{\mathcal{S}\} + [W_{\theta\theta}] \right]^{-1} \left\{ \{\mathcal{S}\}^T [W_{\varepsilon\varepsilon}] \{\delta z\} - [W_{\theta\theta}] (\{\theta\}_j - \{\theta\}_0) \right\} \quad (52)$$

Inserting the iterative subscript 'j' into the above equation [16];

$$\{\theta\}_{j+1} = \{\theta\}_j + \left[\{\mathcal{S}\}_j^T [W_{\varepsilon\varepsilon}] \{\mathcal{S}\}_j + [W_{\theta\theta}] \right]^{-1} \left\{ \{\mathcal{S}\}_j^T [W_{\varepsilon\varepsilon}] (\{z\}_m - \{z\}_j) - [W_{\theta\theta}] (\{\theta\}_j - \{\theta\}_0) \right\} \quad (53)$$

Finite Element Method and Model Testing

Model updating procedure needs engineering insight about the mathematical model of the structure and experimental model of the structures. Mathematical model can be represented with analytical or finite element models. Experimental model is obtained via modal testing.

Finite element method constructs the mass, stiffness and damping matrices of the whole structure according to the elements that are used in the model [17]. Each

element type (quad, beam, etc.) has own shape function to provide stiffness, mass matrices. Since, the use of finite element models increases, there is a need of comparison of the results with the test results. The deficient correlation between finite element and test results are generally due to numerical and physical uncertainties. These uncertainties can be listed as [17]:

1. Physical uncertainties
 - a. Boundary conditions
 - b. Material data errors
 - c. Geometry errors
 - d. The exactness of the application of the loads
2. Numerical uncertainties
 - a. Deficiency for system knowledge
 - b. Discretization errors like the element type used in the finite element analysis (beam elements, solid elements, bar elements, etc.)
 - c. Numerical solution uncertainties (Convergence problems, etc.)

The verification of the finite element model is generally based on the numerical eigenvalue and eigenvector comparison with the modal test results.

After previously given basic parts of the model updating theory, the definition of the model updating can be summarized as the correction of the numerical model based on the test results to represent the dynamic behavior of the structure under defined loading conditions.

By using the modal test results as a reference increases the importance of the modal test application and the quality of the modal test data. Brief information is given about the modal test. The measurement hardware has 4 parts: system to excite the structure; force transducer to measure the forcing input; accelerometers to measure the response of the structure; and analyzer to record and modify the test results like Fast Fourier Transformation method [17].

The test apparatus has great significance in modal testing. In free-free case, which is there is no connection between the structure and the ground, the structure is supported with elastic springs. The requirement for the elasticity of the springs is to have much lower frequencies of rigid body modes than flexible mode frequencies [15]. The point of extracting mathematical model by using modal test or FE analysis is to identify the mechanical behavior of the structure and investigate the effects of the structural modifications.

In modal test procedure, there are 2 ways to excite a structure. One of them is shaker which drives the stinger to apply a force to structure with proportional to voltage input. Stinger is an elastic rod which is used to transfer excitation to structure. Another way is to use impact hammer. Shakers can be electrodynamic or electrohydraulic driven. There is a possibility to make feedback control by comparing the force input to structure with the electrical input signal.

Shaker can create different types of signals each having different types of advantages and disadvantages with respect to each other. The important signal types are [17]:

- Swept Sine
- Burst random
- Sine chirp
- Sine sweep
- Periodic chirp
- Random, etc.

The definitions of the signal types are important while using shakers in modal tests. Swept sine signal is gradually changing sine signal moving from one frequency to another one. There is useful type of this signal that is popular in engineering called analog swept sine excitation. It has advantages like [17]:

- It has really low ratio of signal to noise level.
- It can be used with the nonlinear system identification.

Besides these advantages, some disadvantages occur. It is the slowest of the all methods and leakage is a problem [15].

Random signal is a stationary signal with Gaussian probability distribution which has frequency composition at all frequencies at frequency range that was specified. The test results from the random signal represent a linear approximation of the system. It is a fast method but again leakage is a problem [17].

The burst random excitation has a signal content which is a random signal that has a definite ratio of the data block [17]. After the random signal application part, the signal stops to cause the response of the structure to die out. Leakage problem with the burst random signal application is degraded with the time of dying out of the responses [17].

Sine chirp signal is a fast swept sine signal that has the frequency excitation within the sample interval of the FFT analyzer. It has own self windowing function and all advantages of swept sine signal [17].

There is an additional option as to use more than one shaker to excite the structure. It causes the energy coming from the excitation to be more evenly distributed throughout the structure [17]. The connection between the structure and the shaker is another crucial topic in shaker driven excitations. Because the mass effect of the force transducer and the rigidity of the connection must be taken into concern [15]. Stinger which is used to excite the structure by using the driving force produced by the shaker must be axially stiff, but with the bending it must be flexible [15]. It leads the structure to be separated from the shaker body.

Another method that is used in modal testing is to use impact hammer. An impact hammer includes force transducer below its tip. According to the structure that needs to be excited and the frequency range of interest, the hammer mass or tip

stiffness must be changed [17]. This method has its own advantages and disadvantages. As an advantage, it is fast and easy method to carry out. But there are problems with this method, either. It is hard to excite large scale structures. The amount of energy must be enough to excite the structure which can cause damages at the excitation points and lead to non-linearity [17]. It is also hard to arrange the direction of the excitation.

Transducers which were made with the piezoelectric materials used to measure the force input to excite the structure and response. The strain in the piezoelectric material is changed into voltage by the signal conditioners [17]. Accelerometers consist of mass connected to the casing material by the help of piezoelectric material. This system can be assumed as a spring mass system which has own resonant frequency far beyond the frequency range of concern for example 25 kHz [17]. The way of connection of the accelerometers to the structure varies with the application areas and the physical conditions. These methods can be listed with using glue, magnets, bolts, beeswax. The transducers must not have an additional mass effect on the structure.

The conditioning of the signals and the analysis of the vibration data is performed by digital processes. The signals coming from the transducers are changed into the digital signals by analog to digital converters (ADCs) [17].

Although modal testing has lots of advantages to gain insight to dynamic properties of the structure, there are some limitations and problems with modal testing [15]:

- The ability to attach the number accelerometers is limited. For that reason, the number of degree of freedom of the experimental model is always less than the mathematical model.
- The number of the modes is limited by the selected frequency range and is sensitive to the resolution.
- It is hard to model the hysterical and non-proportional damping of the real structure by finite element modeling. While modal testing can give results of the real structure, means there is always a difference between mathematical and experimental results.
- Because of the non linearities, the lack of excitation of the real structure due to shaker limitations, high of the structure (fixed, free-free, etc.) of the mathematical model, the level of noise can cause some modes of the structure to be misses out. For that reason, modal testing needs lots of control and pre-test work.
- According to the boundary condition same conditions must be satisfied in modal testing. But it is difficult to model the same boundary conditions in modal testing. For example, the rigid body modes will not be zero due to the suspensions used to handle the structure in free-free case.
- It is possible to model the rotational degrees of freedom in finite element model by using the elements which have degrees of freedom apart from translation. But in modal testing, it is not available to measure rotational degrees of freedom.
- In modal testing, noise is always a problem. To overcome that problem, the type of excitation must be selected carefully. The use of a filter shall be compulsory.

After the basic topics given about model updating and modal testing, it can be said that using the advantages of both techniques can be a solution to structural dynamic problems of mechanical components in real dynamic conditions.